PREDICTING THE STRUCTURE OF BINARY- AND TERNARY OXIDE GLASSES USING STATISTICAL MECHANICS

MASTER'S THESIS AND INTEGRATED PHD MIDWAY REPORT

by

Mikkel Sandfeld Bødker

AALBORG UNIVERSITY
DENMARK

.

AALBORG UNIVERSITET

Institute for Chemistry and Bioscience
Fredrik Bajers vej 7H
Phone: 99 40 99 40
Fax 96 35 05 58
http://www.bio.aau.dk/

Title:
Predicting the Structure of Binary- and Ternary Oxide Glasses using Statistical Mechanics

Project period:
September 2017 – August 2019

Author:
Mikkel Sandfeld Bødker

Supervisor:
Morten M Smedskjaer

SUMMARY

Oxide glasses are fairly cheap materials with a huge range of applications in industries like construction, telecommunication and the medical industry. Glasses are extensively researched but because of the amorphous nature of the glassy structure, the number of possible glass compositions is huge, making it a field with potential for research and development. Understanding composition-structure-property relations in oxide glasses would accelerate the design of new compositions with tailored properties. The goal of this thesis is to push the understanding of composition-structure relations in binary- and ternary oxide glasses.

First, we modified a statistical mechanics-based model, theorized by John Mauro to capture the probabilities of interactions between network modifier and network former species in binary oxide glass systems. We applied the model to binary phosphate-, borate- and silicate glasses, obtaining relative enthalpies of each possible interaction between network modifier and network former species in these glasses. We could successfully predict composition-structure relations with only 1-3 glasses as input for each system. Additionally, the model was used to predict the structural dependence on thermal history in these binary glasses.

Second, we used the thermal history dependence of the present statistical mechanics-based model to predict MD simulated composition-structure relations in Na_2O-SiO_2 glasses. By assuming the same enthalpies of interactions in experimentally obtained glasses and MD simulated glasses, we were able to successfully predict the MD simulated structures with only one free parameter.

Third, we used the obtained parameters from the binary systems to predict composition-structure relations in ternary borosilicate glasses by assuming same bond energies between a specific network modifier and network forming species in the binary and ternary glass systems. With this assumption, the statistical mechanics-based model was used to predict composition-structure relations in the Na_2O-B_2O_3-SiO_2 and K_2O-B_2O3-SiO_2 systems with 1 and 0 free parameters, respectively. The predictions were compared to data obtained by both NMR experiments and MD simulations with most accurate results when comparing to MD simulation.

PREFACE

This master's thesis is a part of an ongoing Ph.D. study. My Ph.D. study is an integrated Ph.D. ("4+4 Ph.D. in Danish"), where instead of doing 5 years to obtain a master's degree and then 3 years of Ph.D., this Ph.D. project started after one year of my master's program instead of starting the master's thesis. Because this is an ongoing study, this thesis is written slightly differently from a regular master's thesis. The layout is closer to a Ph.D. dissertation, where the published papers are presented at the end of the thesis. Additionally, general discussion of the current work and perspective of future work has been emphasized.

The work was carried out from September 2017 to August 2019. The work was conducted at the Section of Chemistry at Aalborg University. The project is funded by the Independent Research Fund Denmark (grant no. 7017-00019).

I want to express my gratitude to my supervisor Morten M. Smedskjaer for giving me the opportunity to conduct research and develop my personal and professional skills at the same time. Morten is extremely intelligent and prolific. His supervision is sharp with room for discussions and opinions. He is a perfect match as a supervisor for my working preferences and I am looking forward to working for and with him for another 2 years.

Additionally, I would like to thank all my collaborators, especially John C. Mauro, Randall E. Youngman and Søren S. Sørensen. John has been a great mentor with a huge knowledge of the specific topic I am working in. Additionally, he invited me to stay with his group at Pennsylvania State University, PA, USA for three months where I had the opportunity to work on my programming skills and plan for specific Python scripts to publish for use of the public. Randall for conducting NMR experiments and assistance in interpretation of results. Søren for conducting MD simulations for my research.

TABLE OF CONTENT

CHAPTER 1. INTRODUCTION

Glass has spiked interest and intrigue in mankind ever since the first discovery of small glass beads in the early mesopetania as a byproduct from metal production.[1] At that time, opaque materials were assessed with very high values, with examples being amber and gemstones.[2] With the discovery of colored glass beads, production of glasses started becoming a profession were the skills and experiences would travel and grow from generation to generation. Eventually, glasses could be produced in large enough scale to be used as building materials, allowing for sunlight to flow into the houses while keeping the insides shielded from the weather.[1] However, even with glass being more available as building materials, it was still used as a sign of quality, value and decoration as seen in the mosaiks of old buildings such as churches or in modern builds, were large window sections are frequently used.[3] Entering the industrial age, up till now, glass has become a high tech material, used in a variety of industries, including but not limited to bioactive glass in the medical industry, optical fibers in telecommunication and nuclear waste encapsulant in the energy industry.[4–7] With the large range of applications of glass, finetuning the chemical composition of glasses to obtain very specific physical properties for a certain application has become a large research area.[2,8] To accelerate the design of new functional glasses, composition-property models have been extensively researched and developed but are often limited to very specific glass systems and are not transferable between systems.[9] Recently, the atomic-scale chemical structure of oxide glasses has been found to correlate nicely with several physical properties and structure-property models have been developed, even between systems.[10–12] The issue with structure-property models is obtaining structural data, as physical properties are easier to measure than the atomic scale-structure.[13–15] In this study, we apply a statistical mechanics-based model accounting for the enthalpic and entropic contributions to bond preferences in simple oxide glasses to predict the composition-structure relation, also between systems.[16,17] Coupling the proposed composition-structure model with already developed structure-property models could enable quantitative composition-property predictions in glass systems not yet experimentally studied. In this thesis, however, the focus is on predicting the composition-structure relation in oxide glasses. First, using experimentally obtained data from binary oxide glasses to build enthalpy values, specific to each modifier in each glass system. Second, to transfer these enthalpy values to ternary glasses and predict composition-structure relation without fitting to any experimentally obtained data.

1.1. BACKGROUND

Glasses are non-crystalline amorphous materials with chemical structures resembling that of liquids.[18,19] Due to its liquid-like structure, the number of possible elements that can be included to form a glass extends to over half of the periodic table. As a result, the number of potential glass compositions is huge and only a very small fraction has already been synthesized and analyzed.[2] Today, glass is a key part in many technologies such as bioactive bone growth, telecommunication, nuclear waste encasement and high-tech monitors.[4,20–22] All of these technologies have in common that they are developed through the tedious and time-consuming trial-and error methodology.[2,23] A method of tailoring the structure of the glass to obtain the desired properties would greatly accelerate the research and development. To get closer to such a method, this study focuses on the thermodynamics that determine the short-range order in oxide glasses to ultimately predict structures of multicomponent glasses from composition without any experiments. Additionally, we will review and apply topological constraint theory (TCT) as a structure-property model. In this report, TCT has only been applied after predicting glass structure of specific oxide systems to illustrate the potential of linking statistical mechanics and TCT. Moving forward, TCT will be linked directly to the proposed statistical mechanics-based model to tailor glass compositions by predicting and optimizing their properties.

1.1.1. GLASS FORMATION

Upon cooling, most liquids will spontaneously crystallize once reaching a critical temperature (T_m in Figure 1).[24] The crystallization will result in an abrupt decrease in enthalpy in the material, resulting in a release of energy (heat) to the system. Some liquids, however, will keep their liquid form even after passing T_m if the cooling rate is high enough, hence forming a “supercooled liquid”. Upon further cooling, the viscosity of the liquid will keep increase until reaching the fictive temperature, where the viscosity of the liquid becomes too high for the structure to rearrange, hence forming a glass.[25] As a result, glasses are amorphous solid materials with chemical structures resembling that of liquids.[19] As seen in Figure 1, the faster cooling rate will result in a higher fictive temperature (T_f) which will be an important factor later, when exploring the statistical mechanical description of structure distribution, since a higher T_f will result in higher entropy and more randomly distributed structures in the glass. Since T_f of the glass depends on the cooling rate during quenching, the glass transition temperature (T_g) has been defined as the temperature where the supercooled liquid reaches a viscosity of 10^{12} Pa×S.[26,27] T_f is estimated to be equal T_g when the glass is quenched at a cooling rate of 10 K/min.[25]

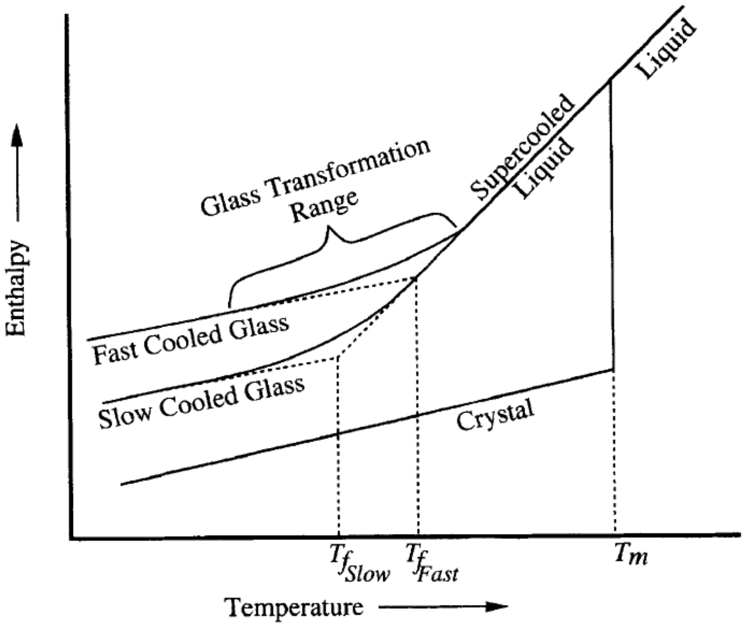

Figure 1. Enthalpy of a glass-forming liquid as a function of temperature, where T_m is the melting temperature of the corresponding crystal, T_{ffast} and slow are fictive temperatures of the glass with a fast and slow cooling rate, respectively.[24]

Some of the most common materials to form glasses upon fast quenching of melts are silica (SiO_2), borate (B_2O_3) and phosphate (P_2O_5), where the Si, B and P atoms form a network through bridging oxygens (BOs), hence they are termed “network formers”.[7,19,28] These glass-formers will have relatively high T_g in their pure form so to reduce the working temperature (and to alter other physical properties) “network modifiers” such as Na_2O, K_2O, and CaO are often added to the glasses.[24] These elements are known as network modifiers because they will break the BOs on the network formers, hence modifying the network.

1.1.2. STRUCTURE OF GLASS

All short-range order (SRO), which refers to the arrangement of atoms over the spacing of only 1-2 atoms, structural groups in the Na_2O-SiO_2 glass system are shown in Figure 2.[29,30] The structural groups are named using the Q^n denotation, where n is the number of BOs pr. silicon atom.

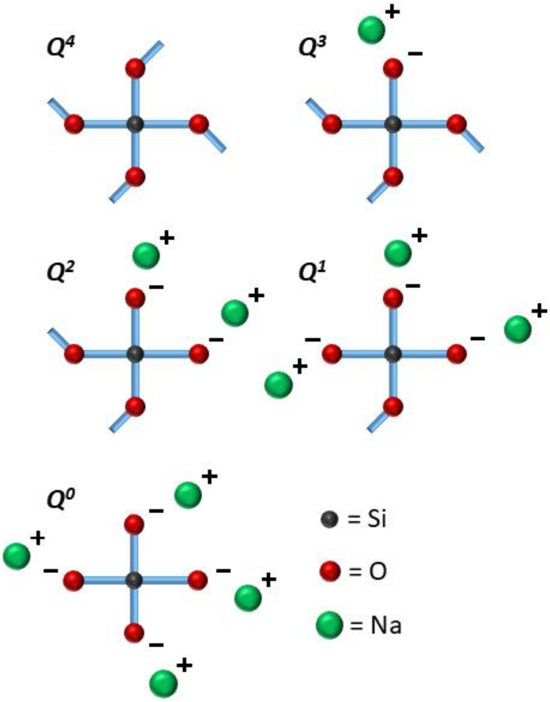

Figure 2. Qn structural units in a Na2O-SiO2 glass system, where green circles are Na+ ions, red circles are oxygen atoms and black circles are silicon atoms. Covalent bonds are represented by a straight blue line.

The more BOs on a silicon atom, the higher the potential energy and hence, a Q^4 unit is more likely to interact with a modifier ion than a Q^3 is.[31] On the other hand, the higher the temperature of the system, the higher the entropic contribution to the free energy of the interaction, hence Q^3 has a closer to equal chance at reacting with a modifier ion as a Q^4 unit.[16] By accounting for the fraction of each structural unit, the energy difference between the interactions, and the energy present from heat at the fictive temperature (where the liquid freezes in time), one would be able to predict the probability of each interaction, leading into statistical mechanical modeling of glass.

1.1.3. STATE OF THE ART

Before descriping the proposed statistical mechanics-based model, an overview of the state of the art is given. Models have already been developed to predict glass properties from their compositions. Below are a few examples, including their strengths and weaknesses.

- Classical additivity models, where properties of glasses are modelled through multiple regression, assuming some linearity between the compositions and the property. This type of model is used for interpolation of properties in specific systems but offers no prediction outside of the glass systems examined.[32,33]

- Structural and semi-empirical models, which, unlike the classical additivity model, allows for predictions of glass properties beyond the limits of the available experimental data. This kind of model extends the experimental data through empirically based structural models, basic principles or general glass chemistry. Hence widening the model application but at the cost of accuracy.[34,35]

- Statistical models are based on statistical analysis such as linear and non-linear regression. These models are often very accurate but limited to the data input in contrast to the structural and semi-empirical models.[9]

- Deductive glass models are based on fundamental laws or theory and are hence not termed as empirical. Examples of deductive glass models include molecular dynamic simulations[36] and thermodynamic modelling[37]. These models are based on the atomic volume, bond strength, atomic size etc. for molecular dynamic simulations and the chemical equilibrium constant, energy of formation etc. for the thermodynamic modelling. Due to the basis of the models, they are often referred to as semi-empirical. Because of the complex amorphous nature of glasses, prediction of complex commercial glasses are hardly possible using deductive glass models as of yet.[38]

The above models aim at predicting the properties of glasses directly from the composition. Molecular dynamics simulations, first established in the late 1980s [39] uses computer simulations of empirical pair potentials between the elements of the glass to predict the short range structure in the glass.[40] Today, detailed molecular dynamics simulations are usually applied on systems containing no more than hundreds of atoms and on time scales of tens of picoseconds.[41] MD simulations offer insight into the structure of oxide glasses but with the main limitation that simulation of glasses must be performed on a system to system basis and is time consuming. Hence, MD simulations do not offer fast prediction of structure of properties of glass systems on a large scale.

Instead of making a direct model to predict the properties of glasses from their composition, this project aims at predicting the structure of the glass from the composition through statistical mechanics and then the properties from the structure. This would give fast prediction of SRO-scale structural units in a large range of glass systems which could then be coupled with structure-property models to easily estimate properties in the systems. Since the proposed statistical mechanical model is semi-empirical, quantitative analysis of the structure of glass systems is a requirement.

Solid state nuclear magnetic resonance spectroscopy

Solid state nuclear magnetic resonance (SS-NMR) is a valuable tool to quantitatively analyse both the short and medium range structures of oxide based glasses.[14] NMR can only be used to probe certain isotopes, since the nuclei investigated must have intrinsic magnetic moment and angular momentum.[42] Common elements used in glass science have NMR active isotopes, which are naturally abundant, such as ^{29}Si, ^{11}B, ^{31}P, ^{27}Al, and ^{23}Na, making SS-NMR a relevant tool to quantitatively analyse the structure of oxide glass systems. Most commercial glasses contain one or more modifiers. These modifiers form non-bridging oxygen (NBO) in the glass network or charge stabilise the network former units. In the SS-NMR results, the peak for the network former nuclei will shift with each added NBO due to increased deshielding. Hence, the Q^n distribution (Figure 2) of most glasses may be quantified using SS-NMR.[31] In mixed network former glasses, 2D NMR has arisen as a powerful tool for predicting the intermediate range structure. Through-bond scalar coupling or internuclear-distance dependent through-space dipolar interactions are exploited to describe the pair-wise connectivity between tetrahedra of different species.[43]

Raman spectroscopy

Raman Spectroscopy is another tool for obtaining short range structural information of a glass system. Like NMR, Raman may be used to probe the Q^n distribution of most glass systems such as silicates, borates or phosphates.[44] Raman utilises the vibrational modes of bonds, since these will shift a reflected beam of light with a specific wavelength to a different wavelength. The shift in wavelength is then specific to the given bond. To be Raman active, the species must have stretching or vibrating bonds, such as the stretching-vibrations of silicon-oxygen bonds.[45] Unlike NMR, quantification of structural units is very difficult using Raman spectroscopy and it is mostly used qualitatively or in combination with SS-NMR.

Neutron diffraction

Finally, neutron diffraction may be used to probe the glass structure. Neutron diffraction works on the basis that a free neutron with a high kinetic energy will transfer kinetic energy to a substrate upon impact. Depending on the energy transferred, the diffraction angle will change and the intensity is detected as a function of diffraction angle. The results may then be Fourier transformed to obtain the pair distribution between atoms in the materials. This method is usually used on crystalline samples and the amorphous nature of glasses makes quantification difficult.[18]

Even though the structural analysis methods of glasses are developed, a general model for predicting the structure of glasses from their composition is still lacking due to their disordered nature.[11]

1.1.4. STATISTICAL MECHANICAL MODELLING OF GLASS

The following description elaborates on the proposed Statistical mechanics-based model by Mauro.[17] We consider that the modifier distribution in simple oxide glasses may be described statistically, using a hypergeometric distribution. Hypergeometric distributions are used to describe the probabilities of a series of events, considering the previous event.[46] An example could be drawing marbles from an urn without replacing them after each draw. In the case of the silicate system in Figure 2, the marbles represent the different structural units, where each unit corresponds to a unique type of marble. The modifiers would then represent the hand drawing a marble from the urn and keeping it. Considering pure SiO_2, the urn would only contain Q^4 marbles. Considering a population of 100 Q^4 marbles, the first random draw would leave 99 remaining Q^4 marbles. The one marble that would be randomly chosen would react with the modifier ion and form a Q^3 unit, hence the marble would be returned to the urn as a Q^3 marble. At the second draw, the urn would contain 99 Q^4 marbles and 1 Q^3 marble and the probability of the modifier to randomly pick a Q^3 marble would be 1 %. If the interaction of the modifier to a network-former species was completely entropically controlled, the hypergeometric distribution would explain the distribution of structural units as a function of modifier concentration. However, in a real glass system, the modifier-former interaction is highly controlled by the system obtaining the lowest possible potential energy, hence the interaction probability is determined by the enthalpies of the different possible interactions and the random hypergeometric distribution is not sufficient. To capture the added enthalpic driving force for a modifier-former interaction, a type of non-central hypergeometric distribution must be applied. In a non-central hypergeometric distribution, each possible event is corrected by a weighting factor, specific to that event. In the case of the marble analogy, the weighting factor would correspond to the marbles having different sizes and the largest marbles would be more likely to be randomly picked. Such a type of distribution is captured mathematically by the Wallenius type non-central hypergeometric distribution:[46,47]

$$p_{i,\omega} = \frac{(g_i - n_{i,\omega-1})w_i}{\sum_{j=1}^{M} \sum_{\omega=0}^{\omega-1} (g_j - n_{j,\omega-1})w_i}, \qquad (1)$$

where $p_{i,\omega}$ is the probability of drawing marble i after ω draws, g_i is the initial population of marble i, $n_{i,\omega-1}$ is the number of marble i already drawn before draw ω and w_i is the weighting factor for marble i. That is, the numerator in Eq. 1 is the number of marbles i before the given draw multiplied by the weighting factor of marble i, and the denominator in Eq. 1 is the total number of marbles before the draw, multiplied by each of their respective weighting factors.

To find a physical meaning of the weighting factor, the non-central hypergeometric distribution is derived from the Boltzmann distribution function. In statistical mechanics, the Boltzmann distribution function[48] describes the probability for a system to be in a given state as a function of the system's temperature and the energy of that state,

$$p_i = \frac{e^{-\frac{\varepsilon_i}{kT}}}{\sum_{j=1}^{M} e^{-\frac{\varepsilon_j}{kT}}}, \tag{2}$$

where p_i is the probability of state i, k is the Boltzmann constant, T is the temperature of the system, ε_i is the total energy of state i, and M is the total number of states. Mauro recently proposed to use the Boltzmann distribution to describe modifier speciation in mixed former glasses.[17] In the glass forming systems, we define the probability states (p_i) to be interactions between modifier ions and network former species i, and consequently, ε_i becomes the free energy of this interaction, which may be described by entropic and enthalpic contributions,

$$p_i = \frac{e^{-\frac{H_i - S_i T}{kT}}}{\sum_{j=1}^{M} e^{-\frac{H_j - S_j T}{kT}}}. \tag{3}$$

Next, we introduce the statistical entropy of the system as,

$$S_i = k \ln \Omega_i, \tag{4}$$

where Ω_i is the number of microstates consistent with a given macrostate for species i,

$$p_i = \frac{e^{-\frac{H_i - k \ln \Omega_i T}{kT}}}{\sum_{j=1}^{M} e^{-\frac{H_j - k \ln \Omega_j T}{kT}}}. \tag{5}$$

We then obtain,

$$p_i = \frac{e^{-\frac{H_i}{kT} + \ln \Omega_i}}{\sum_{j=1}^{M} e^{-\frac{H_j}{kT} + \ln \Omega_j}}, \tag{6}$$

or,

$$p_i = \frac{\Omega_i e^{-\frac{H_i}{kT}}}{\sum_{j=1}^{M} \Omega_j e^{-\frac{H_j}{kT}}}. \tag{7}$$

The number of microstates consistent with the macrostate of species *i* divided by the total number of microstates consistent with the macrostate of the oxide glass will be the same as the relative fraction of species *i* divided by the total number of species. Since the fraction of a given structural species *i* in the glass changes with composition, we obtain

$$\Omega_{i,\omega} = (g_i - n_{i,\omega}), \qquad (8)$$

where ω represents a given modifier concentration, g_i is the degeneracy of species *i* and $n_{i,\omega}$ is the total fraction of species *i* that has already interacted at modifier concentration ω. When calculating the probability of an interaction with species *i* at concentration ω, we must use the fraction of species *i* at the previous concentration step (ω-1),

$$p_{i,\omega} = \frac{(g_i - n_{i,\omega-1})e^{-\frac{H_i}{kT}}}{\sum_{j=1}^{M}\sum_{\omega=0}^{\omega-1}(g_j - n_{j,\omega-1})e^{-\frac{H_j}{kT}}}. \qquad (9)$$

The double summation in the denominator is over all species *M* and each modifier concentration ω up to, but not including the current concentration ω. The probability distribution function in Eq. (9) is a type of non-central hypergeometric distribution function, where the relative enthalpy H_i values are the free parameters when fitting to experimental data. We define $e^{-\frac{H_i}{kT}}$ as the weighting factor w_i for a modifier to interact with the structural group *i*, where *T* is assumed to be equal to T_f for $T < T_f$, since the structure is assumed to freeze in at the fictive temperature:

$$p_{i,\omega} = \frac{(g_i - n_{i,\omega-1})w_i}{\sum_{j=1}^{M}\sum_{\omega=0}^{\omega-1}(g_j - n_{j,\omega-1})w_j}, \qquad (10)$$

where,

$$w_i = e^{-\frac{H_i}{kT_f}}. \qquad (11)$$

In the glass systems, the concentrations of structural units *i* at ω are calculated based on the concentrations of those species at ω-1 and the $p_{i,\omega}$ values that all depend on concentrations at ω-1. Then, the new structural concentrations at ω are used to calculated probabilities $p_{i,\omega+1}$ and so on. By knowing a starting concentration of structural units at ω=0, one can iteratively calculate the concentrations of all structural units at all modifier concentrations ω if w_i for all *i* are known, or fit the model to experimentally obtained data to obtain w_i. In Figure 3, the Q^n distribution after the first draw is illustrated, where the colored spheres illustrate each Q^n unit. Here, we see that even after the first draw, the probability of drawing another Q^4 unit is still 100 % when rounded to 3 decimals. This is due to the effect of the weighting factors seen in the bottom right corner.

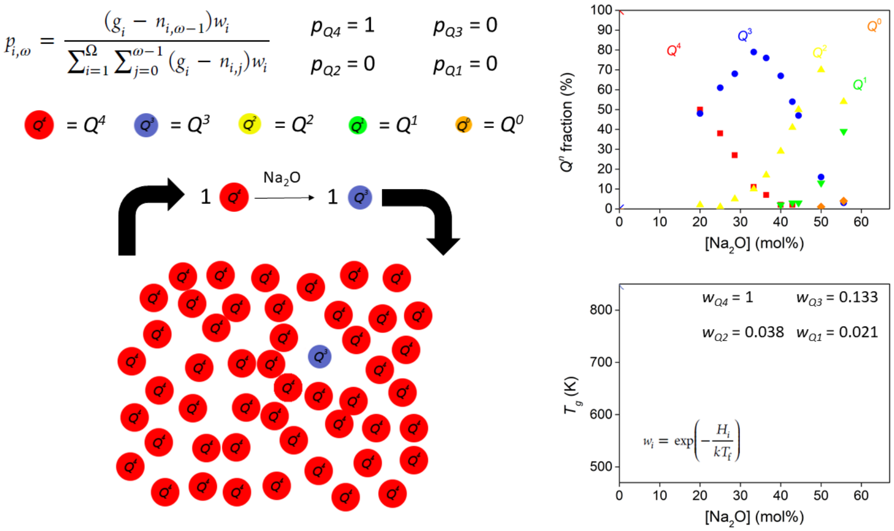

Figure 3. The probabilities of drawing each former specie at 0 % modifier in a Na_2O-SiO_2 glass system. The colored spheres represent the population of structural units in the glass at the first draw. The top right graph shows experimental data of composition-structure relation in the glass system as symbols and the prediction as lines (up until the current concentration). The lower right graph shows the T_g at the composition as a line and the weighting factors calculated for the given composition based on the T_g value.

In Figure 4, the probabilities of drawing each structural unit is calculated for a $50Na_2O$-$50SiO_2$ glass. Observe how the probability to draw a Q^3 unit is still higher than drawing a Q^2 unit despite the larger population of Q^2 units. Figure 3 and 4 should give a picture of the numerical solution to calculating the probabilities of interaction. By knowing the starting concentration and the starting weighting factors, the initial probabilities may be calculated. From the initial probabilities, the fraction of each specie randomly picked for interaction is known and hence the new populations may be calculated, as these units are “returned to the urn” as different units. In the lower right corner of Figure 4, the T_g at the glass composition is tracked and used to calculate new weighting factors for each iteration. Note the difference between the weighting factors in Figures 3 and 4 due to the difference in T_g.

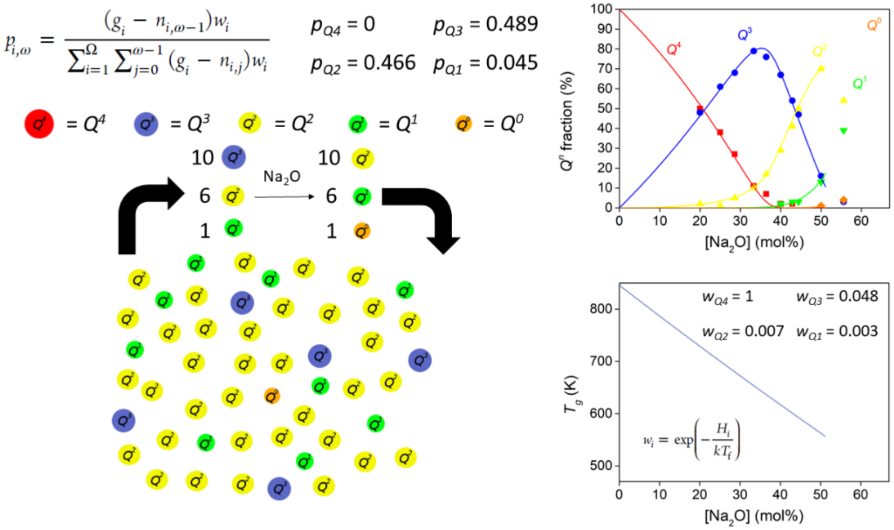

Figure 4. The probabilities of drawing each former specie at 0 % modifier in a Na_2O-SiO_2 glass system. The colored spheres represent the population of structural units in the glass at the first draw. The top right graph shows experimental data of composition-structure relation in the glass system as symbols and the prediction as lines (up until the current concentration). The lower right graph shows the T_g at the composition as a line and the weighting factors calculated for the given composition based on the T_g value.

In case the T_g values of the glass is known, the model can be used to obtain the H_i of modifier former-interactions. Assuming these H_i values are constant for the specific modifier-former interaction, then these can be used in all systems where this interaction occurs. Consequently, the model can be applied to simple glass systems with few components to obtain H_i values, from experimentally obtained data, which in turn may be used to predict structural evolutions in complicated, multicomponent glasses without any fitting. In Appendix A, the python script used to apply this model to the binary phosphate is included with explanation.

1.1.5. TOPOLOGICAL CONSTRAINT THEORY

Topological constraint theory (TCT) was first proposed by Gupta and Cooper to mathematically explain the Zachariasen rules for glass formation.[10] The Gupta-Cooper model is derived for an arbitrary *d*-dimensional space and generalizes the tetrahedral network (as seen in Figure 2) to rigid polytopes of arbitrary dimensionality. At the same time, Phillips published another topological-based model which was later extended and put rigorous mathematical basis by Phillips and Thorpe.[49,50] The Phillips and Thorpe model considers the connectivity of individual atoms in the network and predicted that the glass-forming ability would be maximized when the number of rigid two-and three-body constraints equals the number of atomic degrees of freedom. This prediction was later confirmed experimentally.[12,51] According to Phillips and Thorpe, the glass network can be considered floppy (underconstrained), isostatic (optimally constrained), or stressed rigid (overconstrained), dictated by the relative difference between the average number of constraints per atom (n) and the network dimensionality (d). When $n<d$, the network is underconstrained and contains low-frequency deformation modes (so-called "floppy modes"). The network is isostatic when n=d and stressed rigid when n>d. Gupta and Mauro developed a method to account for temperature dependent constraints in glass-forming liquids.[51] They categorized the constraints by their different onset temperatures, such that $T_\gamma < T_\beta < T_\mu < T_\alpha$, where γ, β, μ, and α are different types of constraints defined as:

- α: Linear constraints. Two α constraints for each oxygen.
- β: Angular constraints on the network former. The quantity depends on the coordination and the number of NBOs associated with the former atom
- γ: Angular constraints on the oxygen. One γ constraint per oxygen.
- μ: Additional modifier rigidity due to clustering effects.

In Figure 5, the influence of the onset temperatures of the constraints is illustrated. When the atomic degrees of freedom passes through zero, the system transition from containing floppy modes to a fully rigid system, where zero corresponds to an isostatic network.[10]

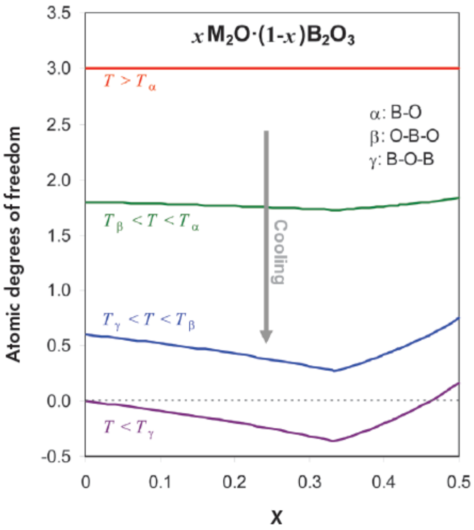

Figure 5. The average atomic degree of freedom as a function of temperature in a binary borate glass system. As the system is cooled, more constraints become rigid and the average degrees of freedom decrease.[10]

Following the discovery of temperature dependent constraint theory in oxide glasses, the concept has been used to predict physical properties such as Tg, fragility, and hardness from the structure on the short-range order scale.[11,12,52–54]

As the topological constraints of a glass is directly calculated from the atomic-scale structure, coupling TCT to the statistical mechanics-based model described in Section 1.1.2 would enable the prediction of physical properties of glasses, effectively amplifying the usefulness of the statistical mechanics-based model.

1.2. CHALLENGES

The statistical mechanics-based model proposed five years ago by Mauro[17] appears to easily solve many of the problems glass scientists are faced with when trying to come up with new and better glass compositions. To reach the end-goal of being able to easily predict structures for a huge range of glass systems from knowing the structures of a few simple systems only, a number of challenges must first be tackled.

First, accurate measurements of the atomic scale structure of oxide glasses is a hard and tedious task and is often neglected in favor of easy measurements of physical properties, which is then correlated to the composition without taking the structure in consideration. To establish and verify the statistical mechanics-based model, systematic measurements of both binary and multicomponent glass structures are required.

Second, the solution to binding probabilities, using the statistical mechanics-based model, is numerical with a set of free parameters. To obtain the most accurate parameters, energy landscaping is required as there may be several global minima when optimizing against the free parameters. Consequently, using the method will require a decent amount of computing power.

Finally, the model also considers the structural dependence on thermal history of the glasses. To establish the model on simple glass systems, the fictive temperatures of the glasses are required as well as quantification of their structural units. Additionally, the structures of the predicted glasses are also depending on their fictive temperatures, making the model seem useless since you need to know a physical property of a glass before you can predict the structure of said glass.

1.3. OBJECTIVES

As this thesis is part of an ongoing Ph.D. study, the following objectives are expected to be completed at the end of the Ph.D.:

I. universal model for predicting the bonding preferences in oxide glasses with different combinations of network formers and modifiers by determining the bond energy parameters for the systems of interest
II. coupling of new structure model with TCT; thus
III. prediction of glass properties as a function of glass chemistry, enabling quantitative design of glass compositions with tailored properties starting at the atomic level.

As the focus of this thesis is on the composition-structure relation in oxide glasses, objectives for the thesis are:

I. Verify the proposed statistical mechanics-based model on experimental data in simple binary oxide glass systems
II. Using the statistical mechanics-based model, obtain relative enthalpy values for binary phosphate-, silicate- and borate glass systems
III. Using the enthalpy parameters obtained in the binary oxide glass systems, modify the statistical mechanics-based model to predict composition-structure relations in ternary oxide glass systems with 0 fitting parameters.

1.4. THESIS CONTENT

The content of this thesis consists of three papers as well as an extended summary of these papers. The papers constitute a large portion of this thesis and may be found after the list of references.

I. M.S. Bødker, J.C. Mauro, S. Goyal, R.E. Youngman, and M.M. Smedskjaer, Predicting Q-Speciation in Binary Phosphate Glasses Using Statistical Mechanics. *The Journal of Physical Chemistry B,* **122** (2018), 7609-7615
II. M.S. Bødker, J.C. Mauro, R.E. Youngman, and M.M. Smedskjaer, Statistical Mechanical Modeling of Borate Glass Structure and Topology: Prediction of Superstructural Units and Glass Transition Temperature, *The Journal of Physical Chemistry B,* **123** (2019), 1206-1213
III. M.S. Bødker, S.S. Sørensen, J.C. Mauro, and M.M. Smedskjaer, Predicting Composition-Structure Relations in Alkali Borosilicate Glasses using Statistical Mechanics, *Frontiers in Materials,* **6** (2019), 175

CHAPTER 2. STATISTICAL MECHANICAL MODELS OF BINARY OXIDE GLASSES

In this chapter, the statistical mechanics-based model will be established and verified in the binary phosphate, silicate and borate glass systems. We will show that the model can predict the compositional structure evolutions in these systems with input data of only a few reference glasses. In the binary phosphates and silicates, we will explore the compositional evolution of their SRO scale structures, while in the borate glass systems, we will also explore the evolution of their intermediate range order (IRO) structures (superstructure).

2.1. BINARY PHOSPHATE GLASSES

Phosphate glasses have seen a high increase in industrial applications over the last 20-30 years, examples being nuclear waste hosts, drug delivery systems, and fast ion conductivity.[21,55,56] As such, phosphate glasses have served as a model system in understanding structure-property relations through topological modeling.[57] Since structure-property relation for the elasticity of phosphate glasses has been established for these systems, predicting their compositional-structure relation would be a useful tool to enable composition-property prediction.

The SRO structure of phosphate glasses are very similar to that of silicate glasses (Figure 2) with the main difference being the extra valence electron on phosphorous compared to silicon.[58,59] As a result, phosphorous is most stable when forming five covalent bonds to oxygen atoms but since the tetrahedral is still the most stable configuration, phosphorous will form a double bond to one oxygen and singe covalent bonds to three oxygen.[60]

In Figure 6, all SRO structural units (Q^3, Q^2, Q^1, and Q^0) are shown as well as the compositional structure evolution of each unit in binary alkali phosphates as predicted by the chemical order model.[28] As seen Figure 6, the chemical order model assumes a purely stepwise conversion of the Q^n units with increasing modifier content. This assumption is commonly explained by the double bond being able to delocalize to any NBO, hence the Q^2 structural configuration is more energetically favorable than the Q^3 configuration.[60] Additionally, the difference in the potential energy between a Q^3 and a Q^2 must be larger than that between a Q^2 and a Q^1, otherwise the Q^2 would be more likely to react with a modifier ion. By applying the statistical mechanics-based model described in Section 1.1.2 to experimentally obtained structure data, we can obtain the enthalpies of these interactions and predict composition-structure relations specific to each glass system.

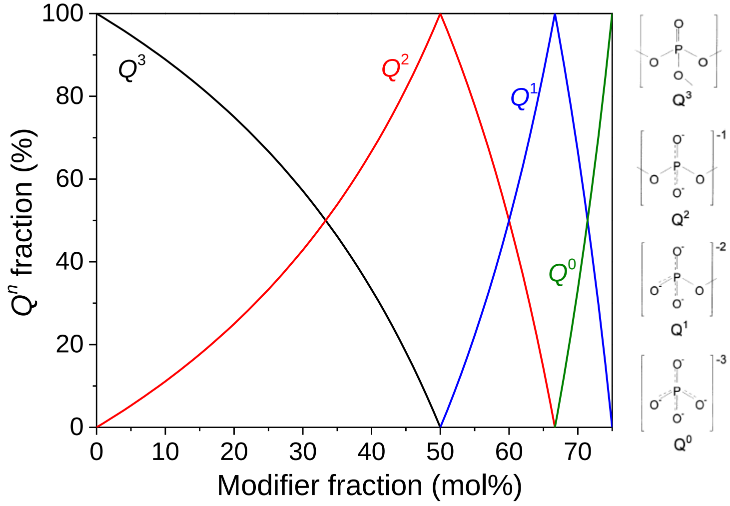

Figure 6. Composition dependence of the molar fraction of Q^n structural units as described by the general chemical order model for a binary phosphate glass. Figure taken from paper I

In paper I, we used the model to predict the fraction of Q^n units in a Na_2O-P_2O_5 glass system as a function of the sodium content.[61] First, lets describe the probability for a sodium to interact with a Q^3 unit at a given composition ω, with the interaction enthalpies as free parameters:

$$p_{Q^3,\omega} = \frac{Q^3_{\omega-1} w_{Q^3,\omega}}{Q^3_{\omega-1} w_{Q^3,\omega} + Q^2_{\omega-1} w_{Q^2,\omega} + Q^1_{\omega-1} w_{Q^1,\omega}}, \qquad (12)$$

where,

$$w_{Q^3,\omega} = e^{-\frac{H_{Na^+,Q^3}}{kT_{f_\omega}}}, \qquad (13)$$

where H_{Na^+,Q^3} is the relative enthalpy value for a sodium ion to interact with a Q^3 structural unit, T_{f_ω} is the fictive temperature in the Na_2O-P_2O_5 glass system at composition ω, and k is the Boltzmann constant (in kJ mol^{-1} K^{-1}). Similar approaches are used to calculate the probabilities for Q^2 and Q^1 at composition ω.

Next, the fractions of Q^3, Q^2, Q^1, and Q^0 at composition ω are calculated:

$$Q_{\omega}^{3} = Q_{\omega-1}^{3} - p_{Q^3,\omega}, \tag{14}$$

$$Q_{\omega}^{2} = Q_{\omega-1}^{2} + p_{Q^3,\omega} - p_{Q^2,\omega}, \tag{15}$$

$$Q_{\omega}^{1} = Q_{\omega-1}^{1} + p_{Q^2,\omega} - p_{Q^1,\omega}, \tag{16}$$

$$Q_{\omega}^{0} = Q_{\omega-1}^{0} + p_{Q^1,\omega}. \tag{17}$$

That is, the fractions of the Q^3, Q^2 and Q^1 units will decrease for each draw ω based on the probabilities for drawing those species, while the fractions of Q^2, Q^1 a and Q^0 will increase for each draw based on the probability of drawing Q^3, Q^2 and Q^1 units, respectively. Since a Q^3 unit is converted to a Q^2 unit, the probability for a modifier to interact with a Q^3 will affect the quantity of both Q^3 and Q^2 units (same argument applies to all other units). Next, the Q_{ω}^{n} fractions are used to calculate probabilities at concentration ω+1 etc.

In Figure 7, the statistical mechanics-based model predictions as well as ^{31}P NMR data for the Li_2O-P_2O_5 glass system from article I is reported.[60,62] The model prediction was made based on structural data of one glass composition only ($50Li_2O$-$50P_2O_5$) and fits very well with the remaining data, with an R^2 of 0.992. All python codes for fitting experimental data to the predicted values with the enthalpy values as free parameters is shown and explained in Appendix A. The model was also applied to binary phosphate glasses with Na_2O, Cs_2O, MgO, and ZnO as the modifier ions as seen in article I.[58,59,63–66] As T_g as a function of modifier concentration were known for all these glass systems, the enthalpy for the interactions were obtained as reported in Table 1.[67]

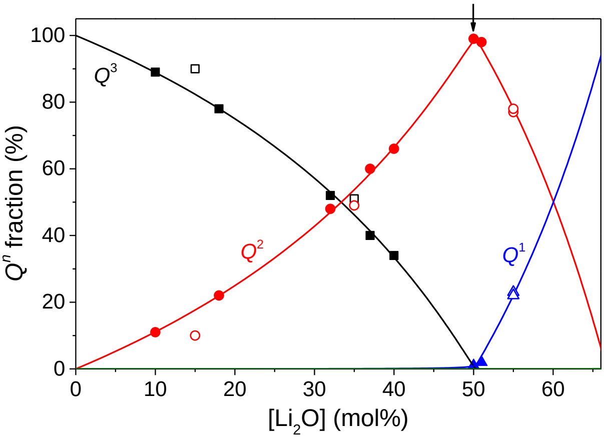

Figure 7. Composition dependence of the fraction of Q^n structural units in binary lithium phosphate glasses. Experimental data from Van Wüllen et al.[62] is represented as closed symbols and from Alam et al.[60] as open symbols. The solid lines represent the prediction using the

present statistical mechanics-based model, which is established only based on experimental data for the glass marked by an arrow. Figure taken from Article I.

Glass modifier	Li_2O	Na_2O	Cs_2O	MgO	ZnO
H_3 (kJ/mol)	0	0	0	0	0
H_2-H_3 (kJ/mol)	33.5	42.8	56.8	31.6	27.0
H_1-H_3 (kJ/mol)	70.4	74.9	85.1	55.0	40.0
R^2	0.992	0.998	0.996	0.942	0.988

Table 1. H_i parameters and coefficient of determination (R^2) values for the fitting of the current model to experimental data for five different binary phosphate glass systems. H_i are scaled relative to that for the Q^3 to Q^2 conversion (H_3), which is set to 0. Table taken from Article I

When introducing the divalent magnesium and zinc cations as modifiers, the enthalpy barriers for the interactions drastically drops, allowing the system to obtain a disproportionate state where more than two structural units are present at a time (contradictory to the chemical order model).

In Figure 8, the structural prediction for the ZnO-P_2O_5 glass system is presented along with the experimental data as points, the chemical order model as the dashed line and a completely entropically controlled distribution as the dotted line.[65,66] This would represent how the statistical mechanics-based model is able to capture the structural evolution by combining the enthalpic and entropic contributions to the bonding preference.

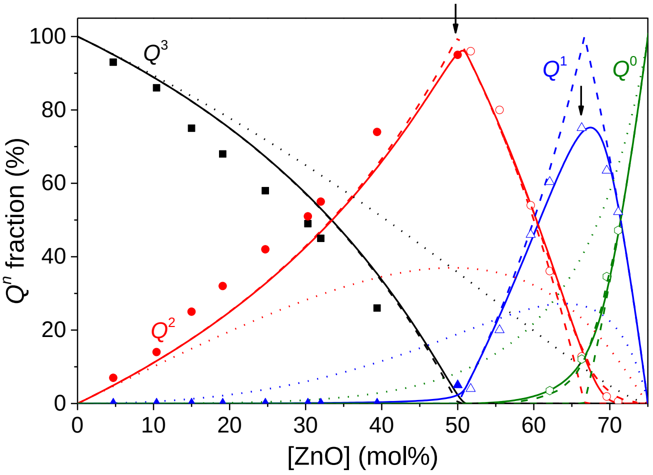

Figure 8. Composition-structure relation of Q^n structural units in zinc phosphate glasses as predicted by different types of models. Closed symbols represent experimental data from Fayon et al.[63] *and the open symbols those from Walter et al.*[64] *The solid lines represent the prediction using the statistical mechanics-based model, established based on experimental data for the glasses marked by an arrow only. The dashed lines represent the chemical order model, and the dotted lines a completely random distribution model. Figure taken from Article I*

Finally, we were able to use the statistical mechanics-based model to predict the structural dependence on the fictive temperature of the glass in article I. It is assumed that a higher fictive temperature will lead to a more entropically controlled, and hence more random distribution of structural units due to the higher energy for making energetically unfavorable interactions.

In Figure 9, the structure of 66ZnO-34P_2O_5 is plotted against the fictive temperature of the glass. As expected, the structure will approach a completely ordered structure with no disproportionation as the fictive temperature approaches 0 and a higher disordered structure as the temperature increases. The dashed lines represent the expected range of experimentally obtainable fictive temperatures for this glass composition.

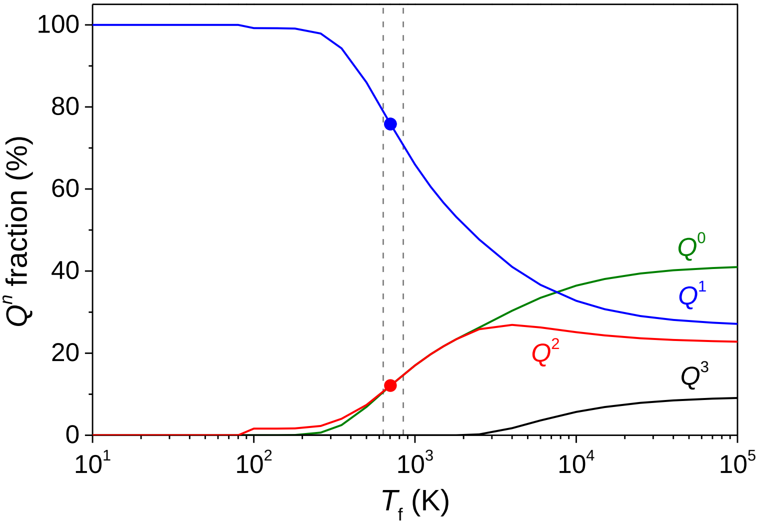

Figure 9. Fraction of Q^n structural units in a 66ZnO-34P_2O_5 glass as a function of fictive temperature. The solid lines show model predictions, while the closed symbols represent the T_f (=T_g) values. The dashed vertical lines represent the extremes of realistically obtainable T_f values (0.9T_g to 1.2T_g). Figure taken from Article I.

2.2. BINARY SILICATE GLASSES

Silicate glasses are probably the most used glass family in industry, most famously known for the soda-lime silicate glasses used for building materials such as windows.[19] The structural units in the silicate glass system are shown in Figure 2 in Section 1.1.1. The Q^n units will interact with a modifier ion in a similar fashion to the phosphate glass system:

$$Q_{\omega}^{n} = Q_{\omega-1}^{n} + p_{Q^{n+1},\omega} - p_{Q^{n},\omega}, \qquad (18)$$

where Q_{ω}^{n} is the fraction of species Q^n at draw ω, and the probabilities $p_{Q^{n},\omega}$ are calculated as:

$$p_{Q^{n},\omega} = \frac{Q_{\omega-1}^{n} w_{Q^{n},\omega}}{\sum_{n=1}^{N} Q_{\omega-1}^{n} w_{Q^{n},\omega}}, \qquad (19)$$

where N is the total number of structural species and $w_{Q^{n},\omega}$is defined as:

$$w_{Q^{n},\omega} = e^{-\frac{H_{M^{+},Q^{n}}}{kT_{f\,\omega}}}. \qquad (20)$$

As in the phosphate glass system, the relative enthalpy values for a modifier ion to interact with a given structural unit is found by fitting the model numerically to structural data with the enthalpy values as free parameters.

The compositional evolution of structural Q^n units in the Na_2O-SiO_2 glass system as obtained by ^{29}Si MAS-NMR experiments is shown in Figure 10, with a very good agreement to the model predictions.[68,69]

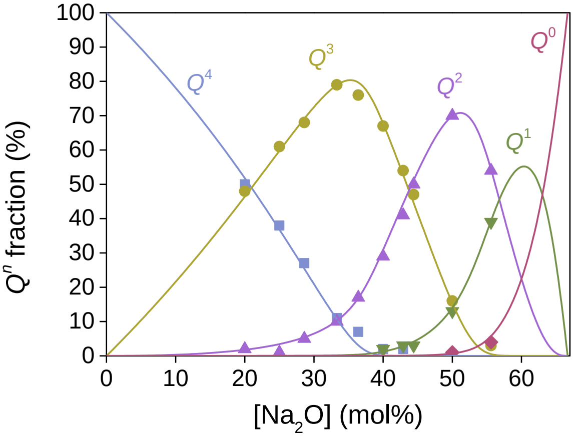

Figure 10. Fraction of Q^n structural units as a function of composition in sodium silicate glasses. Solid lines represent the model predictions and the closed symbols are ^{29}Si MAS NMR experimental data (from Ref. [68]). Figure taken from Article I.

Glass modifier	**Li_2O**	**Na_2O**	**K_2O**
H_4 (kJ/mol)	0	0	0
H_3-H_4 (kJ/mol)	8.4	14.1	18.8
H_2-H_4 (kJ/mol)	16.4	22.9	35.5
H_1-H_4 (kJ/mol)	22.1	27.1	45.8

Table 2. H_i for the fitting of the current model to experimental data for Three different binary silicate glass systems. H_i are scaled relative to that for the Q^4 to Q^2 conversion (H_4), which is set to 0. Table taken from Article I.

As with the phosphate glasses, the larger the alkali ion, the larger the difference between the enthalpies of interactions (Table 2). This is reflected in the higher degree of disproportionation of structural units in the Li_2O-SiO_2 glasses, compared to Na_2O-SiO_2 or K_2O-SiO_2 glasses as found in article III.[40,70]

In Section 2.1, the structural dependence of the fictive temperature was predicted for a 66ZnO-34P_2O_5 glass, using Eq. 19. Molecular dynamics (MD) simulation of oxide glasses has become a powerful tool for probing the SRO scale structure of glasses but suffers from short simulation timescales (nanoseconds to a few microseconds).[71,72] Due to the short simulation timescales, the simulated glasses will attain unrealistically high fictive temperatures and the distributions of structural units differ significantly from those quantified by NMR experiments. As the statistical mechanics based model has the fictive temperature of glasses as an input parameter, it can be a tool to close the gap between MD simulated glass structures and melt-quenched glass structures.

In Figure 11, the distribution of predicted SRO scale structures (line) in the 35Na_2O-65SiO_2 glass is plotted as a function of fictive temperature of the glass (taken from article III). The distribution of Qn units in this glass composition as obtained by MD simulations fall exactly upon the predicted curves.[72,73] This is a first indication, that the enthalpy values obtained by fitting the statistical mechanics-based model to experimentally obtained data may describe both MD simulated- and melt-quenched glasses.

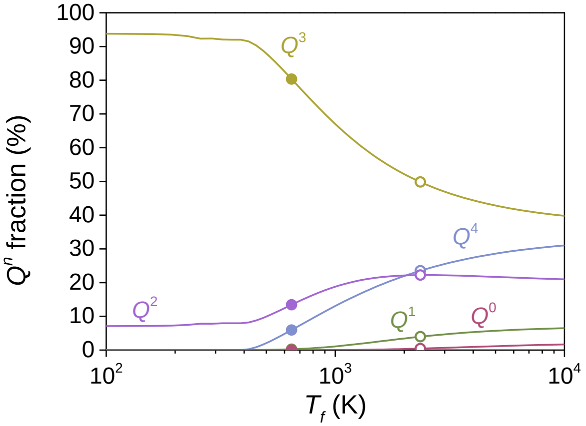

Figure 11. Structural units in 35Na_2O-65SiO_2 plotted against fictive temperature (T_f). The open symbols represent MD simulated data[73], the closed symbols represent ^{29}Si MAS-NMR experimental data[68], and the solid lines represent the model predictions. Figure taken from Article III.

In Figure 12, the structural prediction of MD simulated glasses was performed using the enthalpy values obtained for Na_2O-SiO_2 by using data quantified by ^{29}Si MAS-NMR (Table 2). The model predicts the structural evolution of MD simulated Na_2O-SiO_2 glasses very well with only the T_f scaling factor as a free parameter (MD T_f = 3.6xT_g).

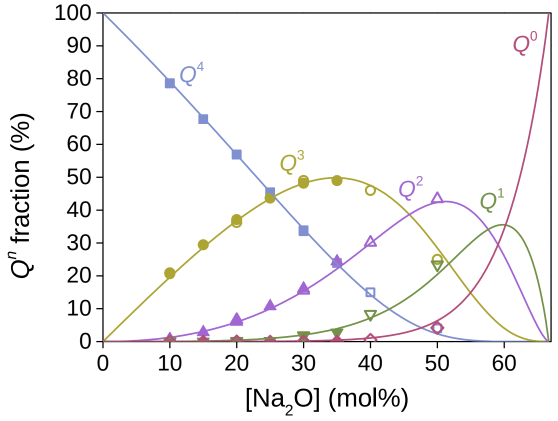

Figure 12. Fraction of Q^n structural units as a function of composition in sodium silicate glasses. The closed and open symbols represent MD simulated data[72,73]. The solid lines represent model predictions, using the same bonding preferences parameter, but a different fictive temperature compared to Figure 10. Figure taken from Article III.

The statistical mechanics-based model was successfully established in the binary silicate glass system in a similar fashion as in the binary phosphate glass system. Additionally, the temperature dependence of the proposed statistical mechanics-based model was used to predict composition-structure relations in MD simulated glasses by using the same enthalpy parameters as in data obtained by MAS-NMR spectroscopy of melt-quenched glasses with only one free parameter.

2.3. BINARY BORATE GLASSES

Unlike phosphate and silicate glasses, the structural backbone of borate glasses is made up of three-fold coordinated trigonal units.[74] Modifiers introduced to the borate glass will either (a) convert a three-fold coordinated boron with three BOs to a four-fold coordinated boron with four BOs with the modifier as charge-compensator for the boron atom or (b) break a BO and form an NBO with the modifier as charge-compensator for the oxygen atom, as in the silicate glasses.[75] In binary borates, conversion (a) is favored at low modifier concentrations (0-30 %), effectively increasing the connectivity of the network by forming additional BOs, resulting in non-monotonic changes in physical properties with modifier content, known as “the boron anomaly”.[75] On the SRO scale, borate glass structures are denoted T^n and Q^n, where T^n units are trigonal boron with n number of BOs and Q^n units are tetrahedral units with n number of BOs.

Additionally, the borate glass will form different intermediate range order (IRO) scale structures as seen in Figure 13.[76,77] The distribution of these “superstructures” depends on the modifier concentration in the glass as well as the thermal history of the glass and may hence be predicted using the statistical mechanics-based model.

These structural units were proposed by Feller in 1982, by assuming all boron atoms to exist in one of the structures in Figure 13.[76] By then using an underutilized ^{10}B NMR technique, they quantified the distribution of these superstructural units in the Li_2O-B_2O_3 glass system. Today, only about 70 % of the boron atoms in a pure borate glass are believed to be found in the boroxol ring configuration, while the rest will be found in non-ring T^3 unit.[78,79] In the following prediction from Article II, the old assumption is used since the data was produced with the same assumption, and the non-ring boron units are assumed to be uniformly distributed among the presumed ring structure-population.

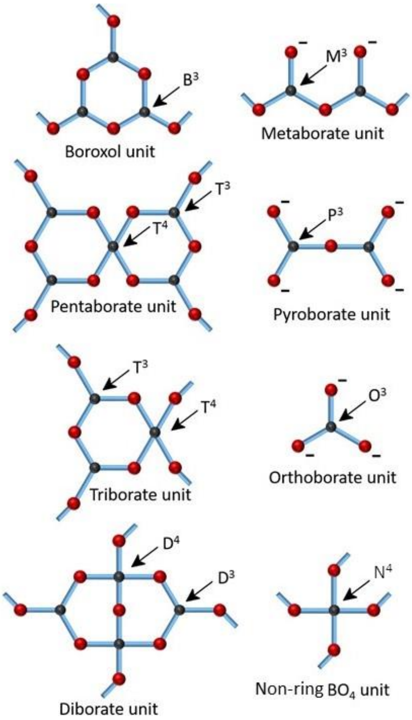

Figure 13. Superstructures in lithium borate glasses. Red circles represent oxygen atoms and black circles boron atoms. The negative signs on oxygen atoms indicate non-bridging oxygen, which are charge-balanced by lithium cations (not shown). A triborate and a pentaborate connect to form a tetraborate unit. The boron structural configurations (quantified by ^{10}B NMR[76]) are marked by arrows, where B^3 is a three-fold coordinated boron in boroxol unit, T^4 is a four-fold coordinated boron in tetraborate unit, etc. Figure taken from Article II

To predict the structural dependence of these IRO scale units, the possible interactions between boron atoms illustrated in Figure 13 and a modifier ion were established based on Feller[76].

$$8B^3 + Li_2O \rightarrow 6T^3 + 2T^4, \tag{21}$$

where the exponents represent the boron coordination number. As lithium oxide interacts with the boroxol structural groups, it changes eight boron atoms in the boroxol configuration into eight boron atoms in the tetraborate configuration, where two of the eight atoms will be four-fold coordinated, and balance the charge from the lithium modifier cation. We assume that the fraction of T^3 is always three times the fraction of T^4 due to the site constraints. Eight boron atoms in the tetraborate configuration will then interact with lithium oxide to form eight boron units diborate configurations, with four of the boron atoms in four-fold coordination, effectively stabilizing the new modifier cations:[76]

$$6T^3 + 2T^4 + Li_2O \rightarrow 4D^3 + 4D^4. \tag{22}$$

It is assumed that the fraction of D^3 is always equal to that of D^4 due to the site constraints. Diborate units may then be transformed into either metaborate or non-ring BO^4 units,[76]

$$2D^3 + 2D^4 + Li_2O \rightarrow 4yM^3 + 4(1-y)N^4. \tag{23}$$

The ratio (y) between metaborate and non-ring BO_4 is assumed to be constant at all modifier concentrations.[76] Other studies[78,80] have found higher concentrations of non-ring BO_4 at low modifier content in alkali borate glasses. These are assumed to part of the tetraborate and diborate structural data by Feller[76]. Metaborate, non-ring BO_4, and orthoborate units are assumed to interact with lithium oxide and form the next structural group at a one-to-one ratio:[76]

$$2M^3 + Li_2O \rightarrow 2P^3, \tag{24}$$

$$2N^4 + Li_2O \rightarrow 2P^3, \tag{25}$$

$$2P^3 + Li_2O \rightarrow 2O^3. \tag{26}$$

When applying the statistical mechanical model in Article III to the borate glass system, each of the structural configurations that the boron atoms undertake in Eqs. (21)-(26) are considered as individual network former species i.

With the interactions established, the probabilities of these interactions may be predicted using Eq. 9 like in the previous subsection:

$$B^3_\omega = B^3_{\omega-1} - 4p_{B^3,\omega}, \tag{27}$$

$$T_\omega = T_{\omega-1} - 4p_{T,\omega} + 4p_{B^3,\omega}, \tag{28}$$

$$T^3_\omega = \frac{3}{4}T_\omega, \quad T^4_\omega = \frac{1}{4}T_\omega. \tag{29}$$

B^3_ω is the fraction of boron atoms in the B^3 configuration at draw ω etc., and the number of probabilities corresponds to the stoichiometries in Eqs. 22-29. The remaining structural units are found with the same methodology, using the stoichiometry in Eqs. 22-29. With these descriptions, the compositional evolution of IRO scale structural units in the Li_2O-B_2O_3 glass system may be predicted with enthalpy values as free parameters, as fictive temperatures are known.[81]

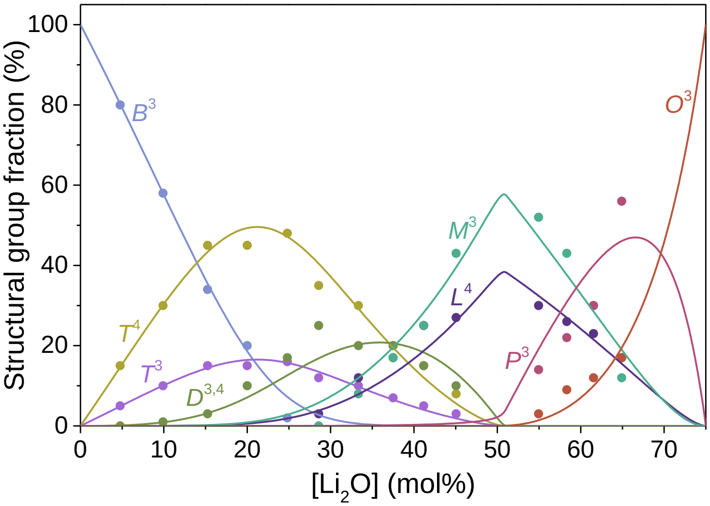

Figure 14. The fraction of IRO superstructural units (see nomenclature in Figure 10) as a function of composition in the lithium borate glasses. The solid lines represent the prediction using the present statistical mechanics-based model and the closed symbols represent experimental data from Feller[76]*. Figure taken from Article II*

The structural evolution is well described by the statistical mechanics-based model with the enthalpy values reported in Table 3.[82]

H_{B^3} (kJ/mol)	H_T (kJ/mol)	H_D (kJ/mol)	H_{N^4} (kJ/mol)	H_{M^3} (kJ/mol)	H_{P^3} (kJ/mol)	y	R^2
0	**8.8**	**1.8**	**29.9**	**28.9**	**31.9**	**0.40**	**0.980**

Table 3. Relative association enthalpies (Hi), where i corresponds to a given boron configuration (see Figure 10), and coefficient of determination (R^2) value for the fitting of the current statistical mechanics-based model to experimental structure data.[76]*. y is a constant determining the ratio between M^3 and N^4 boron species. Table taken from Article II.*

The superstructures predicted in Figure 14 may be converted into their SRO scale counterparts. The focus of this thesis is the composition-structure relation in oxide glasses but in the following, the obtained structures are used in the structure-property relation TCT model as an example.

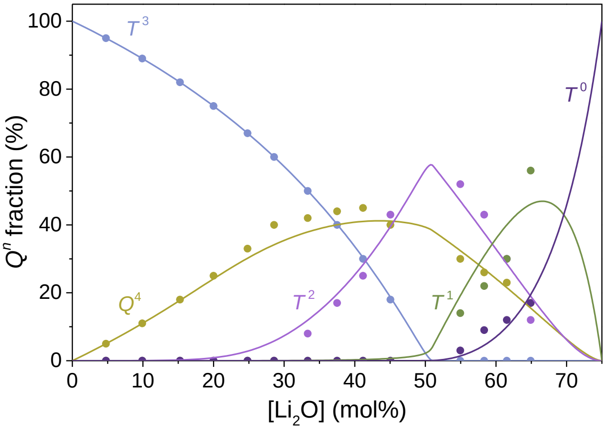

Figure 15. Fraction of SRO structural units as a function of composition in lithium borate glasses. The solid lines represent the prediction using the present statistical mechanical model and the closed symbols represent experimental data from Feller[76]*. Figure taken from Article II.*

Following TCT, the average number of constraints per atom (*n*) can be calculated by averaging over the different network forming species *i* and types of constraints *α*,[51]

$$n(T,x) = \sum_i N_i(x) \sum_\alpha l_{i,\alpha} q_\alpha(T), \qquad (30)$$

where $l_{i,\alpha}$ is the number of α-constraints associated with species *i*, $N_i(x)$ is the mole fraction of species *i* in composition *x*, and $q_\alpha(T)$ accounts for the temperature dependence of constraints *α*.

Based on the work of Smedskjaer *et al.*,[12] the following is used to count the number of constraints for each fraction of structural unit as shown in Figure 15:

- α: B-O and Li^{NB}-O linear constraints. Two α constraints for each oxygen.
- β: O-B-O angular constraints. Five β constraints per Q^4 to form a rigid BO$_4$ tetrahedron and three β constraints per T^3 to keep the BO$_3$ unit planer
- γ: B-O-B angular constraints. One γ constraint per oxygen.
- μ: Additional modifier rigidity due to clustering effects. Two μ constraints per NBO-forming Li atom.

Here, Li^{NB}-O is the fraction of lithium modifiers bonded to non-bridging oxygen..

With the constraint counting rules listed above, Eq. 30 may be applied for the lithium borate glass system to count the average number of constraints:

$$n(x) = 2N(BO) + 5N(Q^4) + 3N(T^3) + 2N(T^2) + 4N(T^1) + 6N(T^0). \tag{31}$$

Here, the fraction of NBO-forming Li atoms that contribute μ constraints is calculated from the fractions of T^2, T^1 and T^0 structural groups.

Following TCT, the composition dependence of T_g is considered to be due to the variation of the configurational entropy S_c.[11] As such, T_g of composition x, where x is the lithium modifier concentration in the present case, may be computed relative to that of some reference composition x_R. The configurational entropy is then largely proportional to the atomic degrees of freedom f:

$$\frac{T_g(x)}{T_g(x_R)} = \frac{S_c[T_g(x_R),x_R]}{S_c[T_g(x),x]} = \frac{f[T_g(x_R),x_R]}{f[T_g(x),x]} = \frac{d-n[T_g(x_R),x_R]}{d-n[T_g(x),x]}, \tag{32}$$

where d=3 is the dimensionality of a three-dimensional glass. With this, T_g may be predicted at any glass composition by knowing T_g and f of a reference glass and f of the glass in question:

$$T_g(x) = \min\left[T_\beta, \frac{3-n(x_R)}{3-n(x)} T_g(x_R)\right], \tag{33}$$

where T_β is the temperature where the β constraint becomes floppy. The resulting T_g prediction is shown in Figure 16.

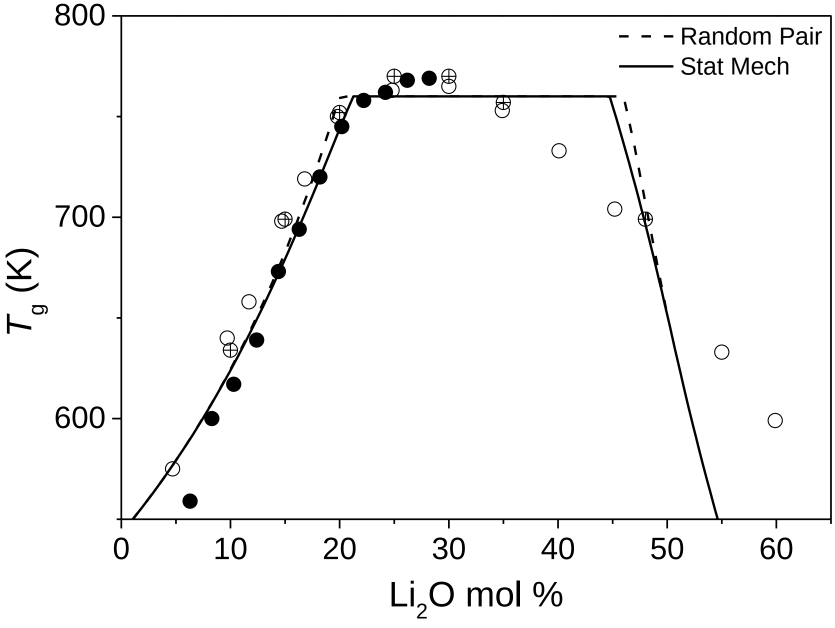

Figure 16. Glass transition temperature (T_g) as a function of fraction of modifier content in the Li_2O*-*B_2O_3 *glasses. The crossed, closed and open symbols represent experimentally data from Chryssikos,*[83] *Kodama*[81] *and Shelby*[84]*, respectively. Both model predictions are based on the TCT structure-property model from Smedskjaer et al.,*[12] *with the dashed and solid lines representing the predictions using the random pair model by Gupta*[85] *and the present statistical mechanical composition-structure model, respectively. Figure taken from Article II.*

TCT combined with statistical mechanics may be used to capture T_g of the Li_2O-B_2O_3 glass system very accurately.

CHAPTER 3. STATISTICAL MECHANICAL MODELING OF TERNARY OXIDE GLASSES

In Chapter 2, the statistical mechanics-based model proposed in Section 1.1.2 was applied to a number of binary oxide glasses to predict the SRO scale structures at any binary composition. With this exercise, we obtained relative enthalpies of interactions specific for each modifier ion and each SRO scale structural unit. In all of the cases in Chapter 2, some experimentally obtained structural data was required to make the predictions and establish the *H* parameters. In this chapter, we will use the parameters established in Chapter 2 to predict structural evolution of multicomponent glasses without using any experimentally obtained structures, except for comparison. That is, assuming the energy of association between modifier and a Q^n unit is the same in binary- and ternary glasses. With this method, the number of glassy systems we are able to predict increases exponentially as we establish enthalpy values in binary glasses linearly.

3.1. BOROSILICATE GLASSES

The borosilicate glass system is one of the most investigated mixed network former oxide glass system due to the large range of industrial applications such as high chemical durable nuclear waste encasement and thermal resistant Pyrex glass.[6,27] The SRO scale structures existing in the borosilicate glasses are summarized when combining Figure 10 and Figure 15 in Sections 2.2 and 2.3, respectively. To predict the compositional depending SRO scale structures in ternary borosilicate glasses, the driving force for the modifier to interact with a given structural unit is assumed to be the same as in the binary glasses but the competitional factor is different since more different units compete for the interaction. That is, the denominator of Eq. 9 is different but the numerator is the same.

With this, the enthalpy values reported in Section 2.2 and 2.3 are summarized in Table 4. First, the Na_2O-SiO_2 and Na_2O-B_2O_3 parameters were used to predict the structures of the Na_2O-B_2O_3-SiO_2 glass system in article III. Since all parameters are relative to their binary systems, the probability for a modifier to interact with boron or silicon in the mixed network former glass must first be established as a Si/B weighting factor.[69]

Glass system	**Na_2O-SiO_2**	**K_2O-SiO_2**	**Na_2O-B_2O_3**	**K_2O-B_2O_3**
H_4 (kJ/mol)	0	0	0	0
H_3-H_4 (kJ/mol)	14.1	18.8	8.4	6.0
H_2-H_4 (kJ/mol)	22.9	35.2	7.4	21.4
H_1-H_4 (kJ/mol)	27.1	32.8	28.5	28.3
α_{B^4/B^2}	-	-	35.5	35.4

Table 4. Relative association enthalpies (H_i), where i corresponds to a given structural configuration. The following structural configurations are considered: Q^4, Q^3, Q^2, and Q^1 for i = 1, 2, 3, and 4, respectively, in the silicate system and T^3, Q^4, T^2 and T^1 for i = 1, 2, 3, and 4, respectively, in the borate system. α_{B^4/B^2} is the average critical modifier concentration, where Eq. (35) starts occurring instead of Eq. (34). Table taken from Article III.

The enthalpy values for the binary borate glasses in Table 4 differ from Section 2.3 since these are based on SRO scale structural units. To establish these parameters, the following interactions were applied:

$$2B^3 + M_2O \rightarrow 2B^4, \qquad (34)$$

$$2B^3 + M_2O \rightarrow 2B^2. \qquad (35)$$

Eqs. 34 and 35 account for the boron anomaly. The α_{B^4/B^2} parameter was introduced in article III, assuming a critical modifier concentration where reaction Eq. 34 stops occurring in place of reaction Eq. 35. In reality these reactions occur somewhat simultaneously but this assumption allow for accurate prediction with only one additional parameter.

$$2B^4 + M_2O \rightarrow 2B^2 + M_2O. \qquad (36)$$

The B^4 units will start converting to B^2 units at high modifier concentrations. To account for this conversion, Eq. 36 is assumed to be a reaction with a corresponding enthalpy parameter.

$$2B^2 + M_2O \rightarrow 2B^1, \qquad (37)$$

$$2B^1 + M_2O \rightarrow 2B^0. \qquad (38)$$

With all the interactions established and the parameters obtained, using experimental data from literature, the structures of borosilicate glasses were predicted using the statistical mechanics-based approach (Appendix A) and compared to experimentally obtained glass structures.[30,86]

Since the ternary glasses are three-component systems, two-dimensional comparison between model prediction and experimental values are shown. For additional compositional prediction presentation, please refer to Article III. The model does not predict the structural evolution in the Na_2O-B_2O_3-SiO_2 glass system very well when using experimental data obtained by NMR (Figure 17). Deconvoluting NMR results in this system can be very difficult and the experimental data has a high uncertainty as well as higher uncertainties in glass chemistry.[13] Another method of quantifying the SRO scale structural units in this glass system is by MD simulations.[87] Since the enthalpy values obtained by the statistical mechanics-based model applies to MD simulated glasses as well, these may serve as a more accurate reference point since the uncertainties are small.

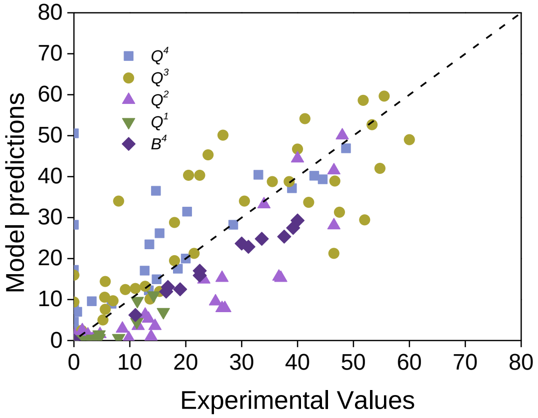

Figure 17. Data obtained by ^{29}Si and ^{11}B MAS NMR [30,86] for sodium borosilicate glasses, compared to model predictions. The dashed line shows a one-to-one correlation. Figure taken from Article III

When comparing to MD simulated glasses in article III, the statistical mechanics-based model predict the structural evolution very well (Figure 18) with the Si/B weighting as the only free parameter ($w_{Si,B}$=0.16).[88]

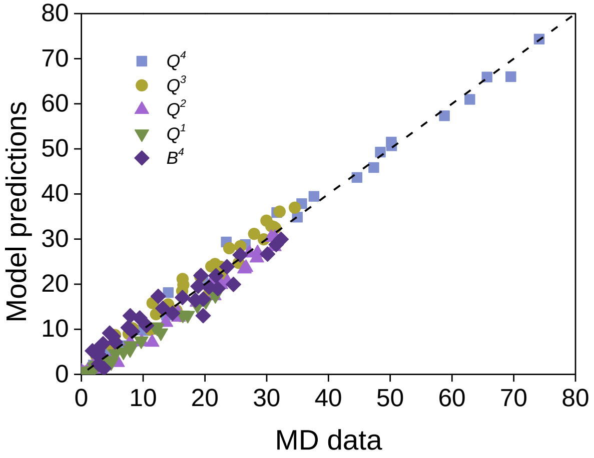

Figure 18. Structural data obtained by MD simulations[88] *for sodium borosilicate glasses compared to model predictions. The dashed line shows a one-to-one correlation. Figure taken from Article III.*

With the $w_{Si,B}$ established the statistical mechanics-based model may be applied to any borosilicate glass with zero free parameters. K_2O-SiO_2- and K_2O-B_2O_3 parameters were established using structural data from literature.[68,78] With these parameters, the structural evolution in the K_2O-B_2O_3-SiO_2 glass system was predicted. To validate the predictions of the current model, MD simulations of the same glass system were made, using already established pair distribution potentials.[88] The MD simulation procedure is explained in detail in Article III.

The model predictions replicate the MD simulations very well with no fitting parameters as seen in Figure 19. This example is the first prediction of SRO scale structures in a multicomponent glass, using only parameters obtained in binary glasses. If the method is universal and not limited to the borosilicate system only, the statistical mechanics-based model may become a useful tool in the future of glass science.

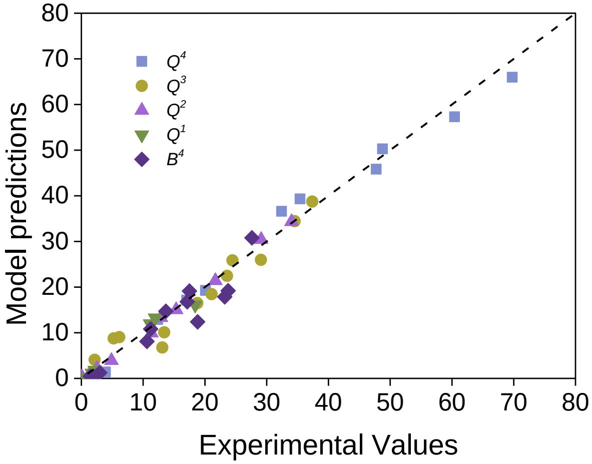

Figure 19. Structural data obtained by MD simulations in the potassium borosilicate system compared to model predictions with zero free parameters. The dashed line shows a one-to-one correlation. Figure taken from Article III

CHAPTER 4. GENERAL DISCUSSION AND PERSPECTIVE

As this thesis is a midway report of my PhD project, this Chapter will mainly focus on the plans for the work to be done. Objectives I and II of the Ph.D. in Section 1.3 have both been mostly fulfilled while all objectives for the master's thesis have been fulfilled. The model may be applied to any combination of network formers and modifiers but the mixed modifier effect is still not verified or compared to experimentally obtained data. The model has been coupled to TCT already but on a very minor scale and not in any multicomponent glasses. This aspect will be further investigated.

4.1. THE PRESENT MODEL

In Chapter 2, the present model was established in binary oxide glasses and provided a more accurate description of experimentally obtained data than some of the commonly used models such as the chemical order model[37] and the Dell-Bray model[76]. The downside of using the statistical mechanics-based model on binary oxide glasses is the requirement of some experimentally obtained data to fit the model against. For each binary glass system, the model must be fitted against data to obtain the enthalpy parameters, however, no more than 2-3 glasses in each system are required to obtain valid predictions. In ternary borosilicate glasses, the model captures the structural evolution of four-fold coordinated boron equally well as the Bray model[89]. Additionally, the model offers prediction of silicate species and considers the effect of changing modifiers without using any experimental data to fit the model, making it superior to any other composition-structure model for ternary oxide glasses, to my knowledge. The downside of using the model in binary or multicomponent glasses is the prior work of establishing enthalpy parameters in binary glasses, but once this part is completed, the model may be applied to a large range of glass systems. The model should be applicable to all combinations of network formers and modifiers, where the enthalpy values are established but has so far only been verified in the ternary alkali borosilicate glasses. Additionally, the thermal history dependence of the model is not well covered. With a structure to T_g model such as TCT, both thermal history and structural units may be predicted simultaneously by first assuming a constant T_g to obtain initial structures, which in turn are used to calculate more accurate T_g values, which would be used to make new structural predictions and so on. This loop would have to go on until neither T_g or structures would change from iteration to iteration. Without a structure to T_g model, one could assume a single, either constant or modifier dependent T_g value/distribution to use for all glasses and hence see the compositional effect on the structural distribution only. This would make the model less precise but still useful.

4.2. FUTURE WORK

To achieve a universal composition-structure model, some structural features still need to be explored. First, the mixed modifier effect will be established and compared to experimental data in the Na_2O-K_2O-SiO_2 glass system. Here, the role of the mixed modifier effect on the fictive temperature will be explored as well. Secondly, some structural units are observed in mixed former glasses which may not be observed in their binary counterparts, such as 5- and 6-fold coordinated silicon in phosphosilicate glasses. These additional structures must be captured by the model.

As the different glass systems and features become established, predicting and describing structural evolutions become more and more challenging. To tackle this challenge, a large portion of the proceeding work will be on software development to produce a single software capable of implementing the statistical mechanics-based model in all the established systems and any combination of their component elements.

Finally, with the composition-structure software developed, the structures predicted using the statistical mechanics-based model will be paired with already established TCT and/or ML models to couple the predicted structures to physical properties. With this, a new software may be developed to optimize glass compositions for desired physical properties by first using the statistical mechanics-based composition-structure model.

4.2.1. SOFTWARE DESIGN

The software development will be done in the object-oriented programming language python. Here, the different network former systems can be combined into one package.

The general structure of the “Stat_Mech_Glass” package is shortly summarized in Figure 20. Here, the blue squares are module files within the package and the green squares are the essential functions in each module. The package would obviously have way more than two modules but Figure 20 should simply illustrate how the modules become increasingly complicated as the number of components of the glass system increases. Following, the inputs and outputs of each function in the SiO2 module will be discussed.

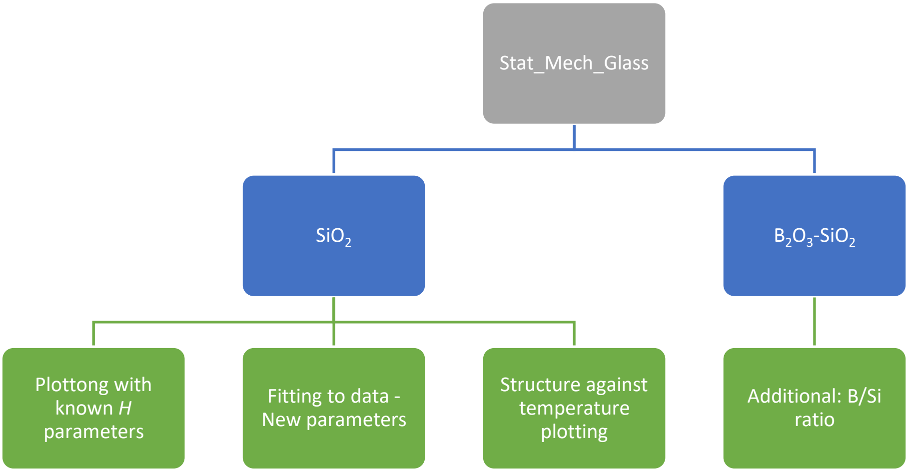

Figure 20. Flow diagram of the "Stat_Mech_Glass" Python package, where the blue boxes are examples of modules and the green boxes are examples of essential functions within each module.

The desired output of the plotting function will be a Q^n distribution as a function of modifier content. Since the solution is not analytical, the user will have the option to get the modifier content and the corresponding structural fractions as a CSV file output. To achieve these outputs, the input for the model has to be the number and types of modifiers (or their corresponding enthalpies), the fraction of each modifier, the fictive temperature of the glass system, and whether the user wants to save the outcome.

The second function will be fitting the model to experimentally obtained data of a binary silicate glass system to get the interaction enthalpies. This will use a second function since the fitting procedure will loop the function over and over so this function must be as simple as possible for short computational lengths. That is, many of the elements of the plotting function should be run outside this function since they do not change with the enthalpies (such as modifier concentration and T_f calculations). The input to this model will be the structural data, the number of iterations and what types of output data the user wants. Output options will include enthalpies, error for each iteration and the resulting prediction as image and data file.

The structure plotted as a function of fictive temperature-function takes the same inputs as the plotting function as well as a single composition. This composition is where the structural dependence on fictive temperature is calculated. This function does not need a T_f for the composition though.

With the structure software above developed, a TCT software may be developed. This software would automatically run the composition-structure models and use the structures to predict physical properties of the glasses. This would enable composition-property plotting. Since the TCT models are still being developed and are specific for each glass system, this software should be tailored specifically for each system.

4.2.2. OUTCOME

Since the statistical-mechanics based model still needs to be verified in mixed modifier glasses and should be expanded to more mixed former glasses, these studies will be published in pier reviewed journals. Each publication should add additional complexity and benefits of using statistical mechanics to predict glass structures. With the model established in the most common glass-forming systems, the focus on the PhD thesis will become software development. A complete composition-structure software will be developed and published for the community to use, including an elaborate user guide. Finally, the usefulness of the published model will be explored by linking it to TCT models. This will also be published in pier reviewed journals but the software will not necessarily be published as it will be tailored for specific applications.

CHAPTER 5. CONCLUSIONS

The focus of this thesis has been the composition-structure relation in oxide glasses. All studies were based on a statistical mechanics-based model proposed by John Mauro in 2013. The statistical mechanics-based model considers the enthalpic and entropic contributions to bond preferences in glass melts to calculate the probabilities of network former to network modifier interactions. From probabilities, the population of structural units may be calculated as a function of composition.

The model was first applied to binary phosphate glasses due to their relatively simple and well documented structures. The composition-structure relation in five different was successfully predicted with only 1-2 glasses as reference in each system. The statistical mechanics-based model captures both the stepwise conversion of structural units as the Chemical Order model and the disproportionation as described by the Brow model. Finally, the model was used to predict the structure of two different binary phosphate glasses as a function of T_f.

In the borate glass system, the composition-structure relation is different from phosphate glasses due to the “boron anomaly”. By using ^{10}B NMR results from literature, the statistical mechanics-based model was modified to predict the composition-structure relation for intermediate range order superstructural units. The results from the model was then used in combination with TCT to predict T_g values as a function of composition, demonstrating how the two model may be combined to make accurate composition-property predictions.

The model was applied to binary silicate glasses with similar structures to the phosphate glasses. Here, the model was used to predict the composition-structure relation in MD simulated Na_2O-SiO_2 glasses. This relation was successfully predicted with the same enthalpy parameters as found by applying the model to ^{29}Si MAS NMR data of Na_2O-SiO_2 glasses and only one free parameter concerning the T_f difference between melt-quenched and MD simulated glasses.

After establishing the statistical mechanics-based model in the binary oxide glasses, it was used to predict the composition-structure relation in ternary Na_2O-B_2O_3-SiO_2 and K_2O-B_2O_3-SiO_2 glass systems with only 1 and 0 free parameters, respectively. This was accomplished by assuming the same enthalpic driving force for a modifier ion to interact with a structural unit in binary- and ternary glass systems.

The model may be modified to predict composition-structure relation in many glass systems since the enthalpy parameters established in binary oxide glasses can be transferring to multicomponent glasses. The model has great potential to be coupled with already established TCT model to tailor glass compositions with specific physical properties.

Finally, the present model provides quick and accurate predictions of a number of glass systems with the parameters already established. Because of the complexity of setting the model up, an easy to use software could be of value to other glass scientists. In such a software, the user should only need to input the glass composition he/she is interested in and have the software calculate the exact distribution of structural units.

LITERATURE LIST

(1) Rasmussen, S. C. *How Glass Changed the World*; SpringerBriefts, 2012; Vol. 3.

(2) Mauro, J. C. Grand Challenges in Glass Science. *Front. Mater.* **2014**, *1*, 1–5.

(3) Day, D. E. Mixed Alkali Glasses - Their Properties and Uses. *J. Non. Cryst. Solids* **1976**, *21* (3), 343–372.

(4) Day, D. E.; Tomsia, A. P.; Jung, S. B.; Sonny Bal, B.; Fu, Q.; Rahaman, M. N.; Bonewald, L. F. Bioactive Glass in Tissue Engineering. *Acta Biomater.* **2011**, *7* (6), 2355–2373.

(5) Hewak, D. *Properties, Processing and Applications of Glass and Rare Earth-Doped Glasses for Optical Fibres*, 1st ed.; Michigan, 1998.

(6) Plodinec, M. J. Borosilicate Glasses for Nuclear Waste Imobilisation. *Glas. Technol.* **2000**, *41* (6), 186–192.

(7) Bengisu, M. Borate Glasses for Scientific and Industrial Applications: A Review. *J. Mater. Sci.* **2016**, *51* (5), 2199–2242.

(8) Mauro, J. C.; Tandia, A.; Vargheese, K. D.; Mauro, Y. Z.; Smedskjaer, M. M. Accelerating the Design of Functional Glasses through Modeling. *Chem. Mater.* **2016**, *28* (12), 4267–4277.

(9) Lyon, K. C. Prediction of the Viscosities of “Soda-Lime” Silica Glasses. *J. Res. Natl. Bur. Stand. Sect. A Phys. Chem.* **1974**, *78A* (4), 497.

(10) Mauro, J. C. Topological Constraint Theory of Glass. *Am. Ceram. Soc. Bull.* **2011**, *90* (4), 31–37.

(11) Micoulaut, M. Concepts and Applications of Rigidity in Non-Crystalline Solids: A Review on New Developments and Directions. *Adv. Phys. X* **2016**, *6149* (April), 1–29.

(12) Smedskjaer, M. M.; Mauro, J. C.; Sen, S.; Yue, Y. Quantitative Design of Glassy Materials Using Temperature-Dependent Constraint Theory. *Chem. Mater.* **2010**, *22* (18), 5358–5365.

(13) Youngman, R. NMR Spectroscopy in Glass Science: A Review of the Elements. *Materials (Basel).* **2018**, *11* (4).

(14) Edén, M. NMR Studies of Oxide-Based Glasses. *Annu. Reports Sect. “C” Phys. Chem.* **2012**, *108*, 177.

(15) Tomozawa, M.; Hong, J. W.; Ryu, S. R. Infrared (IR) Investigation of the Structural Changes of Silica Glasses with Fictive Temperature. *J. Non. Cryst. Solids* **2005**, *351* (12–13), 1054–1060.

(16) Mauro, J. C.; Smedskjaer, M. M. Statistical Mechanics of Glass. *J. Non. Cryst. Solids* **2014**, *396–397*, 41–53.

(17) Mauro, J. C. Statistics of Modifier Distributions in Mixed Network Glasses. *J. Chem. Phys.* **2013**, *138* (12).

(18) Wright, A. C.; Shakhmatkin, B. A.; Vedishcheva, N. M. The Chemical Structure of Oxide Glasses: A Concept Consistent with Neutron Scattering Studies? *Glas. Phys. Chem.* **2001**, *27* (2), 97–113.

(19) Mysen, B. O.; Richet, P. *Silicate Glasses and Melts Properties and Structure*; Elsevier, 2005.

(20) Ovcharenko, N. V; Smirnova, T. V. High Refractive Index and Magneto Optical Glasses in the Systems. *J. Non. Cryst. Solids* **2001**, *291*, 121–126.

(21) Day, D. E.; Wu, Z.; Ray, C. S.; Hrma, P. Chemically Durable Iron Phosphate Glass Wasteforms. *J. Non. Cryst. Solids* **1998**, *241* (1), 1–12.

(22) Januchta, K.; Youngman, R. E.; Goel, A.; Bauchy, M.; Logunov, S. L.; Rzoska, S. J.; Bockowski, M.; Jensen, L. R.; Smedskjaer, M. M. Discovery of Ultra-Crack-Resistant Oxide Glasses with Adaptive Networks. *Chem. Mater.* **2017**, *29* (14), 5865–5876.

(23) Mauro, J. C.; Tandia, A.; Vargheese, K. D.; Mauro, Y. Z.; Smedskjaer, M. M. Accelerating the Design of Functional Glasses through Modeling. *Chem. Mater.* **2016**, *28* (12), 4267–4277.

(24) Shelby, J. E. *Introduction to Glass Science and Technology*, Second Edi.; The Royal Society of Chemistry, 2005.

(25) Yue, Y.; Von der Ohe, R.; Jensen, S. L. Fictive Temperature, Cooling Rate, and Viscosity of Glasses. *J. Chem. Phys.* **2004**, *120* (17), 8053–8059.

(26) Naumis, G. G. Glass Transition Phenomenology and Flexibility: An Approach Using the Energy Landscape Formalism. *J. Non. Cryst. Solids* **2006**, *352* (42-49 SPEC. ISS.), 4865–4870.

(27) Lima, M. M.; Monteiro, R. Characterisation and Thermal Behaviour of a Borosilicate Glass. *Thermochim. Acta* **2001**, *373* (1–2), 69–74.

(28) Brow, R. K. Review: The Structure of Simple Phosphate Glasses. *J. Non. Cryst. Solids* **2000**, *263*, 1–28.

(29) Eckert, H. Spying with Spins on Messy Materials: 60 Years of Glass Structure Elucidation by NMR Spectroscopy. *Int. J. Appl. Glas. Sci.* **2018**, *9* (2), 167–187.

(30) Bhasin, G.; Bhatnagar, A.; Bhowmik, S.; Stehle, C.; Affatigato, M.; Feller, S.; MacKenzie, J.; Martin, S. Short Range Order in Sodium Borosilicate Glasses Obtained via Deconvolution Of29Si MAS NMR Spectra. *Phys. Chem. Glas.* **1998**, *39* (5), 269–274.

(31) Schneider, J.; Mastelaro, V. R.; Zanotto, E. D.; Shakhmatkin, B. A.; Vedishcheva, N. M.; Wright, A. C.; Panepucci, H. Qn Distribution in Stoichiometric Silicate Glasses: Thermodynamic Calculations and 29Si High Resolution NMR Measurements. *J. Non. Cryst. Solids* **2003**, *325* (1–3), 164–178.

(32) Fluegel, A.; Varshneya, A. K.; Seward, T. P.; Earl, D. A.; Street, P. Viscosity of Commercial Glasses in the Softening Range. *Am. Ceram. Soc.* **2003**, *141*, 379–386.

(33) Kucuk, a.; Clare, a. G.; Jones, L. An Estimation of the Surface Tension for Silicate Glass Melts at 1400°C Using Statistical Analysis. *Glas. Technol. - Eur. J. Glas. Sci. Technol. Part A* **1999**, *40* (5), 5.

(34) Priven, A. I. General Method for Calculating the Properties of Oxide Glasses and Glass Forming Melts from Their Composition and Temperature. *Glas. Technol.* **2004**, *45* (6), 244–254.

(35) Ghiorso, M. S.; Kress, V. C. AN EQUATION OF STATE FOR SILICATE MELTS . II . CALIBRATION OF VOLUMETRIC PROPERTIES AT 10 5 Pa. *Am. J. Sci.* **2004**, *304* (8–9), 679–751.

(36) Liang, J.-J.; Cygan, R. .; Alam, T. . Molecular Dynamics Simulation of the Structure and Properties of Lithium Phosphate Glasses. *J. Non. Cryst. Solids* **2000**, *263–264*, 167–179.

(37) Vedishcheva, N. M.; Shakhmatkin, B. A.; Wright, A. C. Thermodynamic Modelling of the Structure of Glasses and Melts: Single-Component, Binary and Ternary Systems. *J. Non. Cryst. Solids* **2001**, *293–295* (1), 312–317.

(38) Goyal, S.; Mauro, J. C. Statistical Mechanical Model of Bonding in Mixed Modifier Glasses. *J. Am. Ceram. Soc.* **2018**, *101* (5), 1906–1915.

(39) Cormack, a. N.; Cao, Y. Molecular Dynamics Simulation of Silicate Glasses.

Mol. Eng. **1996**, *6* (1–2), 183–227.

(40) Ispas, S.; Charpentier, T.; Mauri, F.; Neuville, D. R. Structural Properties of Lithium and Sodium Tetrasilicate Glasses: Molecular Dynamics Simulations versus NMR Experimental and First-Principles Data. *Solid State Sci.* **2010**, *12* (2), 183–192.

(41) Micoulaut, M. Concepts and Applications of Rigidity in Non-Crystalline Solids: A Review on New Developments and Directions. *Adv. Phys. X* **2016**, *6149* (April), 1–29.

(42) Abragram, A. *High-Resolution Nuclear Magnetic Resonance*; McGraw-Hill Book Company: H.J.Bernstein, 1959.

(43) Raguenet, B.; Tricot, G.; Silly, G.; Ribes, M.; Pradel, A. Revisiting the 'Mixed Glass Former Effect' in Ultra-Fast Quenched Borophosphate Glasses by Advanced 1D/2D Solid State NMR. *J. Mater. Chem.* **2011**, *21* (44), 17693.

(44) Yadav, A. K.; Singh, P. A Review of the Structures of Oxide Glasses by Raman Spectroscopy. *RSC Adv.* **2015**, *5* (83), 67583–67609.

(45) Osipov, A.; Osipova, L.; Zainullina, R. Raman Spectroscopy and Statistical Analysis of the Silicate Species and Group Connectivity in Cesium Silicate Glass Forming System. *Int. J. Spectrosc.* **2015**, *2015* (February), 1–15.

(46) Wallenius, K. T. Biased Sampling; the Noncentral Hypergeometric Probability Distribution. *Tech. Report, Off. Nav. Res.* **1963**, No. 70.

(47) Fog, A. Sampling Methods for Wallenius' and Fisher's Noncentral Hypergeometric Distributions. *Commun. Stat. Simul. Comput.* **2008**, *37* (2), 241–257.

(48) Schwabl, F. *Statistical Mechanics*, Second.; Springer US: Garching, Germany, 2006.

(49) Phillips, J. C. Topology of Covalent Non-Crystalline Solids: Short-Range Order in Chalogenide Alloys. *J. Non. Cryst. Solids* **1995**, *215* (2–3), 213–216.

(50) Phillips, J. C.; Thorpe, M. F. Constraint Theory, Vector Percolation and Glass Formation. *Solid State Commun.* **1985**, *53* (8), 699–702.

(51) Mauro, J. C.; Gupta, P. K.; Loucks, R. J. Composition Dependence of Glass Transition Temperature and Fragility. II. A Topological Model of Alkali Borate Liquids. *J. Chem. Phys.* **2009**, *234503* (130).

(52) Smedskjaer, M. M.; Mauro, J. C.; Youngman, R. E.; Hogue, C. L.; Potuzak, M.; Yue, Y. Topological Principles of Borosilicate Glass Chemistry. *J. Phys.*

Chem. B **2011**, *115* (44), 12930–12946.

(53) Kirchner, K. A.; Kim, S. H.; Mauro, J. C. Statistical Mechanics of Topological Fluctuations in Glass-Forming Liquids. *Phys. A Stat. Mech. its Appl.* **2018**, *510*, 787–801.

(54) Smedskjaer, M. M.; Hermansen, C.; Youngman, R. E. Topological Engineering of Glasses Using Temperature-Dependent Constraints. *MRS Bull.* **2017**, *42* (1), 29–33.

(55) Das, S. S.; Singh, N. P.; Srivastava, P. K. Ion Conducting Phosphate Glassy Materials. *Prog. Cryst. Growth Charact. Mater.* **2009**, *55* (3–4), 47–62.

(56) Pickup, D. M.; Newport, R. J.; Knowles, J. C. Sol-Gel Phosphate-Based Glass for Drug Delivery Applications. *J. Biomater. Appl.* **2012**, *26* (5), 613–622.

(57) Wilkinson, C. J.; Zheng, Q.; Huang, L.; Mauro, J. C. Topological Constraint Model for the Elasticity of Glass-Forming Systems. *J. Non-Crystalline Solids X* **2019**, *2* (March).

(58) Click, C. A.; Brow, R. K.; Alam, T. M. Properties and Structure of Cesium Phosphate Glasses. *J. Non. Cryst. Solids* **2002**, *311* (3), 294–303.

(59) Brow, R. K.; Kirkpatrick, R. J.; Turner, G. L. The Short Range Structure of Sodium Phosphate Glasses I. MAS NMR Studies. *J. Non. Cryst. Solids* **1990**, *116* (1), 39–45.

(60) Alam, T. M.; Brow, R. K. Local Structure and Connectivity in Lithium Phosphate Glasses: A Solid-State 31P MAS NMR and 2D Exchange Investigation. *J. Non. Cryst. Solids* **1998**, *223*, 1–20.

(61) Bødker, M. S.; Mauro, J. C.; Goyal, S.; Youngman, R. E.; Smedskjaer, M. M. Predicting Q-Speciation in Binary Phosphate Glasses Using Statistical Mechanics. *J. Phys. Chem. B* **2018**, *122*, 7609–7615.

(62) Van Wüllen, L.; Eckert, H.; Schwering, G. Structure-Property Correlations in Lithium Phosphate Glasses: New Insights from 31P Mutually Implies 7Li Double-Resonance NMR. *Chem. Mater.* **2000**, *12* (7), 1840–1846.

(63) Fayon, F.; Massiot, D.; Suzuya, K.; Price, D. L. 31P NMR Study of Magnesium Phosphate Glasses. *J. Non. Cryst. Solids* **2001**, *283* (1–3), 88–94.

(64) Walter, G.; Vogel, J.; Hoppe, U.; Hartmann, P. Structural Study of

Magnesium Polyphosphate Glasses. *J. Non. Cryst. Solids* **2003**, *320* (1–3), 210–222.

(65) Rajbhandari, P.; Chen, Y.; Doumert, B.; Montagne, L.; Tricot, G. Investigation of Zinc Alkali Pyrophosphate Glasses. Part II: Local and Medium Range Orders Analysed by 1D/2D NMR. *Mater. Chem. Phys.* **2015**, *155*, 23–29.

(66) Meyer, K. Characterization of the Structure of Binary Zinc Ultraphosphate Glasses by Infrared and Raman Spectroscopy. *J. Non. Cryst. Solids* **1997**, *209* (3), 227–239.

(67) Strojek, W.; Eckert, H. Medium-Range Order in Sodium Phosphate Glasses: A Quantitative Rotational Echo Double Resonance Solid State NMR Study. *Phys. Chem. Chem. Phys.* **2006**, *8* (19), 2276.

(68) Maekawa, H.; Maekawa, T.; Kawamura, K.; Yokokawa, T. The Structural Groups of Alkali Silicate Glasses Determined from 29Si MAS-NMR. *J. Non. Cryst. Solids* **1991**, *127* (1), 53–64.

(69) Bødker, M. S.; Sørensen, S. S.; Mauro, J. C.; Smedskjaer, M. M. Predicting Composition-Structure Relations in Alkali Borosilicate Glasses Using Statistical Mechanics. *Front. Mater.* **2019**, *6* (July).

(70) MacDonald, W. M.; Anderson, A. C.; Schroeder, J. Low-Temperature Behavior of Potassium and Sodium Silicate Glasses. *Phys. Rev. B* **1985**, *31* (2), 1090–1101.

(71) Massobrio, C.; Du, J.; Bernasconi, M.; Salmon, P. S. *Molecular Dynamics Simulations of Disordered Materials*; Springer International Publishing: Cham, 2015; Vol. 215.

(72) Du, J.; Cormack, A. N. The Medium Range Structure of Sodium Silicate Glasses: A Molecular Dynamics Simulation. *J. Non. Cryst. Solids* **2004**, *349* (1–3), 66–79.

(73) Adkins, L.; Cormack, A. Large-Scale Simulations of Sodium Silicate Glasses. *J. Non. Cryst. Solids* **2011**, *357* (14), 2538–2541.

(74) Yiannopoulos, Y. D.; Chryssikos, G. D.; Kamitsos, E. I. Structure and Properties of Alkaline Earth Borate Glasses. *Phys. Chem. Glas.* **2001**, *42* (3), 164–172.

(75) Doweidar, H. Consideration of the Boron Oxide Anomaly. *J. Mater. Sci.* **1990**, *25* (1), 253–258.

(76) Feller, S. A.; Dell, W. J.; Bray, P. J. 10B NMR Studies of Lithium Borate

Glasses. *J. Non. Cryst. Solids* **1982**, *51* (1), 21–30.

(77) Faaborg, M.; Goranson, K.; Barnes, N.; Troendle, E.; Rice, R.; Chace, M.; Montgomery, L.; Koehler, A.; Lindeberg, Z.; Holland, D.; et al. A 10B NMR Study of Trigonal and Tetrahedral Borons in Ring Structured Borate Glasses and Crystals. *Phys. Chem. Glas. Eur. J. Glas. Sci. Technol. Part B* **2015**, *56* (5), 177–182.

(78) Youngman, R. E.; Zwanziger, J. W. Network Modification in Potassium Borate Glasses: Structural Studies with NMR and Raman Spectroscopies. *J. Phys. Chem.* **1996**, *100* (41), 16720–16728.

(79) Youngman, R. E.; Zwanziger, J. W. Multiple Boron Sites in Borate Glass Detected with Dynamic Angle Spinning Nuclear Magnetic Resonance. *J. Non. Cryst. Solids* **1994**, *168* (3), 293–297.

(80) Youngman, R. E.; Zwanziger, J. W. On the Formation of Tetracoordinate Boron in Rubidium Borate Glasses. *J. Am. Chem. Soc.* **1995**, *117* (4), 1397–1402.

(81) Kodama, M.; Kojima, S. Anharmonicity and Fragility in Lithium Borate Glasses. *J. Therm. Anal.* **2002**, *69*, 961–970.

(82) Bødker, M. S.; Mauro, J. C.; Youngman, R. E.; Smedskjaer, M. M. Statistical Mechanical Modeling of Borate Glass Structure and Topology: Prediction of Superstructural Units and Glass Transition Temperature. *J. Phys. Chem. B* **2019**, *123*, 1206–1213.

(83) Chryssikos, G. D.; Duffy, J. A.; Hutchinson, J. M.; Ingram, M. D.; Kamitsos, E. I.; Pappin, A. J. Lithoim Borate Glasses: A Quantitative Study of Strength and Fragility. *J. Non. Cryst. Solids* **1994**, *174*, 378–383.

(84) Shelby, J. E. Thermal Expansion of Alkali Borate Glasses. *J. Am. Ceram. Soc.* **1983**, *66* (3), 225–227.

(85) Gupta, P. K. Proceedings of the International Congress on Glass; Unpublished: New Delhi, India, 1986; p 1.

(86) Nanba, T.; Nishimura, M.; Miura, Y. A Theoretical Interpretation of the Chemical Shift of 29Si NMR Peaks in Alkali Borosilicate Glasses. *Geochim. Cosmochim. Acta* **2004**, *68* (24), 5103–5111.

(87) Wang, M.; Anoop Krishnan, N. M.; Wang, B.; Smedskjaer, M. M.; Mauro, J.

C.; Bauchy, M. A New Transferable Interatomic Potential for Molecular Dynamics Simulations of Borosilicate Glasses. *J. Non. Cryst. Solids* **2018**, *498* (December 2017), 294–304.

(88) Deng, L.; Du, J. Development of Boron Oxide Potentials for Computer Simulations of Multicomponent Oxide Glasses. *J. Am. Ceram. Soc.* **2018**, No. September, 1–24.

(89) Bray, P. J. Structural Models for Borate Glasses. *J. Non. Cryst. Solids* **1985**, *75* (1–3), 29–36.

LIST OF PUBLICATIONS

PAPER I

THE JOURNAL OF PHYSICAL CHEMISTRY B

Article

Cite This: J. Phys. Chem. B 2018, 122, 7609−7615

pubs.acs.org/JPCB

Predicting Q-Speciation in Binary Phosphate Glasses Using Statistical Mechanics

Mikkel S. Bødker,[†] John C. Mauro,[‡] Sushmit Goyal,[§] Randall E. Youngman,[§] and Morten M. Smedskjaer*,[†]

[†]Department of Chemistry and Bioscience, Aalborg University, 9220 Aalborg, Denmark

[‡]Department of Materials Science and Engineering, The Pennsylvania State University, University Park, Pennsylvania 16802, United States

[§]Science and Technology Division, Corning Incorporated, Corning, New York 14831, United States

ABSTRACT: Predicting the compositional evolution of the atomic-scale structure of oxide glasses is important for developing quantitative composition−property models. In binary phosphate glasses, the addition of network modifiers generally leads to depolymerization of the networks as described by the Q-speciation, where Q^n denotes PO_4 tetrahedra with n number (between 0 and 3) of bridging P−O−P linkages per tetrahedron. Upon the initial creation of nonbridging oxygens and thus partly depolymerized Q species, a variety of network former−modifier interactions exist. Here, on the basis of ^{31}P magic angle spinning nuclear magnetic resonance spectroscopy data from the literature, we present a statistical description of the compositional evolution of Q-speciation in these glasses by accounting for the relative enthalpic and entropic contributions to the bonding preferences. We show that the entire glass structure evolution can be predicted based on experimental structural information for only a few glass compositions in each series. The model also captures the differences in bonding preferences in glasses with different field strengths (charge-to-size ratio) of the modifier cations.

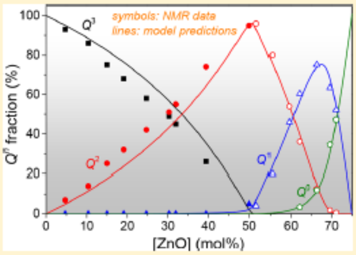

■ INTRODUCTION

Oxide glasses find numerous applications[1−4] because of their unique physical and chemical properties, which vary as a function of temperature, pressure, and chemical composition. The design of new glass compositions requires an accurate structural description but their noncrystalline nature and complex chemical compositions have hindered the construction of a universal structure model. Developing such a model would accelerate the discovery of new glasses by coupling the composition−structure model with existing structure−property models, such as topological constraint theory,[5] thus avoiding the inefficient trial-and-error-based approach.

Although glasses lack the periodicity and long-range order of crystals, they possess characteristic short-range order, which obeys basic crystal-chemical rules. The structural backbone of most oxide glasses consists of network formers such as Si, B, or P.[6] The basic building blocks are the three- or fourfold coordinated network formers, linked together through bridging oxygen (BO).[7] Additionally, network modifier oxides such as Na_2O and CaO are introduced into the glass structure to break the backbone by forming nonbridging oxygen (NBO) or stabilizing negatively charged tetrahedral network formers and hence altering the physical properties of the glass.[8] The structure of glasses is primarily determined from diffraction (scattering) and spectroscopic methods, such as Raman spectroscopy, nuclear magnetic resonance (NMR) spectroscopy, and neutron diffraction.[8] Ab initio and classical molecular dynamics (MD) and reverse Monte Carlo simulations are also used to study the atomic-scale structure of glasses. MD simulations use numerical calculations with interatomic potentials to predict the structure of the glass.[9] Today, detailed MD simulations are usually applied to systems containing many thousands of atoms on time scales of roughly nanoseconds. Despite the ongoing improvement in computational capacity, enough computing power to simulate bulk glasses on a realistic laboratory timescale will not be available in the foreseeable future.[10] On the other hand, because of the lack of stoichiometric requirements, a nearly infinite combination of compositions can lead to successful glass formation. Experimental structure characterization is thus a tedious task, prompting the need for a unified model of glass structure evolution with composition.

Various statistical approaches for structural predictions in oxide glasses have been attempted.[11−13] For example, Bernoulli statistics have been used to predict cluster formation probability in rare earth-doped aluminoborate glasses.[13] For alkali phosphate glasses, a binominal distribution has been applied to predict the fraction of modifiers present in either isolated or cross-linking sites.[12] Recently, Mauro[11] proposed a more general model for predicting the modifier distribution

Received: May 15, 2018
Revised: June 30, 2018
Published: July 11, 2018

DOI: 10.1021/acs.jpcb.8b04604
J. Phys. Chem. B 2018, 122, 7609−7615

and thus network former speciation in oxide glasses. The model is based on a statistical mechanical noncentral multivariate hypergeometric function with Boltzmann weighting factors. The approach can be viewed as analogous to drawing marbles from an urn, with each network former being a marble and the size of the marble depending on the Boltzmann weighting factor. Each network modifier in the glass structure "draws" a marble, where the probability for drawing each marble depends on the number distribution of marbles and their size, that is, the Boltzmann weighting factor. After each "draw", the number distribution of remaining marbles changes, that is, the probability to draw a given marble changes for each draw. However, this statistical mechanical model has not yet been experimentally verified. In this work, we attempt to do so by focusing on binary phosphate glasses, as these have served as model systems in understanding and developing structure−property relationships in complex, multicomponent phosphate glasses for applications such as nuclear waste hosts,[14] fast ion conductivity,[15] and drug delivery systems.[16] The network structure of various binary alkali, alkaline earth, and transition-metal phosphate glasses has therefore been studied extensively using a wide variety of spectroscopic and diffraction techniques.[17] ^{31}P NMR spectroscopy has been an especially powerful tool for studying the connectivity of PO_4 tetrahedra in the structural glass network.[18] Like silica, phosphate forms a tetrahedral cross-linked three-dimensional structure in its pure vitreous form.[17] Because P has one more valence electron than Si, it will share five pairs of electrons with oxygen, resulting in one doubly bonded terminal oxygen and three singly bonded BO per tetrahedron.

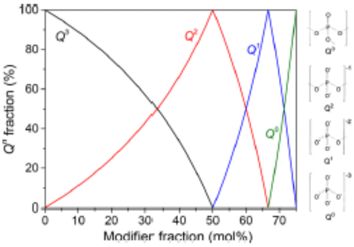

Figure 1. Composition dependence of the molar fraction of Q^n structural units as described by the general chemical order model (eqs 1−6) for a binary phosphate glass.

The connectivity of the phosphate network is described by its Q^n-speciation. The Q^n terminology corresponds to PO_4 tetrahedra, where n ranges from 0 to 3 and denotes the number of BO atoms, that is, P−O−P linkages, per tetrahedron. These linkages progressively break to form NBO upon addition of modifier oxides to P_2O_5. That is, Q^n species are converted to Q^{n-1} species and the network connectivity decreases, as shown schematically in Figure 1. In the case of strictly stepwise $Q^n \rightarrow Q^{n-1}$ conversion, the network would consist of only one or two types of Q-species, that is, a binary distribution. This so-called chemical order model is the most commonly used model for predicting the structure of phosphate glasses, especially alkali and alkaline earth phosphate glasses.[17] With the model, the structure of phosphate glasses is divided into three regions depending on the network modifier concentration (see Figure 1). From 0 to 50 mol % R_2O or RO modifier, the fractions of Q^2 and Q^3 are given by

$$f_{Q^2} = \frac{x}{1-x} \tag{1}$$

$$f_{Q^3} = \frac{1-2x}{1-x} \tag{2}$$

where x is the molar fraction of the modifier. In this range, the fraction of Q^2 approaches 1, whereas the fraction of Q^3 approaches 0 as the modifier content approaches 50 mol %. Accordingly, the chemical order model describes the structural evolution in polyphosphate glasses (50−66.7 mol % modifier) as

$$f_{Q^1} = \frac{2x-1}{1-x} \tag{3}$$

$$f_{Q^2} = \frac{2-3x}{1-x} \tag{4}$$

Finally, for glasses with 66.7−75 mol % modifier, only Q^0 and Q^1 phosphate groups are expected, according to the chemical order model:

$$f_{Q^0} = \frac{3x-2}{1-x} \tag{5}$$

$$f_{Q^1} = \frac{3-4x}{1-x} \tag{6}$$

The chemical order model has been shown to work well for binary alkali and alkaline earth phosphate glasses up to a modifier content of ∼60 mol %.[19−21] However, the work of Brow et al.[20] suggests a different structural evolution for binary zinc phosphate glasses containing up to 71 mol % ZnO. The other extreme structural model would be a purely entropy-dominated distribution of Q species that may result from a random modification of the network. However, the studies in the literature indicate that neither of these extremes in Q species distribution is exactly followed by zinc phosphate[20] and magnesium phosphate glasses.[21] In particular, the binary Q species distribution is more closely followed by phosphate glasses with low field strength (charge-to-size ratio) modifier cation (e.g., Na or K), whereas Q-speciation in glasses with high field strength modifier cation (e.g., Zn or Mg) corresponds more closely to a random distribution.

In this paper, we apply the general statistical mechanical approach proposed by Mauro[11] to model the structure of binary phosphate glasses. Specifically, we predict the Q^n distribution of the entire range of modifier content (covering ultra-, meta-, and pyrophosphates) in binary lithium, sodium, and cesium phosphate glasses based on structural input from only one reference glass. The statistical mechanical approach is also applied on the higher field strength magnesium and zinc phosphate glasses, in which glass formation is possible deeper into the pyrophosphate region. Because of their increased structural complexity, NMR data for two reference glasses are required to predict the structural evolution of these glasses.

■ MODEL

For simple binary phosphate glasses, we consider that the distribution of modifiers in the phosphate network and the resulting Q^n speciation may be described statistically, following a hypergeometric form.[22] Hypergeometric distributions are used in situations where there are N number of draws from a

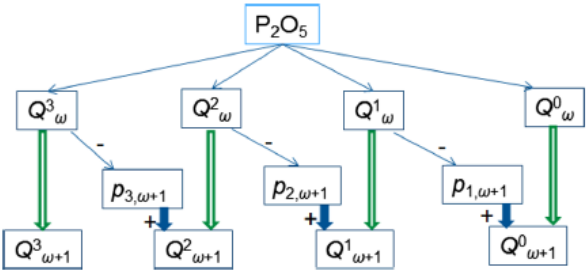

Figure 2. Structural modification of P_2O_5 glass upon modifier addition and thus formation of various Q^n species. The Q^n distribution is shown after ω and $\omega + 1$ modifier–former associations (draws) based on the corresponding probability factors $p_{i,\omega}$.

finite population of size G, without replacement after each draw. In the present system, N represents the number of modifier atoms and G represents the total number of network former sites available for association with a modifier,[11] that is, Q^3, Q^2, and Q^1 are treated as distinct structural sites available for modifier interaction. Each time a modifier "draws" a network former site, the site population changes and so does the probability of association for the next draw. The probability for the modifier to associate with each structural site is different because of various network former–modifier interactions; hence, a kind of noncentral hypergeometric distribution is required to describe the system.[23] Additionally, the distribution must be Boltzmann-weighted according to the thermal history of the glass, as quantified through the fictive temperature (T_f).[22]

The Wallenius[24] noncentral hypergeometric distribution allows for unequal weighting of different types of species in a population, which is needed to describe the glass structure. With this distribution, the probability of selecting a given species of type i at draw number ω is given by[11]

$$p_{i,\omega} = \frac{(g_i - n_{i,\omega-1})w_i}{\sum_{i=1}^{\Omega}\sum_{j=0}^{\omega-1}(g_i - n_{i,j})w_i} \tag{7}$$

where g_i is the degeneracy of species i, $n_{i,j}$ is the accumulated number of successful draws of species i after j number of attempts, Ω is the number of distinct species in the draw population, and w_i is the probability weighting factor for species i. As in the normal hypergeometric distribution, each modifier draw will change the remaining population of network former sites and another draw probability distribution exists for the next draw. With the Wallenius noncentral hypergeometric distribution, each network former site has a certain weighting factor and the site with the highest weighting factor will be depleted first. Because of this complication, there is no rigorous closed form solution for the p_i values, that is, $\langle p_i \rangle$. The most convenient way to surpass this problem is by numerically calculating values for $\langle p_i \rangle$ using recursive methods or through Markov chain Monte Carlo.[11] Here, we use the generalized reduced gradient nonlinear solving method. Each draw is set to be equal to a total of 1% Q^n species, that is, $p_1 + p_2 +, ..., p_i =$ 1%. Hence, the Q^n distribution may be plotted directly against R ($R = x/(100 - x)$, where x is the modifier content in mol %).

In the case of atoms modifying the network formers, the weighting factors w_i in eq 7 depend on the thermal history of the glass, as quantified by its T_f. To capture the nonequilibrium nature of glasses, we assume that the structure of the glass corresponds to the equilibrium structure of the liquid at T_f, which is typically obtained through rapid quenching of the liquid. The weighting factor is therefore

$$w_i = \exp\left(-\frac{H_i}{kT_f}\right) \tag{8}$$

where H_i is the free enthalpy barrier associated with a draw of species i and k is the Boltzmann's constant. With this definition, eq 7 may be rewritten specifically for glass systems as[25]

$$p_{i,\omega} = \frac{(g_i - n_{i,\omega-1})\exp\left(-\frac{H_i}{kT_f}\right)_i}{\sum_{i=1}^{\Omega}\sum_{j=0}^{\omega-1}(g_i - n_{i,j})\exp\left(-\frac{H_i}{kT_f}\right)} \tag{9}$$

Phosphate glass structural sites expressed with the Q^n notation may exist as Q^3, Q^2, Q^1, or Q^0. The Q^n distribution depends on the network modifier type and concentration in the glass. When applying the Wallenius noncentral hypergeometric distribution with Boltzmann's weighting factor on a phosphate glass system, three p_i values are obtained as illustrated in Figure 2. p_3 describes the probability of the modifier ion to associate with a Q^3 structural site, thus forming a new Q^2 structural group. Likewise, p_2 describes the probability for association with Q^2 and so on. By using Monte Carlo draw generating, the evolution of each Q^n species may be modeled to fit a set of obtained structural data with only w_3, w_2, and w_1 as the fitting parameters. When using this approach, the fraction of Q^n values for the phosphate glass system may be modeled according to their respective p_i values as

$$Q_\omega{}^3 = Q_{\omega-1}{}^3 - p_{3,\omega} \tag{10}$$

$$Q_\omega{}^2 = Q_{\omega-1}{}^2 - p_{2,\omega} + p_{3,\omega} \tag{11}$$

Here, $Q_\omega{}^n$ is the fraction of Q^n species after ω number of draws. The number of Q^2 structural units at a given number of draws equals the number of Q^2 structural units before the draw plus the number probability of the modifier ion to "draw" a Q^3 structural unit ($p_{3,\omega}$) and minus the number probability of the modifier ion to "draw" a Q^2 structural unit ($p_{2,\omega}$). As an example, we consider the first and second draws. Before the first draw, all structural groups are Q^3; hence, $p_{3,1}$ (the number probability to draw a Q^3 structural group at the first draw)

DOI: 10.1021/acs.jpcb.8b04604
J. Phys. Chem. B 2018, 122, 7609−7615

equals 1 because $p_{3,1} = \frac{(g_3 - n_{3,0})w_3}{\sum_{i=1}^{3}\sum_{j=0}^{0}(g_i - n_{i,j})w_i} = \frac{100w_3}{100w_3}$. At the second draw, two draw probabilities exist because Q^2 structural groups have been formed and the probabilities depend on the weighting factors. The probability to draw a Q^3 structural group will be $p_{3,2} = \frac{(g_3 - n_{3,1})w_3}{\sum_{i=1}^{3}\sum_{j=0}^{1}(g_i - n_{i,j})w_i} = \frac{99w_3}{99w_3 + 1w_2}$.

Given that the fictive temperature of the glass is known, this can in turn be used to calculate relative H_i values using eq 8. Considering that most glasses are annealed at their glass-transition temperature (T_g), we can set $T_f = T_g$. Therefore, when the T_g values of the glasses of interest are known (as in this study), the model may be fitted with H_3, H_2, and H_1 as the free parameters instead of the weighting factors, making the model generalizable to any thermal history. However, although the physical meaning of the weighting factors is less fundamental than enthalpies, the former may be used when predicting the structure of glasses with unknown T_g values.

To apply this statistical mechanical approach to model the Q^n structural evolution in binary phosphate glasses, certain assumptions need to be fulfilled, including charge stability in the glass and that all modifier ions associate with the network, possibly preventing the model from being applicable on invert glasses. Furthermore, all H_i or w_i values obtained through this model are relative to each other. This could limit the application of the model on more complex systems such as mixed network former glasses because the relative weighting factors cannot be directly transferred from the single network former systems without taking mixed-former interactions into considerations. This will be addressed in future work.

■ RESULTS AND DISCUSSION

Raman and especially ^{31}P magic angle spinning NMR spectroscopy are suitable experimental probes for determining the Q^n speciation in phosphate glass systems.[17,26] The structure of binary phosphate glasses has been extensively studied in the literature, making the system suitable for developing and applying the statistical mechanical structure model. In the following, we first predict the structural evolution of three binary alkali phosphate glass families using experimental structural data from only one glass composition within each series as reference. The predicted Q-speciation is compared to the experimental data within the glass-forming region. The results are shown in Figure 3a−c. The data are obtained for $Cs_2O-P_2O_5$,[27] $Na_2O-P_2O_5$,[19,28] and $Li_2O-P_2O_5$ glasses.[26,29] These simple alkali phosphate glasses can be synthesized using the melt-quenching technique with modifier content up to 60 mol %. Because no Q^0 groups are experimentally detected in any of these alkali phosphate glasses, we find that it is sufficient to use structural reference data for only one glass composition to validate the model. These structural reference data are required because the model is based on a noncentral hypergeometric distribution and hence used to find the Boltzmann association factors used in describing this distribution. We here use the metaphosphate glass with 50 mol % alkali oxide as the reference composition but selecting other compositions has been found to predict the same structural evolution. For phosphate glasses with more than two Q^n species present simultaneously, reference compositions with the most Q^n species present should be selected.

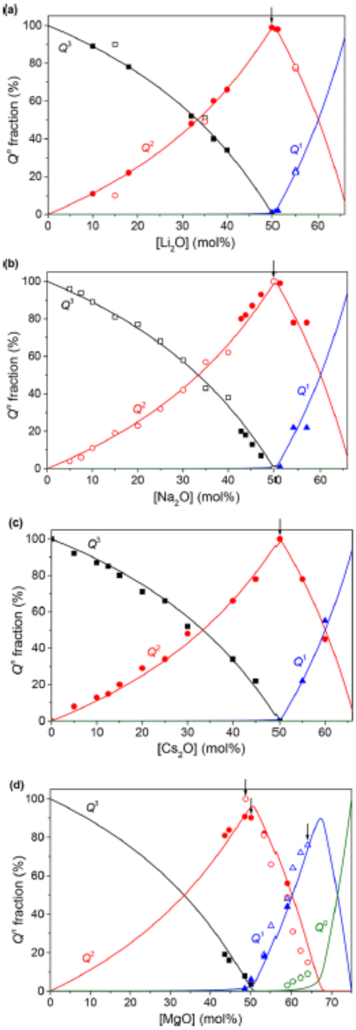

Figure 3. Composition dependence of the fraction of Q^n structural units in binary phosphate glasses with different modifier oxides: (a) Li_2O, (b) Na_2O, (c) Cs_2O, and (d) MgO. In (a), the closed symbols represent experimental data from Van Wüllen et al.[26] and the open symbols represent those from Alam et al.[29] In (b), the closed symbols represent experimental data from Brow et al.[28] and the open symbols represent those from Strojek et al.[19] In (c), the closed symbols represent experimental data from Click et al.[27] In (d), the closed symbols represent experimental data from Fayon et al.[33] and the open symbols represent those from Walter et al.[21] The solid lines represent the prediction using the present statistical mechanical model, which is established only based on experimental data for the glasses marked by an arrow.

DOI: 10.1021/acs.jpcb.8b04604
J. Phys. Chem. B 2018, 122, 7609−7615

As shown in Figure 3a−c, the statistical mechanical model predicts the Q-speciation in the three alkali phosphate glass systems very well, with input from only one reference composition in each series. H_i and coefficients of determination (R^2) of the fits are summarized in Table 1. Note that we set H_3 (the enthalpy barrier associated with draw of Q^3 structural group) equal to 0 to serve as the baseline. The results show that our model is able to reproduce the chemical order model proposed by Van Wazer,[17] without any assumptions. The stepwise conversion of Q^n to Q^{n-1} structural groups with increasing modifier content in alkali phosphate glasses, as described by both the present statistical mechanical model and the chemical order model, occurs because of a higher affinity for modifier cations to associate with the most connected structural phosphate groups. This is ascribed to Q^3 phosphate groups being less stable than Q^2 groups, which are in turn less stable than Q^1 groups, and so on. The stability of the groups is ascribed to the π-bond on the P=O group because the π-bond will be conjugated with NBOs, decreasing the energy of the system.[30] With the present approach, the strictly sequential conversion is expressed as high relative H_i values (∼30−50 kJ/mol) for a modifier ion to associate with (or "draw") a Q^3 structural group over associating with a Q^2 (H_2-H_3) group and so on (Table 1). To estimate standard errors for the H_i values, we have calculated the square root of the inverse Hessian evaluated at the maximum likelihood estimates,[31] obtaining values on the order of 1−20 J/mol. These standard errors represent the precision of the optimization method at the global minimum but do not distinguish between local minima. That is, a result with only a slightly worse fit may display a significantly different H_i value (in the kJ/mol range), despite the relatively low standard errors.

Table 1. Boltzmann Association Factors (H_i) and Coefficient of Determination (R^2) Values for the Fitting of the Current Model to Experimental Data for Five Different Binary Phosphate Glass Systems[a]

glass modifier	Li_2O	Na_2O	Cs_2O	MgO	ZnO
H_3 (kJ/mol)	0	0	0	0	0
H_2-H_3 (kJ/mol)	33.5	42.8	56.8	31.6	27.0
H_1-H_3 (kJ/mol)	70.4	74.9	85.1	55.0	40.0
R^2	0.992	0.998	0.996	0.942	0.988

[a] H_i values are scaled relative to that for the Q^3 to Q^2 conversion (H_3), which is set to 0.

For alkali silicate glasses, it has been found that an increasing field strength of the modifier cation results in a more random distribution of Q^n species, that is, the disproportionation reaction given in eq 12 is shifted to the right with increasing modifier field strength.[32] However, for alkali phosphate glasses, eq 12 has been found to be completely shifted to the left for $n = 2$,[17] that is, no difference in the Q^n distribution is expected for these glass systems.

$$2Q^n \rightleftharpoons Q^{n-1} + Q^{n+1} \tag{12}$$

To investigate the ability of the present model to predict the structural evolution of phosphate glasses at higher modifier content (thus including the Q^0 structural groups) and field strength, we consider the binary $MgO-P_2O_5$[21,33] and $ZnO-P_2O_5$[20,34] glass families. The results for the Mg-glasses are shown in Figure 3d. Because the Q-speciation data found in the literature for $MgO-P_2O_5$ glasses differ significantly in the two references,[21,33] we base the model on the structural reference data of three glasses (one from each reference around 50 mol % modifier and one at 64 mol % modifier), although only two compositions are strictly required. The statistical mechanical model offers a worse fit for the magnesium phosphate compared to the alkali phosphate glasses but the compositional trend in the data is well captured with $R^2 = 0.942$. The fact that some disproportion of Q^2 occurs near the metaphosphate region in the $MgO-P_2O_5$ glasses has been suggested to be due to a change from a ring structure to phosphate chains[33] or because Mg may act as a partial network former in the glass structure (with average coordination number of 3.7 ± 0.3).[21] The unexpected excess of Q^2 and Q^0 structural groups in the pyrophosphate region, compared to the chemical order model, is likely due to the disproportionation.

We next apply the model to zinc phosphate glasses, which have been extensively investigated because of their exceptional glass-forming abilities. Brow et al.[20] have successfully produced glasses and determined short-range structure in compositions with up to 71 mol % ZnO. We use the two glasses with 50 and 66 mol % ZnO as reference data to build the statistical mechanical model (Figure 4). We find a very good agreement between the model and experimental data, with $R^2 = 0.988$ for all data points and $R^2 = 0.995$ considering only the pyrophosphate region above 50 mol % ZnO. As described by Brow et al., the structure of zinc phosphate glasses differs from that of the original chemical order model in that Q^2, Q^1, and Q^0 groups exist in the glass simultaneously. This deviation in Q-speciation is described in terms of the disproportionation reactions (eq 12). Similarly to silicate glasses, the reaction shifts to the right with increasing field strength of the modifier cation.[20] Brow et al.[20] introduced an equilibrium constant for this reaction to quantify the extent of the deviation from the chemical order model. As shown in Figure 4, the present model (solid lines) agrees well with that of Brow (dashed lines). In our model, we quantify the deviation from the binary

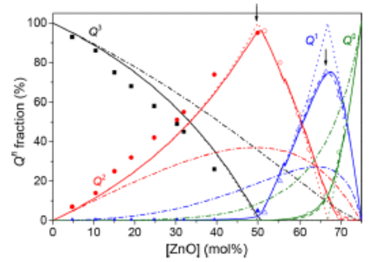

Figure 4. Composition dependence of the fraction of Q^n structural units in zinc phosphate glasses as predicted by different types of models. The closed symbols represent experimental data from Fayon et al.[33] and the open symbols represent those from Walter et al.[21] The solid lines represent the prediction using the present statistical mechanical model, which is established only based on experimental data for the glasses marked by an arrow. The dotted lines represent the chemical order model, whereas the dash dotted lines represent the completely random distribution model. The dashed lines represent the prediction using the thermodynamic model.[20] Note that some lines are on top of each other.

distribution through the Boltzmann association factors, which exhibit similar values for the different Q-groups in the case of random statistical distribution. For example, we find H_2−H_3 ≈ 27 kJ/mol in the ultraphosphate region but H_1−H_2 ≈ 13 kJ/mol in the pyrophosphate region. This translates into stepwise sequential conversion in the ultraphosphate region and more gradual conversion in the pyrophosphate region. To demonstrate the effect of the relative H_i values, the proposed model for zinc phosphate glasses (solid lines) is compared in Figure 4 to the chemical order model (dotted lines) and a completely random distribution (dash dotted lines). In the latter, the probability for a modifier ion to "draw" a network-forming site only depends on the number of network formers. Figure 4 clearly shows that the modifier ions have a higher affinity toward the highest coordinated network formers.

With the model parameters established, we are able to make model predictions of the thermal history dependence of the structural speciation. The predicted Q^n distribution has been plotted against fictive temperature for two fixed glass compositions with different modifier types and contents, that is, the $50Li_2O$−$50P_2O_5$ glass in Figure 5a and the 66ZnO−$34P_2O_5$ glass in Figure 5b. For both glasses, we observe that, as expected, the glass structure becomes the most ordered as T_f approaches 0 K, whereas a random distribution is found as T_f approaches infinity and the behavior of the system becomes dominated by entropy. We note that these calculations are strictly model results, as a realistic range of experimentally obtainable T_f values is typically between $0.9T_g$ and $1.2T_g$.[35] The present model captures the nonequilibrium nature of glasses well because we are able to predict the structural dependence on realistic obtainable T_f values, thus accounting for the cooling rate dependence of the atomic-scale structure. Considering the realistic range of obtainable fictive temperatures (shown by dashed vertical lines in Figure 5), the fraction of the Q^2 structural group for $50Li_2O$−$50P_2O_5$ would vary by ~1.5 at. %, whereas that of the Q^1 structural group for 66ZnO−$34P_2O_5$ would vary by ~10.5 at. %, showing that the fictive temperature has a higher effect on less structurally ordered glasses. Furthermore, the fractions of Q^{n-1} and Q^{n+1} are found to be identical when only three structural groups are present at once in the glass (Figure 5), in agreement with the thermodynamic description (eq 12). We also find that the fractions of Q^1 (Figure 5a) and Q^2 (Figure 5b) vary nonmonotonically and exhibit a maximum with respect to the variation in fictive temperature. This is due to the competition for modifiers among more than two different independently varying structural units.

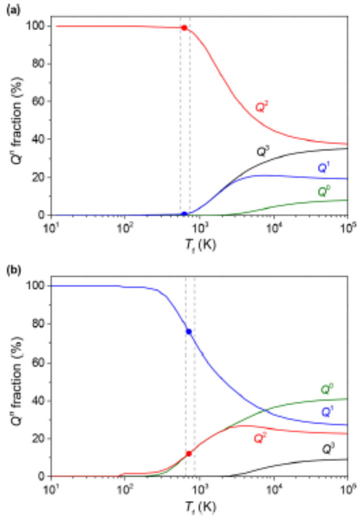

Figure 5. Fictive temperature dependence of the fraction of Q^n structural units in (a) $50Li_2O$−$50P_2O_5$ and (b) 66ZnO−$34P_2O_5$ glasses. The solid lines show model predictions, whereas the closed symbols represent the T_f (=T_g) values of the studied glasses. The dashed vertical lines represent the extremes of realistically obtainable T_f values ($0.9T_g$ to $1.2T_g$).

As shown in Table 1, we have determined a set of relative H_i values for each modifier cation, determining its affinity toward each structural group in phosphate glasses. We find an overall decrease in the H_i differences with increasing modifier field strength. With these H_i parameters being established, they should be transferable to other glass systems containing the same chemical elements. For example, H_i obtained separately in the Na_2O−P_2O_5 and ZnO−P_2O_5 systems should be directly applicable to predict the structure of the Na_2O−ZnO−P_2O_5 system without the need for any additional parameters. This will be investigated in the future by preparing and characterizing the mixed systems. Finally, we note that the present findings suggest that the model can be used to predict the structural evolution using reference data for only a few compositions. This is ideal when applying the model on new glass series where structural data are required. However, considering the long-term objective of building a database of Boltzmann association factors, it is desirable to use all available structural data to ensure accurate parameters.

■ CONCLUSIONS

We have reported the first implementation of a statistical mechanical model using a Wallenius-type noncentral hypergeometric distribution with Boltzmann weighting factors to predict the structural evolution in simple binary phosphate glasses. In binary alkali phosphate glasses, the structural evolution is dominated by sequential Q^n to Q^{n-1} conversion following the chemical order model, which can be predicted based on structural data of only one reference glass composition. Prediction of the Q-speciation in both the ultra- and pyrophosphate regions requires structural data from two reference glasses to obtain reliable parameters for the model. The proposed statistical mechanical approach is also able to predict the structure of zinc phosphate glasses, which feature a more random distribution of the network speciation. This difference in glass structure has previously been described in terms of disproportionation reactions, but here we show that such a macroscopic (thermodynamic) description is physically equivalent to that of the present microscopic (statistical mechanical) description.

■ AUTHOR INFORMATION

Corresponding Author

*E-mail: mos@bio.aau.dk.

ORCID

Morten M. Smedskjaer: 0000-0003-0476-2021

Notes

The authors declare no competing financial interest.

■ ACKNOWLEDGMENTS

This work was supported by the Independent Research Fund Denmark (grant no. 7017-00019).

■ REFERENCES

(1) Mauro, J. C. Grand Challenges in Glass Science. *Front. Mater.* **2014**, *1*, 20.

(2) Januchta, K.; Youngman, R. E.; Goel, A.; Bauchy, M.; Logunov, S. L.; Rzoska, S. J.; Bockowski, M.; Jensen, L. R.; Smedskjaer, M. M. Discovery of Ultra-Crack-Resistant Oxide Glasses with Adaptive Networks. *Chem. Mater.* **2017**, *29*, 5865−5876.

(3) Ovcharenko, N. V.; Smirnova, T. V. High refractive index and magneto-optical glasses in the systems TeO2-WO3-Bi2O3 and TeO2-WO3-PbO. *J. Non-Cryst. Solids* **2001**, *291*, 121−126.

(4) Kasuga, T.; Abe, Y. Calcium Phosphate Invert Glasses with Soda and Titania. *J. Non-Cryst. Solids* **1999**, *243*, 70−74.

(5) Mauro, J. C. Topological Constraint Theory of Glass. *Am. Ceram. Soc. Bull.* **2011**, *90*, 31−37.

(6) Zachariasen, W. H. The Atomic Arrangement in Glass. *J. Am. Chem. Soc.* **1932**, *54*, 3841−3851.

(7) Wright, A. C.; Shakhmatkin, B. A.; Vedishcheva, N. M. The Chemical Structure of Oxide Glasses: A Concept Consistent with Neutron Scattering Studies? *Glass Phys. Chem.* **2001**, *27*, 97−113.

(8) Edén, M. NMR Studies of Oxide-Based Glasses. *Annu. Rep. Prog. Chem., Sect. C: Phys. Chem.* **2012**, *108*, 177.

(9) Ispas, S.; Charpentier, T.; Mauri, F.; Neuville, D. R. Structural Properties of Lithium and Sodium Tetrasilicate Glasses: Molecular Dynamics Simulations versus NMR Experimental and First-Principles Data. *Solid State Sci.* **2010**, *12*, 183−192.

(10) Micoulaut, M. Concepts and Applications of Rigidity in Non-Crystalline Solids: A Review on New Developments and Directions. *Adv. Phys.: X* **2016**, *1*, 147−175.

(11) Mauro, J. C. Statistics of Modifier Distributions in Mixed Network Glasses. *J. Chem. Phys.* **2013**, *138*, 12A522.

(12) Rodrigues, B. P.; Mauro, J. C.; Yue, Y.; Wondraczek, L. Modifier Constraints in Alkali Ultraphosphate Glasses. *J. Non-Cryst. Solids* **2014**, *405*, 12−15.

(13) Gao, G.; Wei, J.; Shen, Y.; Peng, M.; Wondraczek, L. Heavily Eu2O3-Doped Yttria-Aluminoborate Glasses for Red Photoconversion with a High Quantum Yield: Luminescence Quenching and Statistics of Cluster Formation. *J. Mater. Chem. C* **2014**, *2*, 8678−8682.

(14) Day, D. E.; Wu, Z.; Ray, C. S.; Hrma, P. Chemically Durable Iron Phosphate Glass Wasteforms. *J. Non-Cryst. Solids* **1998**, *241*, 1−12.

(15) Das, S. S.; Singh, N. P.; Srivastava, P. K. Ion Conducting Phosphate Glassy Materials. *Prog. Cryst. Growth Charact. Mater.* **2009**, *55*, 47−62.

(16) Pickup, D. M.; Newport, R. J.; Knowles, J. C. Sol-Gel Phosphate-Based Glass for Drug Delivery Applications. *J. Biomater. Appl.* **2012**, *26*, 613−622.

(17) Brow, R. K. Review: The Structure of Simple Phosphate Glasses. *J. Non-Cryst. Solids* **2000**, *263-264*, 1−28.

(18) Losso, P.; Schnabel, B.; Jäger, C.; Sternberg, U.; Stachel, D.; Smith, D. O. 31P NMR Investigations of Binary Alkaline Earth Phosphate Glasses of Ultra Phosphate Composition. *J. Non-Cryst. Solids* **1992**, *143*, 265−273.

(19) Strojek, W.; Eckert, H. Medium-range order in sodium phosphate glasses: A quantitative rotational echo double resonance solid state NMR study. *Phys. Chem. Chem. Phys.* **2006**, *8*, 2276.

(20) Brow, R. K.; Tallant, D. R.; Myers, S. T.; Phifer, C. C. The Short-Range Structure of Zinc Polyphosphate Glass. *J. Non-Cryst. Solids* **1995**, *191*, 45−55.

(21) Walter, G.; Vogel, J.; Hoppe, U.; Hartmann, P. Structural Study of Magnesium Polyphosphate Glasses. *J. Non-Cryst. Solids* **2003**, *320*, 210−222.

(22) Goyal, S.; Mauro, J. C. Statistical Mechanical Model of Bonding in Mixed Modifier Glasses. *J. Am. Ceram. Soc.* **2018**, *101*, 1906−1915.

(23) Fog, A. Sampling Methods for Wallenius' and Fisher's Noncentral Hypergeometric Distributions. *Comm. Stat. Simulat. Comput.* **2008**, *37*, 241−257.

(24) Wallenius, K. T. *Biased Sampling; the Noncentral Hypergeometric Probability Distribution*; Supported by the Army, Navy and Air Force, 1963; Vol. *70*.

(25) Mauro, J. C.; Smedskjaer, M. M. Statistical Mechanics of Glass. *J. Non-Cryst. Solids* **2014**, *396-397*, 41−53.

(26) van Wüllen, L.; Eckert, H.; Schwering, G. Structure−Property Correlations in Lithium Phosphate Glasses: New Insights from31P ↔ 7Li Double-Resonance NMR. *Chem. Mater.* **2000**, *12*, 1840−1846.

(27) Click, C. A.; Brow, R. K.; Alam, T. M. Properties and Structure of Cesium Phosphate Glasses. *J. Non-Cryst. Solids* **2002**, *311*, 294−303.

(28) Brow, R. K.; Kirkpatrick, R. J.; Turner, G. L. The short range structure of sodium phosphate glasses I. MAS NMR studies. *J. Non-Cryst. Solids* **1990**, *116*, 39−45.

(29) Alam, T. M.; Brow, R. K. Local Structure and Connectivity in Lithium Phosphate Glasses: A Solid-State 31P MAS NMR and 2D Exchange Investigation. *J. Non-Cryst. Solids* **1998**, *223*, 1−20.

(30) Hudgens, J. J. The Structure and Properties of Anhydrous, Alkali Ultra-Phosphate Glasses. Retrospective Theses and Dissertations, Iowa State University, 1994.

(31) Nelder, J. A.; Mead, R. A Simplex Method for Function Minimization. *Comput. J.* **1965**, *7*, 308−313.

(32) Maekawa, H.; Maekawa, T.; Kawamura, K.; Yokokawa, T. The Structural Groups of Alkali Silicate Glasses Determined from 29Si MAS-NMR. *J. Non-Cryst. Solids* **1991**, *127*, 53−64.

(33) Fayon, F.; Massiot, D.; Suzuya, K.; Price, D. L. 31P NMR Study of Magnesium Phosphate Glasses. *J. Non-Cryst. Solids* **2001**, *283*, 88−94.

(34) Meyer, K. Characterization of the Structure of Binary Zinc Ultraphosphate Glasses by Infrared and Raman Spectroscopy. *J. Non-Cryst. Solids* **1997**, *209*, 227−239.

(35) Yue, Y.; von der Ohe, R.; Jensen, S. L. Fictive Temperature, Cooling Rate, and Viscosity of Glasses. *J. Chem. Phys.* **2004**, *120*, 8053−8059.

PAPER II

THE JOURNAL OF PHYSICAL CHEMISTRY B
Article
Cite This: J. Phys. Chem. B 2019, 123, 1206–1213
pubs.acs.org/JPCB

Statistical Mechanical Modeling of Borate Glass Structure and Topology: Prediction of Superstructural Units and Glass Transition Temperature

Mikkel S. Bødker,[†] John C. Mauro,[‡] Randall E. Youngman,[§] and Morten M. Smedskjaer*,[†]

[†]Department of Chemistry and Bioscience, Aalborg University, 9220 Aalborg, Denmark

[‡]Department of Materials Science and Engineering, The Pennsylvania State University, University Park, Pennsylvania 16802, United States

[§]Science and Technology Division, Corning Incorporated, Corning, New York 14831, United States

Supporting Information

ABSTRACT: Predicting the compositional evolution of the atomic-scale structure and properties of oxide glasses is important for designing new materials for advanced applications. A statistical mechanics-based approach has recently been applied to predict the composition−structure evolution in binary phosphate glasses, while topological constraint theory (TCT) has been applied in the last decade to predict the structure−property evolution in various oxide and nonoxide glass systems. In this work, we couple these two approaches to enable quantitative predictions of the compositional dependence of glass transition temperature and the population of superstructural units. The object of the study is the lithium borate glass system because they feature interesting structural characteristics (e.g., boron anomaly), and ample structure and property data are available. In these glasses, the average coordination number of boron first increases when lithium modifiers are added and then later decreases accompanied by network depolymerization. First, on the basis of ^{10}B nuclear magnetic resonance spectroscopy data from literature, we present a statistical description of the structural evolution in lithium borate glasses by accounting for the relative enthalpic and entropic contributions to the bonding preferences. We show that the entire glass structure evolution (both short- and intermediate-range) can be predicted based on experimental structural information for only a few glass compositions. We then show that the developed structural model can be combined with a previously established TCT model to predict the compositional evolution of the glass transition temperature. This work thus opens a new avenue for the computational design of glasses with tailored properties.

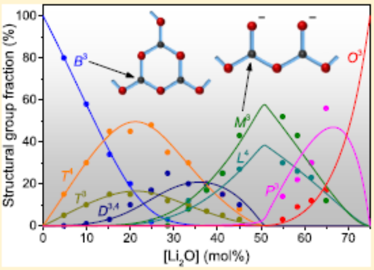

1. INTRODUCTION

Oxide glasses find numerous applications[1−4] because of their unique physical and chemical properties, which vary as a function of temperature, pressure, and chemical composition. To accelerate the design of new glass compositions, an accurate structural description is required, but the noncrystalline nature and complex structural units found in oxide glasses have hindered the construction of a universal structure model. Developing such a model would enable direct prediction of glass properties from their composition by coupling the composition−structure model with existing structure−property models, such as topological constraint theory (TCT),[5] thus avoiding the inefficient trial-and-error-based approach.[6]

Although glasses lack the periodicity and long-range order of crystals, they possess characteristic short-range order (SRO), which obeys the basic rules of crystal chemistry. Borate glasses, which feature low processing temperature,[7] high thermal shock resistance,[8] and high electrical resistivity compared to soda lime silicate glasses,[1] constitute a class of oxide glasses with particularly complicated structural units, including both short- and intermediate-range features.[9−11] Moreover, boron speciation has been found to be challenging to model using classical molecular dynamics simulations,[12] although recent progress has been made in the development of reliable boron oxide potentials.[13,14] The backbone of pure B_2O_3 glass consists of three-fold coordinated boron atoms.[15] While physical properties such as glass transition temperature and hardness of silicate glasses decrease significantly when increasing the amount of modifier ions in the glass network,[3] the same properties will initially increase when adding modifier ions to a borate network because of the so-called "boron anomaly".[16,17] In silicate glasses, the addition of modifier ions breaks the network by forming nonbridging oxygens (NBOs) to charge-balance the modifier cations.[18,19] When introducing modifier oxides to B_2O_3, there are two possible scenarios: (a) formation

Received: December 11, 2018
Published: January 8, 2019

DOI: 10.1021/acs.jpcb.8b11926
J. Phys. Chem. B 2019, 123, 1206−1213

of NBO by breaking the linkage between two trigonally coordinated BO_3 groups or (b) conversion of boron from a three-fold coordinated (B^3) to a four-fold coordinated (B^4) state without the creation of NBO.[20]

Previous studies have successfully linked the short-range structure of simple borate glasses with their macroscopic physical properties, such as glass transition temperature (T_g),[16,21] liquid fragility,[16,21] and micro-hardness.[22] This previous work was based on TCT, which was originally developed by Phillips and Thorpe,[23−25] who treated the atomic structure of a glass as a network of bond constraints. According to this view, the network can be floppy (underconstrained), isostatic (optimally constrained), or stressed rigid (overconstrained), depending on the relative difference between the network dimensionality (d) and the average number (n) of constraints per atom.[23−25] When $n < d$, the network is underconstrained and contains low-frequency deformation modes (so-called “floppy modes”). The network is optimally rigid when $n = d$ and stressed rigid when $n > d$. The studies around 2010 by Mauro et al.[16] and later by Smedskjaer et al.[21] developed topological modeling tools for alkali and alkaline earth borates which account for the temperature-dependent nature of bond constraints. On the basis of structural data obtained by nuclear magnetic resonance (NMR) spectroscopy, the approach was successfully applied to predict the evolution of viscosity and hardness with composition (x) in the modified borate systems.

The application of TCT for prediction of glass properties requires available structural data for each composition, and it is therefore typically used in combination with a structural model for the glass system. Unfortunately, the existing models used to describe the network structure of borate glasses either require up to ten equilibrium constants for each glass system as in the chemical equilibrium concept (CEC) model[26] or generalize the structure without considering different types of modifier size and charge, as in the random pair model of Gupta[27] or the well-known Feller−Bray model.[28] The Feller−Bray model has been especially successful in estimating the structural evolution of borate glasses without specifying the type(s) of modifier ions.[29]

Recently, Mauro[30] proposed an alternative approach for predicting the modifier distribution and thus network former speciation in oxide glasses. The model is based on a statistical mechanical noncentral multivariate hypergeometric function with Boltzmann weighting factors. The approach may be seen as analogous to drawing marbles from an urn, with each network former being a unique type of marble for which the size is determined by the Boltzmann weighting factor. The modifier−former interactions are formed when a modifier “draws” a marble (i.e., a network former), with the probability for a given modifier−former interaction depending on the number distribution of the different former species (based on glass composition) and their size (i.e., Boltzmann weighting factor). After each “draw”, the population of the remaining marbles changes, that is, the probability to draw a given marble changes after each draw. We have recently experimentally demonstrated the applicability of the model for binary phosphate glasses,[31] where the marbles in the urn would represent structural phosphate Q^n units, where n is the number of BOs per phosphate tetrahedron. The probability for a network modifier to “draw” a certain phosphate unit depends on the number distribution of Q^n units at the time of the draw and the size of the marble. By considering that a drawn Q^n unit is replaced by a Q^{n-1} unit, we have successfully predicted the structural evolution in a number of binary phosphate glasses, including $MgO{-}P_2O_5$ and $ZnO{-}P_2O_5$ glasses with a high degree of disproportionation of Q^n units.[31]

Previous attempts at calculating boron coordination in glasses using different statistical mechanical models have been reported.[32−34] However, they differ from the current one, for example, by not considering the system as a noncentral hypergeometric distribution and in the free parameters used for fitting the models. In order to apply the present statistical mechanical approach to predict the borate glass structure as a function of composition, we also consider the evolution of the various superstructural borate units, in addition to the boron anomaly in the coordination number. As such, it is more complicated to apply the present model to the borate system compared to the previously studied phosphate system,[31] in which we only needed to account for the various modifier-Q group interactions. Figure 1 shows the structural groups that exist on the intermediate-range order (IRO) scale in borate glasses over a range of modifier content, including boroxol (six-membered ring with only trigonal boron), pentaborate (two six-membered rings linked through a four-fold coordinated boron), triborate (six-membered ring with one four-fold coordinated boron and two trigonal boron), diborate (two six-membered rings linked through two four-fold coordinated boron), nonring BO_4 (four-fold coordinated boron not in a ring structure), metaborate (trigonal boron chain with one

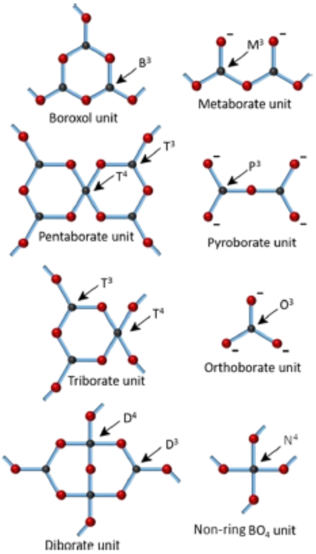

Figure 1. Structural groups in lithium borate glasses. Red circles represent oxygen atoms and black circles boron atoms. The negative signs on oxygen atoms indicate NBO, which are charge balanced by lithium cations (not shown). Two tetraborate units are formed by connecting a triborate unit with a pentaborate unit. The boron structural configurations (quantified by ^{10}B NMR[28]) are marked by arrows, where B^3 is a three-fold coordinated boron in boroxol unit, T^4 is a four-fold coordinated boron in tetraborate unit, etc.

DOI: 10.1021/acs.jpcb.8b11926
J. Phys. Chem. B 2019, 123, 1206−1213

NBO on each boron), pyroborate (two trigonal boron linked with a BO and each trigonal boron having two NBOs), and orthoborate units (trigonal boron with three NBOs). Metaborate is drawn as a chain, but may also be found in a ring-type configuration.[28] These superstructural groups are based on the data provided by Feller,[28] obtained in 1982; however, more recent studies by Youngman and Zwanziger[35] found that around 30% of the boron in pure B_2O_3 glass is in nonring BO_3 groups. These are not included in the presented work because of a lack of quantitative data in literature and the nonring BO_3 groups are assumed to be part of the quantified boroxol structural units.

The aim of the present study is to predict the structural evolution of binary lithium borate glasses using the statistical mechanical model for bonding preferences.[30] Lithium is chosen as the modifier because quantitative data of the fraction of various superstructural units have, to our knowledge, only been reported in binary borates with lithium as the modifier. This is likely because ^{10}B NMR measurements are needed for such quantification,[28] requiring ^{10}B enriched H_3BO_3, specialized field-stepping to account for the very broad resonances,[36] and processing times of several days to accumulate the signal. In contrast, ^{11}B NMR may be performed without enriched components and features measurement times of less than 1 h.[37] As a result, the ^{11}B NMR technique has become widely popular in the field of glass science,[19] as it can be used to extract the boron coordination number, although perhaps it does not capture all of the structural details on the IRO order needed for the present modeling approach. Therefore, in spite of omission of the nonring BO_3 and BO_4 units at low modifier contents, we rely on the mostly complete ^{10}B NMR-based model of Feller for this study, placing emphasis on the evolution of superstructural units as a function of glass composition. Building on the recent work of Kirchner et al.,[38] we also couple the composition−structure model based on statistical mechanics with a structure−property model based on TCT to predict the glass transition temperature (T_g) as a function of composition. We compare the results with experimental data and previous glass structure models.

2. COMPOSITION−STRUCTURE MODEL: STATISTICAL MECHANICS

In the model, we consider that the distribution of modifiers in lithium borate glasses and the resulting IRO group distribution can be described statistically, following a hypergeometric form.[30] Hypergeometric distributions describe situations with a fixed number of draws from a finite population without replacement after each draw. In the present glasses, the population represents the total number of network-forming boron sites available for association with a modifier and the number of draws represents the number of lithium modifier atoms.[39] Each of the structural groups is treated as an individual site available for modifier interaction. Each time a modifier "draws" a network former site, the distribution of structural groups changes and so does the probability of the next draw. Various network former−modifier interactions affect the probability for the modifier to associate with each structural group; hence, a kind of noncentral hypergeometric distribution is required.[40]

As reported previously,[30,31] the Wallenius[41] noncentral hypergeometric distribution is suited to describe the glass structure. With this distribution, the probability of selecting a given species of type i at draw number ω is given by[39]

$$p_{i,\omega} = \frac{(g_i - n_{i,\omega-1})w_i}{\sum_{i=1}^{\Omega} \sum_{j=0}^{\omega-1} (g_i - n_{i,j})w_i} \qquad (1)$$

where g_i is the degeneracy of species i, $n_{i,j}$ is the accumulated number of successful draws of species i after j number of attempts, and w_i is the probability weighting factor for species i. As dictated by eq 1, the draw probability is altered by introducing a weighting factor. The w_i values depend on the energy barrier of the modifier−former interaction, which is different for each type of structural group.[30] Additionally, we assume that the structure of the glass corresponds to the equilibrium structure of the liquid at the fictive temperature (T_f). The Boltzmann weighting factor used in this model is therefore given as

$$w_i = \exp\left(-\frac{H_i}{kT_f}\right) \qquad (2)$$

where H_i is the enthalpy barrier associated with a draw of species i, and k is Boltzmann's constant. With this definition, eq 1 may be rewritten specifically for glass systems as[42]

$$p_{i,\omega} = \frac{(g_i - n_{i,\omega-1})\exp\left(-\frac{H_i}{kT_f}\right)}{\sum_{i=1}^{\Omega} \sum_{j=0}^{\omega-1} (g_i - n_{i,j})\exp\left(-\frac{H_i}{kT_f}\right)} \qquad (3)$$

In the following, we describe the different types of modifier−former interactions that must be considered to establish the composition−structure model. On the basis of the structural groups depicted in Figure 1, we use the following abbreviations: B for boroxol, T for tetraborate, D for diborate, M for metaborate, N for nonring BO_4, P for pyroborate, and O for orthoborate. Upon addition of a lithium modifier to pure B_2O_3, the following transformation occurs[28]

$$8B^3 + Li_2O \rightarrow 6T^3 + 2T^4 \qquad (4)$$

where the exponents represent the boron coordination number. When lithium oxide reacts with the boroxol structural groups, it alters the IRO configuration of eight boron atoms in the boroxol configuration into eight boron atoms in the tetraborate configuration, where two of the eight atoms will be four-fold coordinated, and hence, balance the charge from the lithium modifier cation. We assume that the fraction of T^3 is always three times the fraction of T^4 because of the site constraints. Then, eight boron atoms in the tetraborate configuration interact with lithium oxide to form eight boron units in diborate configuration, with four of the boron atoms in four-fold coordination, effectively stabilizing the newly introduced modifier cations[28]

$$6T^3 + 2T^4 + Li_2O \rightarrow 4D^3 + 4D^4 \qquad (5)$$

We assume here that the fraction of D^3 is always equal to that of D^4 because of the site constraints. Following interaction between lithium oxide and boron atoms in diborate configuration, the latter may be transformed into either metaborate or nonring BO^4 units[28]

$$2D^3 + 2D^4 + Li_2O \rightarrow 4yM^3 + 4(1 - y)N^4 \qquad (6)$$

Here, we assume that the ratio (y) between metaborate and nonring BO_4 is constant at all modifier concentrations.[28] Other

DOI: 10.1021/acs.jpcb.8b11926
J. Phys. Chem. B 2019, 123, 1206−1213

studies[43,44] have found higher concentrations of nonring BO_4 at a low modifier content in alkali borate glasses. Here, we assume that these are part of the tetraborate and diborate structural data by Feller.[28] Finally, we assume that metaborate, nonring BO_4, and orthoborate units will all associate with lithium oxide and form the next structural group at a one-to-one ratio[28]

$$2M^3 + Li_2O \rightarrow 2P^3 \tag{7}$$

$$2N^4 + Li_2O \rightarrow 2P^3 \tag{8}$$

$$2P^3 + Li_2O \rightarrow 2O^3 \tag{9}$$

When applying the statistical mechanical model to the borate glass system, each of the structural configurations that the boron atoms undertake in eqs 4–9 is considered as individual network former species i. Following the marble analogy, we may have thus eight different types of marbles (B^3, T^3, T^4, D^3, D^4, M^3, N^4, and P^3, where O^3 is excluded because it does not interact with another modifier). However, because the fractions of T^3 and T^4, and D^3 and D^4, respectively, are constrained by each other, each pair may be treated as a single type of unit (marble).

To perform the structural modeling, we apply eq 3 to calculate numerically the probability of drawing species i, with each species having its own weighting factor w_i. Each of these w_i values is used in the structural modeling as a fitting parameter. We thus obtain seven model parameters, including y. Here, $p_{B^3,\omega}$ describes the probability of the modifier ion to associate with four B^3 atoms, thus forming three new T^3 and one new T^4 configured boron atoms at draw ω, following the stoichiometry in eq 4. Likewise, $p_{T,\omega}$ describes the probability for lithium association with three T^3 and one T^4 configured boron atoms (eq 5, and so on for the remaining reactions in eqs 6–9). We then estimate the fractions of species i at a given draw ω from the $p_{i,\omega}$ values and the fraction of that structural group at draw number $\omega - 1$. Examples of these calculations are given in eqs 10 and 11 for B^3 and T units, respectively. The T speciation stoichiometry is given in eq 12.

$$B_{\omega}{}^3 = B_{\omega-1}{}^3 - 4p_{B^3,\omega} \tag{10}$$

$$T_{\omega} = T_{\omega-1} - 4p_{T,\omega} + 4p_{B^3,\omega} \tag{11}$$

$$T_{\omega}{}^3 = \frac{3}{4}T_{\omega}, \qquad T_{\omega}{}^4 = \frac{1}{4}T_{\omega} \tag{12}$$

By using a Monte Carlo algorithm for draw generation, the compositional evolution of each structural group may be predicted based on the above equations and a set of experimental structural data. The Boltzmann weighting factors (w_{B^3}, w_T, w_D, w_{M^3}, w_{N^4}, and w_{P^3}) and y are used as the fitting parameters. To further clarify this protocol, let us consider the first two draws (i.e., lithium association with boron network former units) of the model. Before the first draw, the only structural group present is B^3, keeping in mind that nonring BO_3 units are not captured in the model or the data on which this model is based. Hence, $p_{B^3,1}$ (the number probability for Li to draw a B^3 structural group at the first draw) equals 1 because $p_{B^3,1} = \frac{(g_{B^3} - n_{B^3,0})w_{B^3}}{\sum_{i=1}^{6}\sum_{j=0}^{0}(g_i - n_{i,j})w_i} = \frac{100w_{B^3}}{100w_{B^3}} = 1$. On the second draw, two draw probabilities exist because tetraborate structural groups have been formed and the probabilities depend on the weighting factors. The probability to draw a B^3 structural group will be equal to $p_{B^3,2} = \frac{(g_{B^3} - n_{B^3,1})w_{B^3}}{\sum_{i=1}^{6}\sum_{j=0}^{1}(g_i - n_{i,j})w_i} = \frac{96w_{B^3}}{96w_{B^3} + 4w_T}$. The conversion of four boron atoms from the B^3 configuration to the T configuration (three T^3 and one T^4) at the first draw follows the stoichiometry given by eq 4.

Given that the fictive temperature of the glass is known, the above procedure to obtain weighting factors can in turn be used to calculate relative interaction enthalpies H_i using eq 3. Assuming that the present glasses from literature are frozen-in or annealed at their glass transition temperature (T_g), we set $T_f = T_g$. Therefore, when the T_g values of the glasses of interest are known experimentally, the model may be fitted with H_{B^3}, H_T, H_D, H_{M^3}, H_{N^4}, H_{P^3}, and y as the seven free parameters instead of the weighting factors, making the model generalizable to any thermal history. However, although the physical meaning of the weighting factors is less fundamental than enthalpies, the former may be used when predicting the structure of glasses with unknown T_g values. The fit of the model to the experimental reference data is performed in the object-oriented programming language Python. Here, the Basinhopping optimization method (part of the SciPy package) is used[45] because it attempts to find the global minimum in the parameter space by repeating the optimization with different guessed values of the starting parameters and solving for the structure in a self-consistent fashion.

3. STRUCTURE–PROPERTY MODEL: CONSTRAINT THEORY

As recently found by Kirchner et al.,[38] the statistical mechanics of the glass structure may be theoretically linked to TCT by accounting for the interplay between enthalpic and entropic effects. Following TCT, the composition dependence of T_g is considered to be due to the variation of the configurational entropy S_c. As such, T_g of composition x, where x is the lithium modifier concentration in the present case, may be computed relative to that of some reference composition x_R[16]

$$\frac{T_g(x)}{T_g(x_R)} = \frac{S_c[T_g(x_R), x_R]}{S_c[T_g(x), x]} \tag{13}$$

According to energy landscape modeling,[46,47] the configurational entropy is largely proportional to the atomic degrees of freedom f. The latter is in turn proportional to the number of low-frequency "floppy modes", hence incorporating topological constraints

$$\frac{T_g(x)}{T_g(x_R)} = \frac{f[T_g(x_R), x_R]}{f[T_g(x), x]} = \frac{d - n[T_g(x_R), x_R]}{d - n[T_g(x), x]} \tag{14}$$

where $d = 3$ is the dimensionality of the three-dimensional network and n is the average number of constraints per atom in the system. n can be calculated by averaging over the different network forming species i (although for the TCT model, only the boron coordination number and number of NBOs per boron are needed) and types of constraints α[16]

$$n(T, x) = \sum_i N_i(x) \sum_{\alpha} l_{i,\alpha} q_{\alpha}(T) \tag{15}$$

where $N_i(x)$ is the mole fraction of species i in composition x, $l_{i,\alpha}$ is the number of α-constraints associated with species i, and

$q_\alpha(T)$ accounts for the temperature dependence of constraints α.

TCT thus connects structural (number of structural units) and topological information (types and rigidity of constraints associated with each unit) with the macroscopic properties (here, glass transition temperature). To apply eqs 13–15 to predict $T_g(x)$, we first count the different types of constraints associated with each network-forming species and rank them according to their relative bond strengths (i.e., constraint onset temperature). On the basis of the work of Smedskjaer et al.,[21] we consider the following types of bond constraints:

- α: B–O and Li^{NB}–O linear constraints. Two α constraints for each oxygen.
- β: O–B–O angular constraints. Five β constraints per Q^4 to form a rigid BO_4 tetrahedron and three β constraints per Q^3 to keep the BO_3 unit planar.
- γ: B–O–B angular constraints. One γ constraint per oxygen.
- μ: Additional modifier rigidity due to clustering effects. Two μ constraints per NBO-forming Li atom.

Here, Li^{NB}–O is the fraction of lithium modifiers bonded to NBO. The constraint onset temperatures are ordered such that[16,21]

$$T_\gamma < T_g < T_\beta < T_\mu < T_\alpha \tag{16}$$

where the linear constraints freeze in at the highest temperature because these bonds are the strongest. If the temperature at the time of observation exceeds the onset temperature of a given constraint, that constraint is broken and $q_\alpha(T)$ in eq 15 becomes zero for that type of constraint. For example, T_g is assumed to be higher than the onset temperature of the γ constraint,[16] hence no γ constraints are considered in the T_g calculation.

Following the constraint counting listed above, the number of constraints in the lithium borate system at the glass transition temperature is given by

$$\begin{aligned} n(x) = {} & 2N(\mathrm{BO}) + 5N(Q^4) + 3N(Q^3) + 2N(Q^2) \\ & + 4N(Q^1) + 6N(Q^0) \end{aligned} \tag{17}$$

Here, the fraction of NBO-forming Li atoms that contribute μ constraints is calculated from the fractions of Q^2, Q^1, and Q^0 structural groups. When combining eqs 14 and 17, we may describe the evolution of T_g as a function of composition x

$$T_g(x) = \min\left[T_\beta, \frac{3 - n(x_R)}{3 - n(x)} T_g(x_R)\right] \tag{18}$$

where T_β is the temperature above which the β constraints are no longer rigid (equal to 760 K following ref 16), the minimum function results from the breakdown of eq 17 when $T_g(x) > T_\beta(x)$ because eq 17 assumes that the β constraints are rigid which is violated when the calculated T_g rises above T_β.

4. RESULTS AND DISCUSSION

To quantify the fractions of the various borate groups at both SRO and IRO length scales, ^{10}B NMR measurements are required, as described by Feller.[28] Because of the small number of borate glasses analyzed by this technique, it complicates the extension of the proposed model to other borate systems. In addition, it is recognized that this measurement and the resulting structural model proposed by Feller is incomplete, failing to account for nonring BO_3 and BO_4 units at the low modifier content. ^{11}B NMR data on binary potassium and rubidium borate glasses indicate that the former is eliminated from the network structure by approximately 30 mol % alkali oxide.[43,44] By assuming here that these structural units are part of the boroxol, tetraborate, and diborate signals of the analyzed ^{10}B NMR data,[28] the present model will capture the evolution of SRO structural units correctly, despite the inconsistencies of the data. In the following, we first predict the IRO structural evolution in the binary lithium borate glass system and then compare the prediction with the experimental data[28] within the glass-forming region. The results are shown in Figure 2. The proposed model shows good agreement with the experimentally obtained data with a coefficient of determination (R^2) value of 0.98. To capture the compositional trend most accurately, all experimental data points were included in modeling. However, a reasonably good agreement can also be obtained by using as few as three reference glasses, as shown in Figure S1 in the Supporting Information.

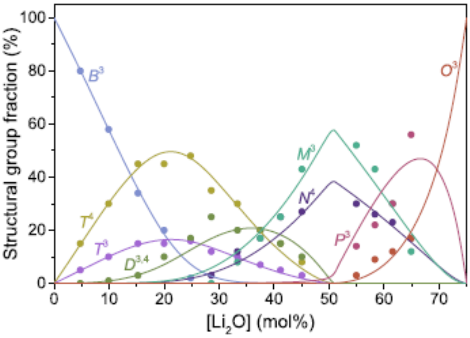

Figure 2. Composition dependence of the fraction of IRO superstructural units (see nomenclature in Figure 1) in the lithium borate glasses. The closed symbols represent experimental data from Feller[28] and the solid lines represent the prediction using the present statistical mechanical model, with the assumption that the glass structure corresponds to the structure of the glass forming liquid at $T_f = T_g$.

The empirical model of Feller divides the structural evolution into three regions, each exhibiting a linear stepwise conversion among the structural groups. On the other hand, the present model captures the disproportionation of the structural groups and expresses the stability of each group through the relative association enthalpy (Table 1). We set H_{B^3} equal to 0 kJ/mol, while all remaining H values are calculated relative to that of H_{B^3}. The probability for a modifier to "draw" species i decreases with the increasing H_i value. For example, the values of H_{M^3} and H_{N^4} are very high compared to the preceding relative H_i values, suggesting that they are less likely to be "drawn" than the diborate and tetraborate groups. As a result, M^3 and N^4 exist almost exclusively at 50 mol % Li_2O concentration (Figure 2). In other words, the energy barrier for a modifier ion to associate with either a metaborate or a nonring BO_4 structural unit is much higher than that for it to associate with either boroxol, tetraborate, or diborate groups. As such, the latter groups must first be depleted before metaborate or nonring BO_4 units are converted upon association with lithium modifier cations.

DOI: 10.1021/acs.jpcb.8b11926
J. Phys. Chem. B 2019, 123, 1206−1213

Table 1. Relative Association Enthalpies (H_i), Where *i* Corresponds to a Given Boron Configuration (See Figure 1), and Coefficient of Determination (R^2) Value for the Fitting of the Current Statistical Mechanical Model to Experimental Structure Data.[28a]

$H_B{}^3$ (kJ/mol)	H_T (kJ/mol)	H_D (kJ/mol)	$H_N{}^4$ (kJ/mol)	$H_M{}^3$ (kJ/mol)	$H_P{}^3$ (kJ/mol)	y	R^2
0	8.8	1.8	29.9	28.9	31.9	0.40	0.980

[a] The uncertainty of the association enthalpy parameters are on the order of ±0.05 kJ/mol. The association enthalpies are scaled relative to that for the B^3 to T conversion ($H_B{}^3$), which is set to 0. y is the constant determining the ratio between M^3 and N^4 boron species.

To couple the present statistical mechanical model with the previously proposed TCT model[16] to predict the composition dependence of T_g, the structural evolution must also be expressed on the SRO length scale, that is, in terms of the fractions (N) of Q^n units, where n ranges from 0 to 4 and denotes the number of BO atoms (i.e., B−O−B linkages) per boron atom. We calculate the fractions of the Q^n units from those of the IRO structural groups as $N(Q^3) = N(B^3) + N(T^3) + N(D^3)$, $N(Q^4) = N(T^4) + N(D^4) + N(L^4)$, $N(Q^2) = N(M^3)$, $N(Q^1) = N(P^3)$, and $N(Q^0) = N(O^3)$. The compositional evolution of SRO is shown in Figure 3, revealing good agreement between model and data. Good agreement is also found when using only three reference compositions (see Figure S2 in the Supporting Information). The boron anomaly is captured by the non-monotonic conversion of Q^3 to either Q^4 or Q^2, depending on the lithium concentration. In this study, we have built a structural model based on the compositional evolution of IRO superstructural units in borate glasses. This IRO model can then be used to calculate the Q^n structural evolution at SRO, and hence, the boron anomaly.

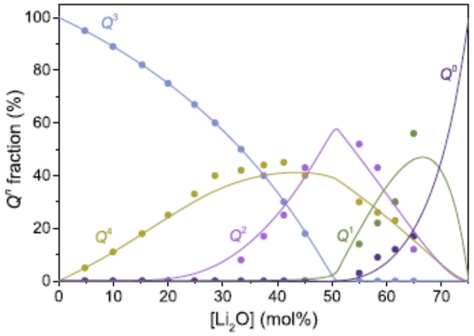

Figure 3. Composition dependence of the fraction of SRO Q^n structural units in lithium borate glasses. The closed symbols represent experimental data from Feller[28] and the solid lines represent the prediction using the present statistical mechanical model, including the assumption that the glass structure corresponds to the structure of the glass forming liquid at $T_f = T_g$.

With the structural model parameters established, we are able to make model predictions of the thermal history dependence of the structural boron speciation. The Q^n distribution (Figure 4a) and the distribution of superstructural units (Figure 4b) have been predicted as a function of fictive temperature for the $40Li_2O-60B_2O_3$ glass composition. As expected, the glass structure becomes more ordered as T_f approaches 0 K, while a random distribution is found as T_f approaches infinity and the system's behavior becomes dominated by entropy. We note that these calculations are strictly model results. We also find that the fraction of Q^4 (Figure 4a) varies nonmonotonically and exhibits a maximum with respect to the variation in fictive temperature. This is due to the competition for modifiers among more than two different independently varying structural units as seen in the evolution of the population of superstructural units with T_f (Figure 4b), where all groups vary monotonically but to different extents. That is, the fractions of tetraborate and diborate structural units are more temperature-dependent at lower fictive temperatures (0−1000 K) than in the higher temperature region, resulting in the nonmonotonic evolution of Q^4 units. The vertical dashed lines in Figure 4 indicate the range of realistically obtainable T_f values ($0.9T_g$ to $1.2T_g$) for each composition. This illustrates how the model captures the non-equilibrium nature of glasses by assuming that the structure of the glass represents that of the metastable supercooled liquid at its T_f. When combining the present composition−structure model with a structure−property model such at TCT, it is thus possible that the optimal property for a given chemical composition is found for $T_f \neq T_g$.

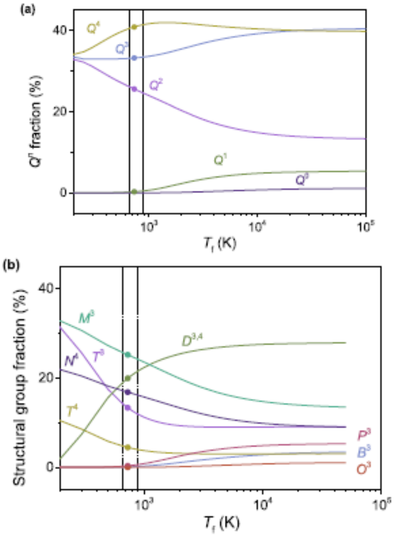

Figure 4. Fictive temperature dependence of the fraction of (a) Q^n structural units and (b) superstructural units in $40Li_2O-60B_2O_3$ (mol %). The solid lines show model predictions, while the closed symbols represent the T_f ($=T_g$) values of the studied glasses and the dashed vertical lines are the limits for the realistically obtainable T_f values.

To investigate the applicability of the present statistical mechanical model, we here attempt to couple it with an already developed TCT structure−property model in order to predict macroscopic glass properties (in this case, glass transition temperature). Using the TCT approach described in Section 3 with the structural input from the statistical mechanical model, the computed values of T_g are compared to experimental values obtained by Chryssikos,[48] Kodama,[49] and Shelby[50] in Figure 5. The dashed line is found by using the same TCT model as in this study, but with the random pair model by Gupta[27] as the structural model for input. The latter does not distinguish between modifier types when predicting the glass structure. With both the random pair model and the present statistical mechanical model as input, good agreement between the measured and predicted values of T_g is found for the lithium borate system, especially at a relatively low modifier content. The prediction becomes less accurate in the high modifier content region, likely because of the inability of the TCT model to accurately account for the effect of Li modifiers on the network rigidity.

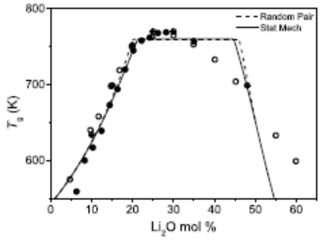

Figure 5. Dependence of the glass transition temperature (T_g) on the fraction of the modifier content in the $Li_2O-B_2O_3$ glasses. The crossed, closed, and open symbols represent experimentally data from Chryssikos,[48] Kodama,[49] and Shelby,[50] respectively. Both model predictions are based on the TCT structure−property model from Smedskjaer et al.,[21] with the dashed and solid lines representing the predictions using the random pair model by Gupta[27] and the present statistical mechanical composition−structure model, respectively.

5. CONCLUSIONS

We have demonstrated that the proposed statistical mechanical model, using a Wallenius-type noncentral hypergeometric distribution with Boltzmann weighting factors, can be used to predict the SRO and IRO structural evolution of binary lithium borate glasses. Specifically, we have found that describing the evolution of IRO structural groups with increasing modifier content is needed to predict the Q^n distribution (SRO) and thus the boron anomaly. This is because the probability for a modifier ion to associate with a given boron species depends on both the IRO environment as well as the local coordination environment of the boron species. Finally, we have shown that the statistical mechanical structure model can be coupled with TCT models to directly predict the composition dependence of the glass transition temperature without any empirical fitting parameters.

■ ASSOCIATED CONTENT

Supporting Information

The Supporting Information is available free of charge on the ACS Publications website at DOI: 10.1021/acs.jpcb.8b11926.

Statistical mechanical calculations of IRO and SRO structural evolution as a function of composition using only three reference glass compositions to fit the model (PDF)

■ AUTHOR INFORMATION

Corresponding Author
*E-mail: mos@bio.aau.dk.

ORCID
John C. Mauro: 0000-0002-4319-3530
Morten M. Smedskjaer: 0000-0003-0476-2021

Notes

The authors declare no competing financial interest.

■ ACKNOWLEDGMENTS

The authors thank C. S. Svendsen and J. K. Nørgaard (Aalborg University) for valuable discussions. This work was supported by the Independent Research Fund Denmark (grant no. 7017-00019).

■ REFERENCES

(1) Bengisu, M. Borate Glasses for Scientific and Industrial Applications: A Review. *J. Mater. Sci.* **2016**, *51*, 2199−2242.
(2) Brow, R. K. Review: The Structure of Simple Phosphate Glasses. *J. Non-Cryst. Solids* **2000**, *263*−*264*, 1−28.
(3) Mysen, B. O.; Richet, P. *Silicate Glasses and Melts Properties and Structure*; Elsevier, 2005.
(4) Hewak, D. *Properties, Processing and Applications of Glass and Rare Earth-Doped Glasses for Optical Fibres*, 1st ed.; INSPEC: Michigan, 1998.
(5) Mauro, J. C. Topological Constraint Theory of Glass. *Am. Ceram. Soc. Bull.* **2011**, *90*, 31−37.
(6) Mauro, J. C.; Tandia, A.; Vargheese, K. D.; Mauro, Y. Z.; Smedskjaer, M. M. Accelerating the Design of Functional Glasses through Modeling. *Chem. Mater.* **2016**, *28*, 4267−4277.
(7) Kuppinger, C. M.; Shelby, J. E. Viscosity and Thermal Expansion of Mixed-Alkali Borate Glasses. *J. Am. Ceram. Soc.* **1986**, *69*, C-292−C-293.
(8) Mahapatra, M. K.; Lu, K.; Reynolds, W. T. Thermophysical Properties and Devitrification of SrO-La2O3-Al2O3-B2O3-SiO2-Based Glass Sealant for Solid Oxide Fuel/Electrolyzer Cells. *J. Power Sources* **2008**, *179*, 106−112.
(9) Youngman, R. E.; Haubrich, S. T.; Zwanziger, J. W.; Janicke, M. T.; Chmelka, B. F. Short-and Intermediate-Range Structural Ordering in Glassy Boron Oxide. *Science* **1995**, *269*, 1416−1420.
(10) Wright, A. C. My Borate Life: An Enigmatic Journey. *Int. J. Appl. Glass Sci.* **2015**, *6*, 45−63.
(11) Lelong, G.; Cormier, L.; Hennet, L.; Michel, F.; Rueff, J.-P.; Ablett, J. M.; Monaco, G. Lithium borate crystals and glasses: How similar are they? A non-resonant inelastic X-ray scattering study around the B and O K -edges. *J. Non-Cryst. Solids* **2017**, *472*, 1−8.
(12) Micoulaut, M. Concepts and Applications of Rigidity in Non-Crystalline Solids: A Review on New Developments and Directions. *Adv. Phys.: X* **2016**, *1*, 147−175.
(13) Wang, M.; Anoop Krishnan, N. M.; Wang, B.; Smedskjaer, M. M.; Mauro, J. C.; Bauchy, M. A New Transferable Interatomic Potential for Molecular Dynamics Simulations of Borosilicate Glasses. *J. Non-Cryst. Solids* **2018**, *498*, 294−304.
(14) Deng, L.; Du, J. Development of Boron Oxide Potentials for Computer Simulations of Multicomponent Oxide Glasses. *J. Am. Ceram. Soc.* **2018**, 1−24.
(15) Zachariasen, W. H. The Atomic Arrangement in Glass. *J. Am. Chem. Soc.* **1932**, *54*, 3841−3851.
(16) Mauro, J. C.; Gupta, P. K.; Loucks, R. J. Composition Dependence of Glass Transition Temperature and Fragility. II. A Topological Model of Alkali Borate Liquids. *J. Chem. Phys.* **2009**, *130*, 234503.

(17) Uhlmann, D. R.; Shaw, R. R. The Thermal Expansion of Alkali Borate Glasses and the Boric Oxide Anomaly. *J. Non-Cryst. Solids* **1969**, *1*, 347−359.

(18) Wright, A. C.; Shakhmatkin, B. A.; Vedishcheva, N. M. The Chemical Structure of Oxide Glasses: A Concept Consistent with Neutron Scattering Studies? *Glass Phys. Chem.* **2001**, *27*, 97−113.

(19) Edén, M. NMR Studies of Oxide-Based Glasses. *Annu. Rep. Prog. Chem., Sect. C: Phys. Chem.* **2012**, *108*, 177.

(20) Kamitsos, E. I.; Chryssikos, G. D. Borate Glass Structure by Raman and Infrared Spectroscopies. *J. Mol. Struct.* **1991**, *247*, 1−16.

(21) Smedskjaer, M. M.; Mauro, J. C.; Sen, S.; Yue, Y. Quantitative Design of Glassy Materials Using Temperature-Dependent Constraint Theory. *Chem. Mater.* **2010**, *22*, 5358−5365.

(22) Smedskjaer, M. M.; Mauro, J. C.; Yue, Y. Prediction of Glass Hardness Using Temperature-Dependent Constraint Theory. *Phys. Rev. Lett.* **2010**, *105*, 115503.

(23) Phillips, J. C. Topology of Covalent Non-Crystalline Solids: Short-Range Order in Chalogenide Alloys. *J. Non-Cryst. Solids* **1995**, *215*, 213−216.

(24) Phillips, J. C.; Thorpe, M. F. Constraint Theory, Vector Percolation and Glass Formation. *Solid State Commun.* **1985**, *53*, 699−702.

(25) He, H.; Thorpe, M. F. Elastic Properties of Glasses. *Phys. Rev. Lett.* **1985**, *54*, 2107−2110.

(26) Ota, R.; Yasuda, T.; Fukunaga, J. Structure of Alkali Borate Glasses Based on the Chemical Equilibrium Concept. *J. Non-Cryst. Solids* **1990**, *116*, 46−56.

(27) Gupta, P. K. *Proceedings of the International Congress on Glass*; Unpublished: New Delhi, India, 1986; p 1.

(28) Feller, S. A.; Dell, W. J.; Bray, P. J. 10B NMR Studies of Lithium Borate Glasses. *J. Non-Cryst. Solids* **1982**, *51*, 21−30.

(29) Xiao, S. Z. Discussion about the Structural Model of "Nuclear Magnetic Resonance Studies of Glasses in the System Na2OB2O3-SiO2. *J. Non-Cryst. Solids* **1981**, *45*, 29−38.

(30) Goyal, S.; Mauro, J. C. Statistical Mechanical Model of Bonding in Mixed Modifier Glasses. *J. Am. Ceram. Soc.* **2018**, *101*, 1906−1915.

(31) Bødker, M. S.; Mauro, J. C.; Goyal, S.; Youngman, R. E.; Smedskjaer, M. M. Predicting Q-Speciation in Binary Phosphate Glasses Using Statistical Mechanics. *J. Phys. Chem. B* **2018**, *122*, 7609−7615.

(32) Araujo, R. J. Statistical Mechanical Model of Boron Coordination. *J. Non-Cryst. Solids* **1980**, *42*, 209−229.

(33) Araujo, R. J. Statistical Mechanics of Chemical Disorder: Application to Alkali Borate Glasses. *J. Non-Cryst. Solids* **1983**, *58*, 201−208.

(34) Bray, P. J.; Mulkern, R. V.; Holupka, E. J. Boron and silicon coordination in oxide glasses: A statistical mechanical model. *J. Non-Cryst. Solids* **1985**, *75*, 37−43.

(35) Youngman, R. E.; Zwanziger, J. W. Multiple Boron Sites in Borate Glass Detected with Dynamic Angle Spinning Nuclear Magnetic Resonance. *J. Non-Cryst. Solids* **1994**, *168*, 293−297.

(36) Faaborg, M.; College, C.; Goranson, K.; Barnes, N.; Troendle, E.; Rice, R.; Chace, M.; Montgomery, L.; Koehler, A.; Lindeberg, Z.; et al. A 10B NMR Study of Trigonal and Tetrahedral Borons in Ring Structured Borate Glasses and Crystals. *Phys. Chem. Glasses: Eur. J. Glass Sci. Technol., Part B* **2015**, *56*, 177−182.

(37) Jellison, G. E.; Bray, P. J. A Structural Interpretation of B10 and B11 NMR Spectra in Sodium Borate Glasses. *J. Non-Cryst. Solids* **1978**, *29*, 187−206.

(38) Kirchner, K. A.; Kim, S. H.; Mauro, J. C. Statistical Mechanics of Topological Fluctuations in Glass-Forming Liquids. *Phys. A* **2018**, *510*, 787−801.

(39) Mauro, J. C. Statistics of Modifier Distributions in Mixed Network Glasses. *J. Chem. Phys.* **2013**, *138*, 12A522.

(40) Fog, A. Sampling Methods for Wallenius' and Fisher's Noncentral Hypergeometric Distributions. *Commun. Stat. Simul. Comput.* **2008**, *37*, 241−257.

(41) Wallenius, K. T. *Biased Sampling; the Noncentral Hypergeometric Probability Distribution*; Technical Report Office of Naval Research, 1963; No. 70.

(42) Mauro, J. C.; Smedskjaer, M. M. Statistical Mechanics of Glass. *J. Non-Cryst. Solids* **2014**, *396−397*, 41−53.

(43) Youngman, R. E.; Zwanziger, J. W. Network Modification in Potassium Borate Glasses: Structural Studies with NMR and Raman Spectroscopies. *J. Phys. Chem.* **1996**, *100*, 16720−16728.

(44) Youngman, R. E.; Zwanziger, J. W. On the Formation of Tetracoordinate Boron in Rubidium Borate Glasses. *J. Am. Chem. Soc.* **1995**, *117*, 1397−1402.

(45) Jones, E.; Oliphant, T.; Peterson, P. *SciPy: Open Source Scientific Tools for Python*, 2001.

(46) Naumis, G. G. Energy Landscape and Rigidity. *Phys. Rev. E: Stat., Nonlinear, Soft Matter Phys.* **2005**, *71*, 026114.

(47) Naumis, G. G. Glass Transition Phenomenology and Flexibility: An Approach Using the Energy Landscape Formalism. *J. Non-Cryst. Solids* **2006**, *352*, 4865−4870.

(48) Chryssikos, G. D.; Duffy, J. A.; Hutchinson, J. M.; Ingram, M. D.; Kamitsos, E. I.; Pappin, A. J. Lithium borate glasses: a quantitative study of strength and fragility. *J. Non-Cryst. Solids* **1994**, *172−174*, 378−383.

(49) Kodama, M.; Kojima, S. Anharmonicity and Fragility in Lithium Borate Glasses. *J. Therm. Anal.* **2002**, *69*, 961−970.

(50) Shelby, J. E. Thermal Expansion of Alkali Borate Glasses. *J. Am. Ceram. Soc.* **1983**, *66*, 225−227.

PAPER III

frontiers in Materials

ORIGINAL RESEARCH
published: 26 July 2019
doi: 10.3389/fmats.2019.00175

Predicting Composition-Structure Relations in Alkali Borosilicate Glasses Using Statistical Mechanics

Mikkel S. Bødker[1], **Søren S. Sørensen**[1], **John C. Mauro**[2] **and Morten M. Smedskjaer**[1]*

[1] Department of Chemistry and Bioscience, Aalborg University, Aalborg, Denmark, [2] Department of Materials Science and Engineering, The Pennsylvania State University, University Park, PA, United States

Predicting the atomic-scale structure of multicomponent glasses from their composition and thermal history would greatly accelerate the discovery of new engineering and functional glasses. A statistical mechanics-based approach has recently been applied to predict the composition-structure evolution in binary oxide glasses by determining the relative entropic and enthalpic contributions to the bonding preferences. In this work, we first establish the network modifier-former interaction parameters in sodium silicate and sodium borate glasses to predict the structural evolution in sodium borosilicate glasses. Due to the significant variations in the experimentally determined structural speciation in borosilicate glasses, we perform classical molecular dynamics (MD) simulations to establish and validate our structural model. We also show that the statistical mechanical model naturally accounts for the difference in structural speciation from MD simulations and NMR experiments, which in turn arises from the difference in cooling rate and thus thermal history of the glasses. Finally, we demonstrate the predictive capability of the model by accurately accounting for the structural evolution in potassium borosilicate glasses without using any adjustable model parameters. This is possible, because all the interaction parameters are already established in the potassium silicate, potassium borate, and sodium borosilicate glasses, respectively.

Keywords: glass, borosilicates, modeling, statistical mechanics, structure

Edited by:
Matthieu Micoulaut,
Sorbonne Universités, France

Reviewed by:
Jean-Marc Delaye,
Commissariat à l'Energie Atomique et aux Energies Alternatives (CEA), France
Roman Golovchak,
Austin Peay State University, United States

***Correspondence:**
Morten M. Smedskjaer
mos@bio.aau.dk

Specialty section:
This article was submitted to Glass Science,
a section of the journal Frontiers in Materials

***Received:** 22 May 2019*
***Accepted:** 08 July 2019*
***Published:** 26 July 2019*

Citation:
Bødker MS, Sørensen SS, Mauro JC and Smedskjaer MM (2019) Predicting Composition-Structure Relations in Alkali Borosilicate Glasses Using Statistical Mechanics.
Front. Mater. 6:175.
doi: 10.3389/fmats.2019.00175

INTRODUCTION

A multitude of applications of oxide glasses exist, including in the fields of construction materials (Almutawa et al., 2013), electronic substrates (Rahman and Padavettan, 2012), medical technology (Day et al., 2011), etc. There is thus a need to continually develop new glass compositions with physical and chemical properties tuned for each specific application (Naumis, 2005; Mauro, 2014; Mauro et al., 2016) while fulfilling a number of criteria related to their production, including glass-forming ability, cost, emissions, toxicity, refractory compatibility, etc. To accelerate the pace of glass composition development, correlations between the atomic-scale structure of glasses and their macroscopic properties need to be established, for example based on topological constraint theory (Mauro, 2011; Micoulaut, 2016; Smedskjaer et al., 2017; Bauchy, 2019).

Oxide glasses are composed of network formers (such as Si, B, or P), which form the structural backbone and are linked together through bridging oxygen (BO). Network modifiers (such as Na or Ca) break the backbone by forming non-bridging oxygen (NBO) or stabilizing negatively charged network formers. Such short range order (SRO) rearrangements have been intensively investigated using various analytical tools, including solid state nuclear magnetic resonance (NMR) spectroscopy (Youngman, 2018), neutron diffraction (Fischer et al., 2006), and Raman spectroscopy (Neuville et al., 2014). Despite the significant advances within these technologies, the SRO analysis of glasses remains a tedious task due to their non-crystalline nature (Mauro, 2014) and the fact that they feature wide bond angle and length distributions. The SRO of glasses can be accurately characterized in simple compositions with only two to maybe three oxide components, whereas the accuracy drops for multicomponent compositions (Eckert, 2018). Moreover, predicting the structural descriptors (such as average coordination number of network formers) in multicomponent glasses is often impossible with the current models available. Recently, a statistical mechanics based model (Mauro, 2013) has been applied to determine relative enthalpy barriers for modifiers to associate with the various network former units in binary modifier-former glasses (Bødker et al., 2018, 2019). In this work, we attempt to transfer the enthalpy barriers established for binary alkali borate and alkali silicate glasses to predict the structural evolution in ternary alkali borosilicate glasses.

Borosilicate glasses are among the most utilized glasses, e.g., as thermal shock resistant glassware (Lima and Monteiro, 2001) and nuclear waste immobilization (Plodinec, 2000), and their composition-structure relations have thus been intensively investigated (Martens and Müller-Warmuth, 2000). Addition of modifier cations can increase the connectivity of the glass by charge-stabilizing tetrahedral boron (Lelong et al., 2017), but also reduce it by depolymerizing silicon structural units, and at high modifier concentrations also boron. The network formers' competition for modifier cations depends on the Si/B ratio, as described by Bray (1985) and Araujo (1980). However, to our knowledge, a comprehensive composition-structure model, accounting for the quantitative boron and silicon speciation as function of Si/B ratio and modifier content and type(s), has not yet been developed. Knowledge of the evolution of structural units with modifier concentration and Si/B ratio is needed for predicting the properties of borosilicate glasses directly from their composition (for a fixed thermal and pressure history; Smedskjaer et al., 2011).

To gain additional information about the structure of borosilicate glasses, molecular dynamics (MD) simulations have also been conducted based on recent force field developments (Deng and Du, 2018; Wang et al., 2018). The timescales in MD simulations are typically reduced to the nanosecond scale (Micoulaut, 2016), resulting in typical quenching rates in the range of 1–10 K/ps. This leads to a much higher fictive temperature (T_f) in simulated glasses compared to experimental glasses. As a result, the structures of the MD-generated glasses have been frozen in at a higher temperature than the experimental counterparts, giving rise to distributions of structural units that are more entropically dominated (Tomozawa et al., 2005). Despite this disadvantage of the MD simulations, they provide additional structural details, including the complete atomic configuration (Massobrio et al., 2015). Moreover, structural analysis of the experimentally synthesized glasses also comes with some disadvantages, such as uncertainties related to the actual chemical composition (especially if it is not analyzed), inhomogeneity or phase separation, partial crystallization, and thermal history differences. In addition, there are uncertainties related to the data analysis, such as deconvolution of NMR spectra. For alkali borosilicate glasses, we have found that the reported structures (determined by NMR spectroscopy) differ significantly from study to study and even within the same studies for the nominally same glass compositions. For example, the fraction of Si with four BOs in Na_2O-B_2O_3-$2SiO_2$ has been found to be 0 and 57% by Bhasin et al. (1998) and Nanba et al. (2004), respectively, while the fraction of four-fold coordinated boron in Na_2O-B_2O_3-$1.33SiO_2$ has been reported to be both 44 and 62% in the same study (Martens and Müller-Warmuth, 2000).

To overcome these problems in this study, we first show how the statistical mechanics model of SRO structure established based on experimental NMR data can be linked to that based on MD simulations data. With this link established, we will then show that we can predict the structure of MD-simulated ternary sodium borosilicate glasses by first establishing relative enthalpic and entropic bonding preferences in binary sodium borates and silicates. To do so, we only need one additional parameter, namely, the modifiers' relative preference for associating with a silicate structural group relative to a borate structural group. This newly established parameter is then used to predict the structural evolution in potassium borosilicate glasses without any free parameters. These iterations will be based on structural data obtained by NMR experiments and MD simulations, including results from literature (Maekawa et al., 1991; Bhasin et al., 1998; Du and Cormack, 2004; Adkins and Cormack, 2011; Schuch et al., 2011; Deng and Du, 2018) for sodium borate, sodium silicate, and sodium borosilicate glasses as well as new MD simulations performed in this study for potassium borosilicate glasses.

MOLECULAR DYNAMICS SIMULATIONS

Glass Preparation

Twelve glasses in the family of RK_2O-B_2O_3-$KSiO_2$ (see **Table S1**) were simulated by MD using LAMMPS (Plimpton, 1995). A combined potential of the Coulomb and Buckingham potential was used in combination with a potential spline for low values of separation to avoid the Buckingham catastrophe. We refer to the work of Deng and Du for details on the potential and potential spline (Deng and Du, 2018). The force field parameters and quenching procedure have also been taken from that study (Deng and Du, 2018). This includes using varying values for the B-O interaction according to the values of R and K. Cut-offs for all short-range interactions were 11 Å while long range Coulombic interactions were computed directly below 11 Å and using the Particle-Particle-Particle-Mesh (PPPM) method with a relative accuracy of 10^{-5} above 11 Å. A timestep of 1 fs was used for all simulations. Initially ~3,000 atoms were placed randomly in a simulation box with a density ~2% lower than the experimental value to allow for more realistic dynamics in the melt, while avoiding any unrealistic overlaps. This was followed by a potential energy minimization and 60 ps of equilibration in the NVT ensemble at 300 K. The temperature was then set to 6,000 K, allowing the system to equilibrate for 100 ps, followed by a step function to 5,000 K and another isothermal equilibration for 100 ps, both in the NVT ensemble. The system was then quenched from 5,000 to 300 K at 5 K/ps in the NVT ensemble, followed by structural relaxation at 300 K for 60 ps at zero pressure in the NPT ensemble. Finally, this was followed by another 60 ps of structural relaxation in the NVT ensemble.

Structural and Thermal Analysis

The number of BOs and NBOs associated with each silicon species was evaluated by first counting the number of oxygens within the first coordination shell of every boron and oxygen atom. In addition to providing the degree of connectivity around the Si atoms, it also yields the coordination number of boron as a function of composition. The potential used in the simulations has already been verified elsewhere (Deng and Du, 2018). This analysis was followed by counting the number of boron and silicon within the first coordination shell of all oxygens, hence categorizing each oxygen as either bridging or non-bridging. These two pieces of information were then combined to yield the number of NBOs associated with every boron and silicon atom in each simulation. All structural characteristics were averages of 10 structures from the final NVT equilibration.

Fictive temperatures (T_f) were found by employing the method of Liu et al. (2018). This method uses local ground-state enthalpy as a function of temperature to estimate T_f, giving very well-defined transitions compared to common methods of temperature-enthalpy plots as the method only considers the enthalpy of the atomic configuration at each temperature, leaving out contributions of atom dynamics.

STATISTICAL MECHANICAL STRUCTURE MODEL

The statistical mechanical model used herein to predict the modifier-former associations in mixed network former glasses was first proposed by Mauro (2013) and later implemented and validated on binary oxide glasses by Bødker et al. (2018, 2019). The model is based on the assumption that the probability for the initially added network modifier to interact with a certain network former atom depends on the relative statistical entropy (i.e., the fraction of microstates consistent with the macrostate of each network former) and the relative enthalpic barrier for the modifier to break the bonds associated with each network former. Here, the microstates refer to the SRO structural units as each of these correspond to a specific potential energy, while the macrostate is the sum of structural units consistent with a given network former. Using Na_2O-B_2O_3-SiO_2 as an example, the probability for sodium to associate with a borate unit depends on the statistical entropy of boron (i.e., the fraction of boron to silicon content) and the enthalpic energy barrier for this interaction, relative to the enthalpic barrier of the sodium-silicon interaction. This is analogous to calculating the probabilities for drawing a red marble from an urn with both red and blue marbles with different sizes. If we know the relative fraction of the red marbles, i.e., the statistical entropy, and their relative size compared to blue marbles (analogous to the enthalpy barrier in the glass system), we can calculate the probability to draw a red marble over a blue using a non-central (weighted) distribution function (Mauro and Smedskjaer, 2014). In the glass system, we assume that the energy barrier for a modifier to interact with the network former is constant regardless of the composition. The statistical entropy of each network former species does, however, change upon interactions with a modifier ion, since a drawn species is not replaced. This results in a hypergeometric distribution that describes the evolution of network former species as a function of the modifier concentration. As the entropy of the system changes with composition, so does the probability for the modifier-former interaction, requiring a numerical solution to predict the structural evolution of network former species.

To establish the model (Mauro, 2013), we first consider the Boltzmann distribution function (Schwabl, 2006) that describes the probability (i.e., the weighting factor) for a system to be in a given state as a function of the system's temperature and the energy of that state,

$$p_i = \frac{e^{-\frac{\varepsilon_i}{kT}}}{\sum_{i=1}^{M} e^{-\frac{\varepsilon_i}{kT}}}, \tag{1}$$

where p_i is the probability of state i, k is the Boltzmann constant, T is the temperature of the system, ε_i is the total energy of state i, and M is the total number of states. Here, p_i describes the probability for a network modifier to interact with a given network former species i, and consequently, ε_i becomes the free energy of this interaction, which may be described by entropic and enthalpic contributions,

$$p_i = \frac{e^{-\frac{H_i - S_i T}{kT}}}{\sum_{i=1}^{M} e^{-\frac{H_i - S_i T}{kT}}}. \tag{2}$$

Next, we introduce the statistical entropy of the system as,

$$S_i = k \ln \Omega_i \tag{3}$$

where, Ω_i is the number of microstates consistent with a given macrostate for species i,

$$p_i = \frac{e^{-\frac{H_i - k \ln \Omega_i T}{kT}}}{\sum_{i=1}^{M} e^{-\frac{H_i - k \ln \Omega_i T}{kT}}}. \tag{4}$$

We then obtain,

$$p_i = \frac{e^{-\frac{H_i}{kT} + \ln \Omega_i}}{\sum_{i=1}^{M} e^{-\frac{H_i}{kT} + \ln \Omega_i}}, \tag{5}$$

or,

$$p_i = \frac{\Omega_i e^{-\frac{H_i}{kT}}}{\sum_{i=1}^{M} \Omega_i e^{-\frac{H_i}{kT}}}. \tag{6}$$

The number of microstates consistent with the macrostate of species i divided by the total number of microstates consistent with the macrostate of the oxide glass will be the same as the relative fraction of species i divided by the total number of species. Since the fraction of a given structural species i in the glass changes with composition, we obtain

$$\Omega_{i,\omega} = (g_i - n_{i,\omega}), \tag{7}$$

where ω represents a given modifier concentration, g_i is the degeneracy (initial fraction) of species i, and $n_{i,\omega}$ is the total fraction of species i that has already interacted at modifier concentration ω. ω represents an absolute quantity of modifier ions, but we have converted it to a relative concentration for easy comparison with the experimental data. When calculating the probability of an interaction with species i at concentration ω, we must use the fraction of species i at the previous concentration step ($\omega-1$),

$$p_{i,\omega} = \frac{(g_i - n_{i,\omega-1})e^{-\frac{H_i}{kT}}}{\sum_{i=1}^{M}\sum_{j=0}^{\omega-1}(g_i - n_{i,j})e^{-\frac{H_i}{kT}}}. \tag{8}$$

The double summation in the denominator is over all species M and the accumulated number of successful interactions of species i after j number of attempts ($n_{i,j}$) up to but not including the current modifier concentration ω. For each concentration step, the fraction $n_{i,\omega}$ of network former species i interacting with the modifier ion can be calculated from the probability of the interaction and its fraction at the previous concentration step $\omega-1$. Then, that fraction is subtracted from the remaining amount of network forming species i at the next concentration, which is used to calculate the new probability and so on. Hence, the probability distribution function in Equation (8) is a type of non-central hypergeometric distribution function, where the relative enthalpy H_i values are the free parameters when fitting to experimental data. We define $e^{-\frac{H_i}{kT}}$ as the weighting factor w_i for a modifier to interact with the structural group i, where T is assumed to be equal to T_f for $T < T_f$, since the structure is assumed to freeze in at the fictive temperature:

$$p_{i,\omega} = \frac{(g_i - n_{i,\omega-1})w_i}{\sum_{i=1}^{M}\sum_{j=0}^{\omega-1}(g_i - n_{i,j})w_i}, \tag{9}$$

where,

$$w_i = e^{-\frac{H_i}{kT_f}}. \tag{10}$$

The application of Equation (9) to predict the structure of binary oxide glasses has been described in detail elsewhere (Bødker et al., 2018, 2019). Here, we will use the M_2O-B_2O_3-SiO_2 system, where M is an alkali metal, to explain the numerical procedure when calculating the compositional dependence of structural units with the present model. The SRO structural units of interest in the silicate part of the borosilicate network are the Q^n units, where n is the number of BO per tetrahedron ($n = 0, 1, 2, 3$, or 4), while those of interest in the borate part are the B^n units, again with $n = 0, 1, 2, 3$, or 4.

First, following our previous study of alkali borate glasses (Bødker et al., 2019), we consider the reaction mechanisms for B^3 and B^4 structural groups when interacting with an alkali modifier oxide (M_2O),

$$2B^3 + M_2O \rightarrow 2B^4, \tag{11}$$

$$2B^3 + M_2O \rightarrow 2B^2. \tag{12}$$

These two reactions describe the boron anomaly, where a three-fold coordinated B^3 structural unit may either form a four-fold coordinated B^4 structural unit without NBOs or a three-fold coordinated B^2 unit with one NBO. Previous studies (Uhlmann and Shaw, 1969; Yiannopoulos et al., 2001) have shown that Equation (11) dominates at low modifier concentration, while Equation (12) dominates at higher modifier concentration. To capture this so-called boron anomaly in this study, we introduce a critical concentration above which a parameter ($\alpha_{B4/B2}$) changes from 1 to 0, allowing only one of the two reactions to occur at any point. This is a structural simplification, but as it will be shown, it enables us to establish a simple model, yet predict the structural evolution with sufficient accuracy. An additional complication occurs when a network modifier interacts with a B^4 unit,

$$2B^4 + M_2O \rightarrow 2B^2 + M_2O. \tag{13}$$

As the modifier concentration increases, the B^4 structural units will begin to become converted to B^2 units, forming new NBOs on either boron or silicon units close to the initial B^4 unit. Then the modifier cations interact with the newly created NBOs. Equation (9) is used to calculate the fraction of the introduced modifier at each concentration step that initiates the conversion of a B^4 structural unit; hence the fraction of free modifier is also known and must be included in the interactions at each ω. Analogous to our work on alkali phosphate glasses[13], the following depolymerization reactions occur for all silicate structural units [and similarly for the B^2 and B^1 structural units (Bødker et al., 2019)],

$$2Q^n + M_2O \rightarrow 2Q^{n-1}. \tag{14}$$

With all the possible modifier interactions established, the fractions of the structural units at concentration ω are calculated as,

$$B^3_{\omega} = B^3_{\omega-1} - p_{B^3,\omega} - p_{B^4,\omega} \cdot p_{B^3,\omega}, \tag{15}$$

$$B^4_{\omega} = B^4_{\omega-1} + p_{B^3,\omega} \cdot \alpha_{B^4/B^2} - p_{B^4,\omega}. \tag{16}$$

That is, the fraction of B^3 at modifier concentration step ω ($B^3{}_{\omega}$) equals the fraction of B^3 at the previous concentration step ($B^3_{\omega-1}$) minus the fraction that reacts at ω ($p_{B^3,\omega}$) and also minus the fraction of B^4 that is converted to B^2 multiplied by the probability for the B^3 to react ($p_{B^4,\omega} \cdot p_{B^3,\omega}$). The latter is needed, since the extra modifier from a B^4 group (Equation 13) will react according to the bonding preference at this composition. In Equation (16), the number of B^4 units will increase proportionally to the fraction of B^3 units drawn (Equation 11), but only until the critical modifier concentration, where $\alpha_{B4/B2}$ changes from 1 to 0. Additional examples are given for B^2 and Q^3 structural units as,

$$B^2_\omega = B^2_{\omega-1} + p_{B^3,\omega}\cdot\left(1-\alpha_{B^4/B^2}\right) + p_{B^4,\omega} + p_{B^4,\omega}\cdot p_{B^3,\omega} - p_{B^2,\omega} - p_{B^4,\omega}\cdot p_{B^2,\omega} \tag{17}$$

$$Q^3_\omega = Q^3_{\omega-1} + p_{Q^4,\omega} + p_{B^4,\omega}\cdot p_{Q^4,\omega} - p_{Q^3,\omega} - p_{B^4,\omega}\cdot p_{Q^3,\omega} \tag{18}$$

In Equation (17), the fraction of B^2 units will increase when a B^3 is drawn (Equation 12) only when $\alpha_{B4/B2}$ is 0 and always when B^3 is drawn by the modifiers released by B^4 ($p_{B^4,\omega}\cdot p_{B^3,\omega}$). Additionally, the fraction of B^2 will increase when a B^4 is converted and become reduced when the modifier draws a B^2 either initially ($p_{B^2,\omega}$) or after being released from a B^4 ($p_{B^4,\omega}\cdot p_{B^2,\omega}$). The fractions of Q^4, Q^3,… Q^0, B^1, and B^0 will increase according to the probability of their n+1 species to be drawn, but at the same time decrease according to the probability for the modifier to interact with that unit as shown in the Q^3 example in Equation (18). Further explanation of the modeling procedure is given elsewhere (Bødker et al., 2019). Typically, the fitting parameters of the model would be all the relative H_i values (or w_i, if T_f is unknown), but in this study, the relative H_i values are first established in binary sodium borate glasses and sodium silicate glasses (as demonstrated in section Validating Structure Model for Alkali Silicate and Borate Glasses below). These H_i values are then transferred to predict the structural evolution in the sodium borosilicate glasses with only one free parameter, the conversion factor ($w_{Si,B}$). This parameter is needed, since all enthalpy values are calculated relatively within each system, i.e., the H_{Q3} in the sodium silicate is relative to the H_{Q4} parameter, while the H_{B2} in sodium borate is relative to the H_{B3} parameter.

Modeling of the composition-structure evolution in the binary and ternary systems to obtain the H_i values was performed in the object-oriented programming language Python. Here, the Basinhopping optimization method (part of the SciPy package) is used (Jones et al., 2001), since it attempts to find the global minimum in the parameter space by repeating the optimization with different guessed values of the starting parameters and solving for the structure in a self-consistent fashion. Additionally, all simulations were repeated five to 10 times with different starting values.

RESULTS AND DISCUSSION

Validating Structure Model for Alkali Silicate and Borate Glasses

The statistical mechanical model has previously been established in binary phosphate (Bødker et al., 2018) and borate glasses (Bødker et al., 2019), but not yet in binary silicate glasses. The modeling procedure for silicate glasses is the same as for binary phosphate glasses (Bødker et al., 2018). Here, we apply this approach to sodium silicates (**Figure 1A**) and potassium silicates (**Figure 1B**) based on ^{29}Si MAS NMR data from literature (Schroeder et al., 1973; Maekawa et al., 1991). To obtain relative H_i values for these glasses, we extrapolated the T_g values found in literature (**Table S2**) (Schroeder et al., 1973; MacDonald et al., 1985; Belova et al., 2015) using simple regression to estimate a T_g value for each modifier concentration step (ω). As shown in **Figure 1**, the model accurately captures the evolution of structural Q^n units with the modifier concentration using the fitted H_i values as reported in **Table 1**. Similarly, the modeling of the structure of sodium borate (Shelby, 1983; Schuch et al., 2011) and potassium borate (Zhong and Bray, 1989) systems based on ^{11}B MAS NMR data is shown in **Figures S1a,b**, with the corresponding T_g values from literature in **Table S2**. Only the fraction of B^4 is obtained from ^{11}B MAS NMR so these fits have been made using Equations (15) and (16) in section Statistical Mechanical Structure Model. Due to the limited amount of experimental data, these H_i values are very sensitive to any experimental uncertainties, which is especially the case for H_3 and H_4 of the borate glasses in the high modifier regions.

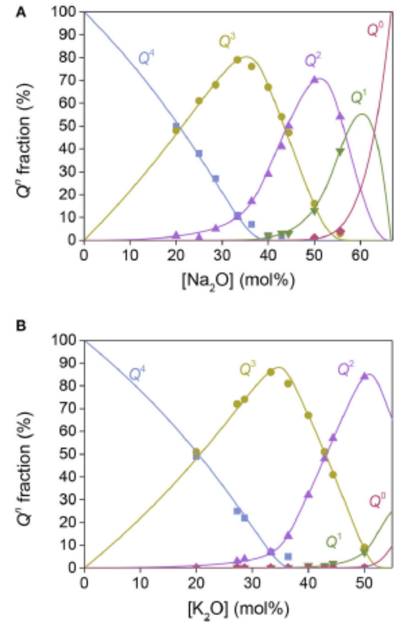

FIGURE 1 | Composition dependence of the fraction of Q^n structural units in **(A)** sodium silicate and **(B)** potassium silicate glasses. The closed symbols represent ^{29}Si MAS NMR experimental data (from Maekawa et al., 1991 for sodium and Schroeder et al., 1973 and Maekawa et al., 1991 for potassium) and the solid lines represent the model predictions.

TABLE 1 | Relative association enthalpies (H_i), where *i* corresponds to a given structural configuration, for the fitting of the current statistical mechanical model to experimental structure data.

Glass system	Na_2O-SiO_2	K_2O-SiO_2	Na_2O-B_2O_3	K_2O-B_2O_3
H_1 (kJ/mol)	0	0	0	0
H_2 (kJ/mol)	14.1	18.8	8.4	6.0
H_3 (kJ/mol)	22.9	35.2	7.4	21.4
H_4 (kJ/mol)	27.1	32.8	28.5	28.3
α_{B^4/B^2}	–	–	35.5	35.4

The following structural configurations are considered: Q^4, Q^3, Q^2, and Q^1 for i = 1, 2, 3, and 4, respectively, in the silicate system and B^3, B^4, B^2, and B^1 for i = 1, 2, 3, and 4, respectively, in the borate system. The uncertainty of the association enthalpy parameters is on the order of ±0.05 kJ/mol. α_{B^4/B^2} is the fitted average critical modifier concentration, where Equation (12) starts occurring instead of Equation (11).

Reconciling Structure Data From Experiments and MD Simulations

Simulated quenching of liquid to glasses using MD requires the use of high cooling rates, in turn yielding higher T_f values for MD glasses compared to experimental glasses. In other words, the structure freezes in at a higher temperature and becomes more entropically controlled. Assuming that the enthalpic contributions to the modifier-former interactions are the same for experimental and MD simulated glasses, the present statistical mechanical model should be able to predict the structural evolution in a MD simulated glass system based on the difference in fictive temperature. **Figure 2A** shows the Q^n speciation in a 35Na_2O-65SiO_2 glass as a function of T_f, including model predictions, experimental data from ^{29}Si NMR spectroscopy (Maekawa et al., 1991), and simulations data from a previous MD study (Adkins and Cormack, 2011). The good agreement between model and data confirms the hypothesis that the present model can be used to describe the MD simulated structure of oxide glasses based on experimentally obtained NMR data (or vice versa) with only T_f as the free parameter. Likewise, **Figure 2B** shows the fraction of four-fold coordinated boron (B^4) in a 40Li_2O-60B_2O_3 glass as a function of T_f, including model predictions from our previous study (Bødker et al., 2019) based on the fractions of superstructural units, experimental data from ^{10}B NMR spectroscopy (Feller et al., 1982). Since the fraction of B^4 varies non-monotonically with the fictive temperature according to the model (Bødker et al., 2019), the values of B^4 fraction from NMR and MD are almost identical, in agreement with previous studies (Xu et al., 1988; Ohtori et al., 2001).

In **Figure 1A**, the structural units in the Na_2O-SiO_2 system are plotted against the modifier concentration, where the solid symbols represent ^{29}Si NMR data (Maekawa et al., 1991) and the lines as model predictions with known T_g values (MacDonald et al., 1985; Belova et al., 2015) with the resulting H_i parameters as reported in **Table 1**. Next, we use the obtained H_i values from the binary sodium silicate glasses (**Table 1**) to predict the structural evolution of the MD simulated Na_2O-SiO_2 glasses (Du and Cormack, 2004; Adkins and Cormack, 2011), with only an adjustable conversion factor from experimental T_g values to predicted T_f values (**Figure 3**). The excellent agreement suggests that we can predict MD simulated structures based on input from experimental structure data and the thermal history of the MD simulated glasses. With the link established between experimental and MD simulated glass structures, we are now able to utilize the proposed model to predict realistic glass structures of alkali borosilicates based only on knowledge of MD simulated glass structures. As it will be shown below, this becomes useful for multicomponent systems with composition fluctuations, phase separation, uncertain NMR deconvolutions, etc.

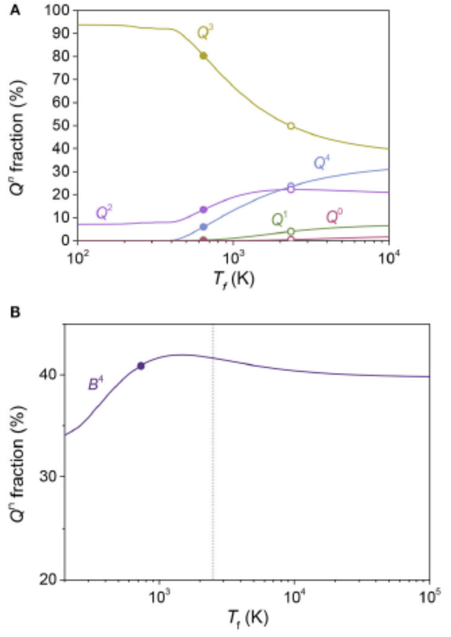

FIGURE 2 | The fraction of structural units in **(A)** 35Na_2O-65SiO_2 and **(B)** 40Li_2O-60B_2O_3 glasses as a function of fictive temperature (T_f). **(A)** The closed symbols represent ^{29}Si MAS-NMR experimental data (Maekawa et al., 1991), the open symbols represent MD simulated data (Adkins and Cormack, 2011), and the solid lines represent the model predictions. **(B)** The closed symbol represent ^{10}B NMR experimental data (Feller et al., 1982) and the dashed line is an estimate of T_f of the MD simulated glass. The solid line represents the model prediction.

Structure Model for Sodium Borosilicate Glasses

^{29}Si NMR data of silica-containing glasses can be challenging to deconvolute, e.g., due to the bond angle distribution contributing to very broad and overlapping peaks (Mahler and Sebald, 1995).

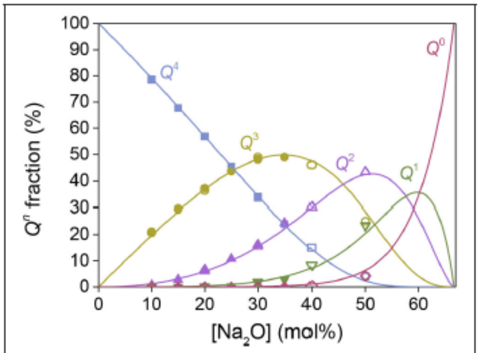

FIGURE 3 | Composition dependence of the fraction of Q^n structural units in sodium silicate glasses. The closed and open symbols represent MD simulated data obtained by Du and Cormack (2004) and Adkins and Cormack (2011), respectively. The solid lines represent model predictions, using the same bonding preferences parameter, but a different fictive temperature compared to **Figure 1A**.

In binary alkali silicate glasses, the chemical composition of the glasses may be used to constrain the deconvolution by assuming neutral charge balance in the glass and that all modifiers interact with the structure, significantly improving the accuracy of the deconvolution. However, in borosilicate glasses, determination of the boron speciation typically only involves quantification of the boron coordination number with no distinction of symmetric (only BO) and asymmetric (one or more NBO) trigonal boron units. In this case, the chemical composition of the glasses cannot be used to constrain the ^{29}Si NMR deconvolution, since the fraction of modifier associated with the boron species is unknown. **Figure 4A** shows the statistical mechanics-based model predictions compared to experimental data obtained by ^{11}B and ^{29}Si NMR spectroscopy techniques (Bhasin et al., 1998; Nanba et al., 2004) in the sodium borosilicate system. These predictions were made with only the relative Si/B weighting factor ($w_{\mathrm{Si},\mathrm{B}}$) as a free parameter. All H_i values and α_{B^4/B^2} were transferred from the binary silicate and borate glasses, as reported in **Table 1**. The compositional evolution of $\mathrm{Q^n}$ and $\mathrm{B^n}$ speciation are shown in **Figures 4B,C**, respectively, for glasses with $K = 2$. Model vs. experiments comparisons for other B/Si ratios (i.e., K value) are shown in **Figure S2**. Overall we find that although the major trends in Q^n and B^n with composition are captured by the model (with only one adjustable parameter), there are relatively large deviations in the absolute values Q^n and B^n between model and experiments.

To overcome the abovementioned experimental uncertainties associated with structure determination in borosilicate glasses, we next attempt to predict the composition dependence of silicon and boron speciation in MD simulated sodium borosilicate glasses, again based on the relative H_i values obtained separately in sodium silicate and sodium borate glasses (**Table 1**). **Figure 5A** shows the comparison of model predictions with MD simulated

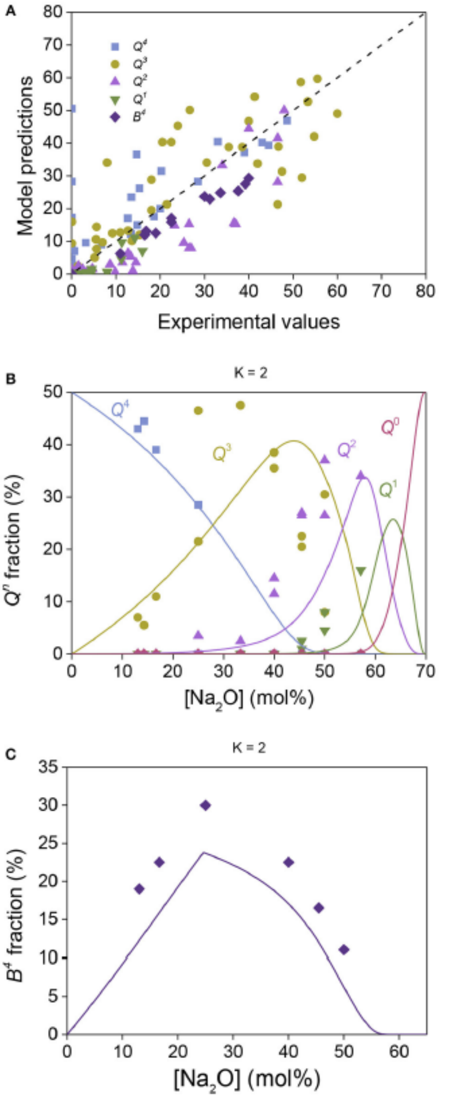

FIGURE 4 | Sodium borosilicate structural data obtained by ^{29}Si and ^{11}B MAS NMR (Bhasin et al., 1998; Nanba et al., 2004) compared to model predictions. **(A)** All experimental data plotted against the model predictions, with the dashed line showing a one-to-one correlation. **(B)** Composition dependence of Q^n fractions in sodium borosilicate glasses with $K = 2$, where the symbol represents experimental data by ^{29}Si MAS NMR and the lines are

(Continued)

FIGURE 4 | model predictions. **(C)** Composition dependence of the fraction of four-fold coordinated boron (B^4) in sodium borosilicate glasses with $K = 2$ as obtained by ^{11}B MAS-NMR (symbols) and the model predictions (line).

data (Deng and Du, 2018), obtained with only $w_{Si,B}$ as a fitting parameter found to be 0.16. The compositional evolution of Q^n and B^n speciation are shown in **Figures 5B,C**, respectively, for glasses with $K = 2$, with additional comparisons given in **Figure S3**. Overall, we observe excellent agreement between the model predictions and MD data with only one adjustable parameter, supporting the assumption that the H_i values can be transferred from simple binary systems to multi-component systems containing the same interactions as in the binary glasses.

Structure Prediction of Potassium Borosilicate Glasses Without Free Parameters

To further test the validity and universality of the present model, the obtained $w_{Si,B}$ weighting factor from the sodium borosilicate glasses is transferred (along with the H_i values from **Table 1**) to predict the structural evolution in potassium borosilicate glasses. The structure data for these glasses are determined based on the MD simulations performed in this study (see section Molecular Dynamics Simulations). **Figure 6A** illustrates the general agreement between model predictions and MD data, while **Figures 6B,C** show the predicted Q^n and B^n speciation, respectively, as a function of the modifier concentration for $K = 2$ (similar plots for $K = 4$ and 6 are shown in **Figure S4**). All the parameters used in the model have been obtained from different systems, namely, H_i and α_{B^4/B^2} values from potassium silicate and potassium borate glasses (**Table 1**) and $w_{Si,B} = 0.16$ from the sodium borosilicate glasses (section Structure model for sodium borosilicate glasses). In other words, no fitting is needed to obtain the model predictions. We note that a small amount of four-fold coordinated boron with one NBO is observed in the MD simulations (up to ~2% of the structure), but since this unit is not observed in the experimental data, it has been included as three-fold coordinated boron with two NBOs. This discrepancy is likely due to the use of the Buckingham potential and the higher fictive temperatures of the MD simulated glasses, resulting in a higher probability for energetically unfavorable structures.

To correct for the thermal history difference, the T_f values for the MD simulated glasses have been determined by extrapolating experimental data (Grandjean et al., 2008) the same way as shown in **Figure 2A**, i.e., all T_f values have been scaled with a constant relative to the experimental values. The predicted T_f values by this method are generally in good agreement with those determined by using the method of Liu et al. (2018) (see **Figure S5**).

Perspectives

Taking alkali borosilicate glasses as an example, we have found good agreement between the predicted values and those determined by MD simulations and also established a link

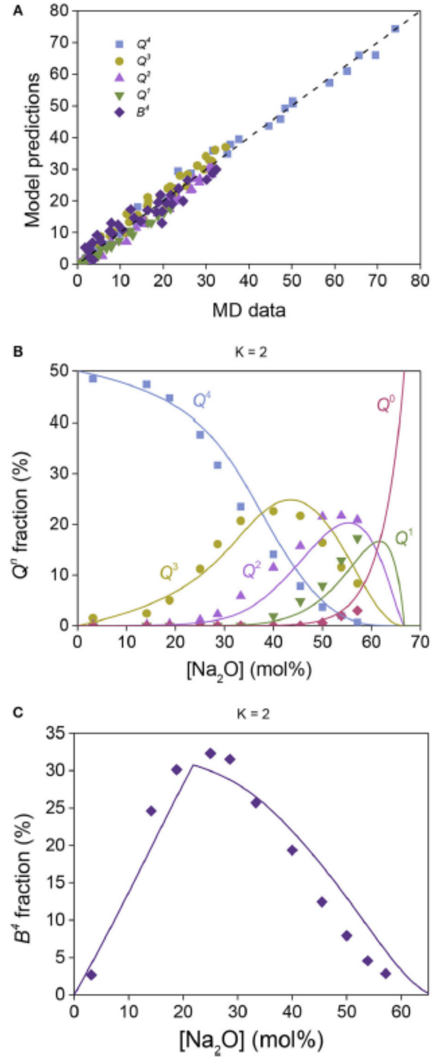

FIGURE 5 | Sodium borosilicate structural data obtained by MD simulations (Deng and Du, 2018) compared to model predictions. **(A)** All experimental data plotted against the model predictions, where the dashed line shows the one-to-one correlation. **(B)** Q^n fractions for silicate structural groups (symbols) and model predictions (lines) plotted against the overall modifier concentration for glasses with $K = 2$. **(C)** Fraction of four-fold coordinated boron as obtained by MD simulations (symbols) and the model predictions (line) against the overall modifier concentration for glasses with $K = 2$.

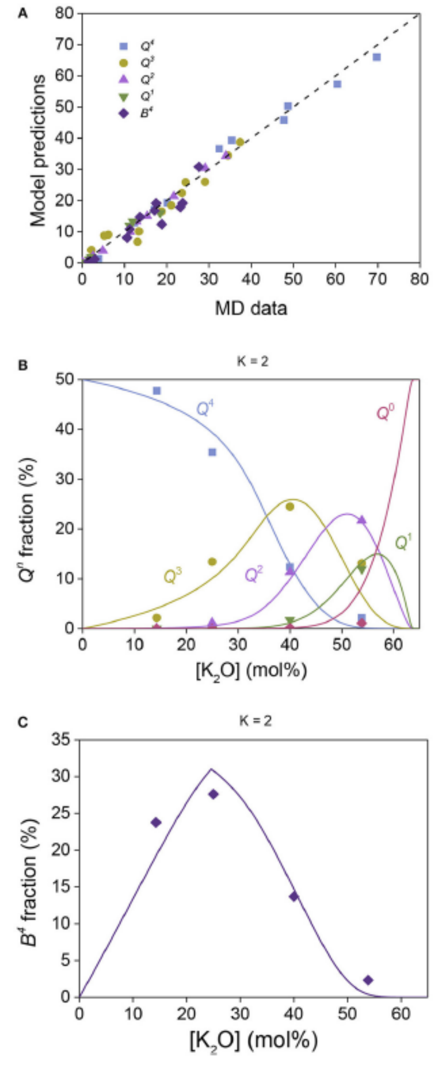

FIGURE 6 | Potassium borosilicate structural data obtained by MD simulations compared to model predictions with zero free parameters. **(A)** All experimental data plotted against the model predictions, where the dashed line shows the one-to-one correlation. **(B)** Q^n fractions for silicate structural groups (symbols) and model predictions (lines) plotted against the overall modifier concentration for glasses with $K = 2$. **(C)** Fraction of four-fold coordinated boron as obtained by MD simulations (symbols) and model predictions (line) plotted against the overall modifier concentration for glasses with $K = 2$.

between MD simulated structures in glasses and their melt-quenched counterparts. We expect this approach can be applied to predict the structure of various multicomponent glasses based on knowledge of the structure of the binary glasses that they are constituted by. This would greatly reduce the experimental or simulation time needed to predict the composition-structure evolution in multicomponent glasses. In this study, we included model predictions of glasses that contained two or three of the following four components: Na_2O, K_2O, B_2O_3, and SiO_2. This required model simulations on four types of binary glasses, namely, Na_2O-SiO_2, K_2O-SiO_2, Na_2O-B_2O_3, and K_2O-B_2O_3. Building on these four simulations, we would in principle be able to predict seven different glass systems, such as K_2O-Na_2O-B_2O_3-SiO_2, K_2O-B_2O_3-SiO_2, K_2O-Na_2O-SiO_2, etc. However, to predict the composition-structure evolution in all these systems, the effect of mixing different types of modifiers on the structure should be accounted for. The probability distributions of interactions in mixed modifier systems have already been developed (Goyal and Mauro, 2018), but still need to be verified experimentally. Another limitation of the model is the T_f dependence of the predicted structural units. If the model is used to predict the structural evolution in compositions not yet established by MD or experiments, a model of thermal history dependence must be incorporated to iteratively estimate the structural evolution and evolution of T_f simultaneously.

As the number of oxide components increases, the number of required simulations would increase linearly, whereas the number of systems predicted from the simulations would increase exponentially. This makes the present approach a promising tool for screening the atomic scale structure of many multicomponent oxide-based glasses. Such prediction would especially be useful when it is coupled with a relevant structure-property model. Finally, we note that the present approach predicts the mean structures of a given composition. Recently, Kirchner et al. (2018) and Kirchner and Mauro (2019) proposed a statistical mechanics-based method to explore topological fluctuations in the glass structure and properties, which would be interesting to couple with the present composition-structure model for borosilicate glasses in future work.

CONCLUSIONS

We have shown that a structure model based on the Boltzmann distribution can be used to predict the structure of ternary borosilicate glasses by transferring model parameters from simpler glasses with some of the same components. We started by using experimental structure data for sodium silicate and sodium borate glasses to determine the relative enthalpy values for sodium to interact with each structural group within the network. Using these values, we then applied the model to predict the structural evolution in sodium borosilicate glass system with only one free parameter to account for the relative propensity for the sodium modifier to interact with the silicate and borate part of the network. This parameter is required since the determined enthalpy values are relative, not absolute. With the $w_{Si,B}$ parameter established for the sodium borosilicate system, we used the model to accurately predict the structural evolution in potassium borosilicate glasses without any free parameters, in this case building on transferred enthalpy values from experimental data of potassium silicate and potassium borate glasses. Finally, we have also shown that the statistical mechanical model is able to predict both experimental and MD structure data using only the fictive temperature as the scaling parameter.

DATA AVAILABILITY

The datasets generated for this study are available on request to the corresponding author.

AUTHOR CONTRIBUTIONS

MS and MB designed the study. MB performed the statistical mechanical modeling and Python programming. SS performed the MD simulations. MB and MS wrote the manuscript with revisions from JM and SS. All authors participated in discussing the data.

FUNDING

This work was supported by the Independent Research Fund Denmark (grant no. 7017-00019). Computational resources were provided by the DeIC National HPC Center (ABACUS 2.0) at the University of Southern Denmark and funded by Aalborg University.

ACKNOWLEDGMENTS

We thank Sushmit Goyal (Corning Inc.), Randall E. Youngman (Corning Inc.), Jincheng Du (University of North Texas), and Mathieu Bauchy (University of California, Los Angeles) for valuable discussions.

SUPPLEMENTARY MATERIAL

The Supplementary Material for this article can be found online at: https://www.frontiersin.org/articles/10.3389/fmats.2019.00175/full#supplementary-material

REFERENCES

Adkins, L., and Cormack, A. (2011). Large-scale simulations of sodium silicate glasses. *J. Non Cryst. Solids* 357, 2538–2541. doi: 10.1016/j.jnoncrysol.2011.03.012

Almutawa, F., Vandal, R., Wang, S. Q., and Lim, H. W. (2013). Current status of photoprotection by window glass, automobile glass, window films, and sunglasses. *Photodermatol. Photoimmunol. Photomed.* 29, 65–72. doi: 10.1111/phpp.12022

Araujo, R. J. (1980). Statistical mechanical model of boron coordination. *J. Non Cryst. Solids* 42, 209–230. doi: 10.1016/0022-3093(80)90023-X

Bauchy, M. (2019). Deciphering the atomic genome of glasses by topological constraint theory and molecular dynamics: a review. *Comput. Mater. Sci.* 159, 95–102. doi: 10.1016/j.commatsci.2018.12.004

Belova, E. V., Kolyagin, Y. A., and Uspenskaya, I. A. (2015). Structure and glass transition temperature of sodium-silicate glasses doped with iron. *J. Non Cryst. Solids* 423–424, 50–57. doi: 10.1016/j.jnoncrysol.2015.04.039

Bhasin, G., Bhatnagar, A., Bhowmik, S., Stehle, C., Affatigato, M., Feller, S., et al. (1998). Short range order in sodium borosilicate glasses obtained via deconvolution of ^{29}Si MAS NMR spectra. *Phys. Chem. Glass.* 39, 269–274.

Bødker, M. S., Mauro, J. C., Goyal, S., Youngman, R. E., and Smedskjaer, M. M. (2018). Predicting Q-speciation in binary phosphate glasses using statistical mechanics. *J. Phys. Chem. B* 122, 7609–7615. doi: 10.1021/acs.jpcb.8b04604

Bødker, M. S., Mauro, J. C., Youngman, R. E., and Smedskjaer, M. M. (2019). Statistical mechanical modeling of borate glass structure and topology: prediction of superstructural units and glass transition temperature. *J. Phys. Chem. B* 123, 1206–1213. doi: 10.1021/acs.jpcb.8b11926

Bray, P. J. (1985). Structural models for borate glasses. *J. Non Cryst. Solids* 75, 29–36. doi: 10.1016/0022-3093(85)90198-X

Day, D. E., Tomsia, A. P., Jung, S. B., Sonny Bal, B., Fu, Q., Rahaman, M. N., et al. (2011). Bioactive glass in tissue engineering. *Acta Biomater.* 7, 2355–2373. doi: 10.1016/j.actbio.2011.03.016

Deng, L., and Du, J. (2018). Development of boron oxide potentials for computer simulations of multicomponent oxide glasses. *J. Am. Ceram. Soc.* 102, 2482–2505. doi: 10.1111/jace.16082

Du, J., and Cormack, A. N. (2004). The medium range structure of sodium silicate glasses: a molecular dynamics simulation. *J. Non Cryst. Solids* 349, 66–79. doi: 10.1016/j.jnoncrysol.2004.08.264

Eckert, H. (2018). Spying with spins on messy materials: 60 years of glass structure elucidation by NMR spectroscopy. *Int. J. Appl. Glas. Sci.* 9, 167–187. doi: 10.1111/ijag.12333

Feller, S. A., Dell, W. J., and Bray, P. J. (1982). ^{10}B NMR studies of lithium borate glasses. *J. Non Cryst. Solids* 51, 21–30. doi: 10.1016/0022-3093(82)90186-7

Fischer, H. E., Barnes, A. C., and Salmon, P. S. (2006). Neutron and x-ray diffraction studies of liquids and glasses. *Rep. Prog. Phys.* 69, 233–299. doi: 10.1088/0034-4885/69/1/R05

Goyal, S., and Mauro, J. C. (2018). Statistical mechanical model of bonding in mixed modifier glasses. *J. Am. Ceram. Soc.* 101, 1906–1915. doi: 10.1111/jace.15364

Grandjean, A., Malki, M., Montouillout, V., Debruycker, F., and Massiot, D. (2008). Electrical conductivity and 11B NMR studies of sodium borosilicate glasses. *J. Non Cryst. Solids* 354, 1664–1670. doi: 10.1016/j.jnoncrysol.2007.10.007

Jones, E., Oliphant, T., and Peterson, P. (2001). *SciPy: Open Source Scientific Tools for Python*. Available online at: http://www.scipy.org/ (accessed May 15, 2019).

Kirchner, K. A., Kim, S. H., and Mauro, J. C. (2018). Statistical mechanics of topological fluctuations in glass-forming liquids. *Phys. A Stat. Mech. Appl.* 510, 787–801. doi: 10.1016/j.physa.2018.07.028

Kirchner, K. A., and Mauro, J. C. (2019). Statistical mechanical model of the self-organized intermediate phase in glass-forming systems with adaptable network topologies. *Front. Mater.* 6:11. doi: 10.3389/fmats.2019.00011

Lelong, G., Cormier, L., Hennet, L., Michel, F., Rueff, J. P., Ablett, J. M., et al. (2017). Lithium borate crystals and glasses: how similar are they? A non-resonant inelastic X-ray scattering study around the B and O K-edges. *J. Non Cryst. Solids* 472, 1–8. doi: 10.1016/j.jnoncrysol.2017.06.012

Lima, M. M., and Monteiro, R. (2001). Characterisation and thermal behaviour of a borosilicate glass. *Thermochim. Acta* 373, 69–74. doi: 10.1016/S0040-6031(01)00456-7

Liu, Z., Hu, Y., Li, X., Song, W., Goyal, S., Micoulaut, M., et al. (2018). Glass relaxation and hysteresis of the glass transition by molecular dynamics simulations. *Phys. Rev. B* 98:104205. doi: 10.1103/PhysRevB.98.104205

MacDonald, W. M., Anderson, A. C., and Schroeder, J. (1985). Low-temperature behavior of potassium and sodium silicate glasses. *Phys. Rev. B* 31, 1090–1101. doi: 10.1103/PhysRevB.31.1090

Maekawa, H., Maekawa, T., Kawamura, K., and Yokokawa, T. (1991). The structural groups of alkali silicate glasses determined from 29Si MAS-NMR. *J. Non Cryst. Solids* 127, 53–64. doi: 10.1016/0022-3093(91)90400-Z

Mahler, J., and Sebald, A. (1995). Deconvolution of 29Si magic-angle spinning nuclear magnetic resonance spectra of silicate glasses revisited -

some critical comments. *Solid State Nucl. Magn. Reson.* 5, 63–78. doi: 10.1016/0926-2040(95)00027-N

Martens, R., and Müller-Warmuth, W. (2000). Structural groups and their mixing in borosilicate glasses of various compositions - an NMR study. *J. Non Cryst. Solids* 265, 167–175. doi: 10.1016/S0022-3093(99)00693-6

Massobrio, C., Du, J., Bernasconi, M., and Salmon, P. S. (2015). *Molecular Dynamics Simulations of Disordered Materials*. Cham: Springer International Publishing.

Mauro, J. C. (2011). Topological constraint theory of glass. *Am. Ceram. Soc. Bull.* 90, 31–37.

Mauro, J. C. (2013). Statistics of modifier distributions in mixed network glasses. *J. Chem. Phys.* 138:12A522. doi: 10.1063/1.4773356

Mauro, J. C. (2014). Grand challenges in glass science. *Front. Mater.* 1:20. doi: 10.3389/fmats.2014.00020

Mauro, J. C., and Smedskjaer, M. M. (2014). Statistical mechanics of glass. *J. Non Cryst. Solids* 396–397, 41–53. doi: 10.1016/j.jnoncrysol.2014.04.009

Mauro, J. C., Tandia, A., Vargheese, K. D., Mauro, Y. Z., and Smedskjaer, M. M. (2016). Accelerating the design of functional glasses through modeling. *Chem. Mater.* 28, 4267–4277. doi: 10.1021/acs.chemmater.6b01054

Micoulaut, M. (2016). Concepts and applications of rigidity in non-crystalline solids: a review on new developments and directions. *Adv. Phys. X* 6149, 1–29. doi: 10.1080/23746149.2016.1161498

Nanba, T., Nishimura, M., and Miura, Y. (2004). A theoretical interpretation of the chemical shift of ^{29}Si NMR peaks in alkali borosilicate glasses. *Geochim. Cosmochim. Acta* 68, 5103–5111. doi: 10.1016/j.gca.2004.05.042

Naumis, G. G. (2005). Energy landscape and rigidity. *Phys. Rev. E Stat. Nonlin. Soft Matter Phys.* 71:026114. doi: 10.1103/PhysRevE.71.026114

Neuville, D. R., de Ligny, D., and Henderson, G. S. (2014). Advances in Raman spectroscopy applied to earth and material sciences. *Rev. Mineral. Geochem.* 78, 509–541. doi: 10.2138/rmg.2013.78.13

Ohtori, N., Takase, K., Akiyama, I., Suzuki, Y., Handa, K., Sakai, I., et al. (2001). Short-range structure of alkaline-earth borate glasses by pulsed neutron diffraction and molecular dynamics simulation. *J. Non Cryst. Solids* 293–295, 136–145. doi: 10.1016/S0022-3093(01)00662-7

Plimpton, S. (1995). Fast parallel algorithms for short-range molecular dynamics. *J. Comput. Phys.* 117, 1–19. doi: 10.1006/jcph.1995.1039

Plodinec, M. J. (2000). Borosilicate glasses for nuclear waste imobilisation. *Glas. Technol.* 41, 186–192.

Rahman, I. A., and Padavettan, V. (2012). Synthesis of silica nanoparticles by sol-gel: size-dependent properties, surface modification, and applications in silica-polymer nanocomposites—a review. *J. Nanomater.* 2012:132424. doi: 10.1155/2012/132424

Schroeder, J., Mohr, R., Macedo, P., and Montrose, C. (1973). Rayleigh and Brillouin scattering in K_2O-SiO_2 glasses. *J. Am. Ceram. Soc.* 10, 510–514. doi: 10.1111/j.1151-2916.1973.tb12399.x

Schuch, M., Trott, C., and Maass, P. (2011). Network forming units in alkali borate and borophosphate glasses and the mixed glass former effect. *RSC Adv.* 1, 1370–1382. doi: 10.1039/c1ra00583a

Schwabl, F. (2006). *Statistical Mechanics. 2nd Edn*. Garching: Springer US.

Shelby, J. E. (1983). Thermal expansion of alkali borate glasses. *J. Am. Ceram. Soc.* 66, 225–227. doi: 10.1111/j.1151-2916.1983.tb10023.x

Smedskjaer, M. M., Hermansen, C., and Youngman, R. E. (2017). Topological engineering of glasses using temperature-dependent constraints. *MRS Bull.* 42, 29–33. doi: 10.1557/mrs.2016.299

Smedskjaer, M. M., Mauro, J. C., Youngman, R. E., Hogue, C. L., Potuzak, M., and Yue, Y. (2011). Topological principles of borosilicate glass chemistry. *J. Phys. Chem. B* 115, 12930–12946. doi: 10.1021/jp208796b

Tomozawa, M., Hong, J. W., and Ryu, S. R. (2005). Infrared (IR) investigation of the structural changes of silica glasses with fictive temperature. *J. Non Cryst. Solids* 351, 1054–1060. doi: 10.1016/j.jnoncrysol.2005.01.017

Uhlmann, D. R., and Shaw, R. R. (1969). The thermal expansion of alkali borate glasses and the boric oxide anomaly. *J. Non Cryst. Solids* 1, 347–359. doi: 10.1016/0022-3093(69)90018-0

Wang, M., Anoop Krishnan, N. M., Wang, B., Smedskjaer, M. M., Mauro, J. C., and Bauchy, M. (2018). A new transferable interatomic potential for molecular dynamics simulations of borosilicate glasses. *J. Non Cryst. Solids* 498, 294–304. doi: 10.1016/j.jnoncrysol.2018.04.063

Xu, Q., Kawamura, K., and Yokokawa, T. (1988). Molecular dynamics calculations for boron oxide and sodium borate glasses. *J. Non Cryst. Solids* 104, 261–272. doi: 10.1016/0022-3093(88)90397-3

Yiannopoulos, Y. D., Chryssikos, G. D., and Kamitsos, E. I. (2001). Structure and properties of alkaline earth borate glasses. *Phys. Chem. Glas.* 42, 164–172.

Youngman, R. (2018). NMR spectroscopy in glass science: a review of the elements. *Materials* 11, E476. doi: 10.3390/ma11040476

Zhong, J., and Bray, P. J. (1989). Change in boron coordination in alkali borate glasses, and mixed alkali effects, as elucidated by NMR. *J. Non Cryst. Solids* 111, 67–76. doi: 10.1016/0022-3093(89)90425-0

Conflict of Interest Statement: The authors declare that the research was conducted in the absence of any commercial or financial relationships that could be construed as a potential conflict of interest.

Appendix A. Binary Phosphate Python Script

As an example of the procedure of fitting the statistical mechanics-based model to experimentally obtained data, below is shown the python script used to accomplish that in the binary phosphate glasses (the simplest system and simplest code).

First the file from which the data is imported is defined by the same name as in the folder on the computer. Next, empty lists are made for each column of data, that is the modifier concentration and the corresponding Q^n units for that modifier concentration. With the open command, the file is opened and read as a .csv file. Then, the data is appended to the empty lists created at the top of the script. On lines 31 to 35, all values in the lists are converted to floats – floats refer to numbers with decimals and this is done since the data is always imported as string values (as letters). Finally, the lists are converted to numpy arrays which are basically the same as lists but allows for more math operations.

```
 7 import numpy as np
 8 import matplotlib.pyplot as plt
 9 import csv
10 import scipy.optimize
11 import math
12 import os
13
14 fil = 'ZnO_phosphate'
15
16 mod_data = []
17 Q3_data = []
18 Q2_data = []
19 Q1_data = []
20 Q0_data = []
21
22 with open(f"{fil}.csv", newline='') as csvfile:
23     spamreader = csv.reader(csvfile, delimiter=';', quotechar='|')
24     for row in spamreader:
25         mod_data.append(row[0])
26         Q3_data.append(row[1])
27         Q2_data.append(row[2])
28         Q1_data.append(row[3])
29         Q0_data.append(row[4])
30
31 mod_data = [float(i) for i in mod_data]
32 Q3_data = [float(i) for i in Q3_data]
33 Q2_data = [float(i) for i in Q2_data]
34 Q1_data = [float(i) for i in Q1_data]
35 Q0_data = [float(i) for i in Q0_data]
36
37 Q3_data = np.array(Q3_data)
38 Q2_data = np.array(Q2_data)
39 Q1_data = np.array(Q1_data)
40 Q0_data = np.array(Q0_data)
```

On line 42 and 43, a numpy array is formed consisting of draw numbers running from 1 to 300. Next, the modifier concentration corresponding to each draw (when 100 draws equal 1 modifier ion for 1 P atom). Finally, on line 57 the Tg estimation function for zinc phosphates is defined (based on literature data).

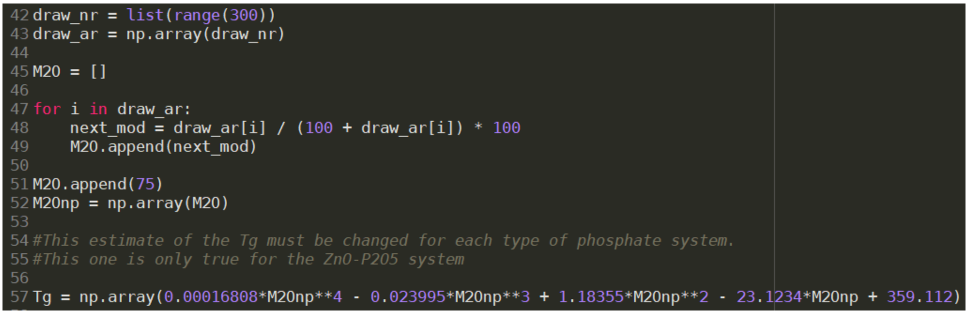

```
42 draw_nr = list(range(300))
43 draw_ar = np.array(draw_nr)
44
45 M20 = []
46
47 for i in draw_ar:
48     next_mod = draw_ar[i] / (100 + draw_ar[i]) * 100
49     M20.append(next_mod)
50
51 M20.append(75)
52 M20np = np.array(M20)
53
54 #This estimate of the Tg must be changed for each type of phosphate system.
55 #This one is only true for the ZnO-P2O5 system
56
57 Tg = np.array(0.00016808*M20np**4 - 0.023995*M20np**3 + 1.18355*M20np**2 - 23.1234*M20np + 359.112)
```

On line 59 the model function which will be used to fit the enthalpy values is defined and takes a list of enthalpy parameters as input. Inside the function, an array of parameters is defined from the function input on line 61. Since the weighting factors for the statistical mechanics-based model changes with the T_g, a specific weighting factor is calculated for each draw number in lines 66 to 89.

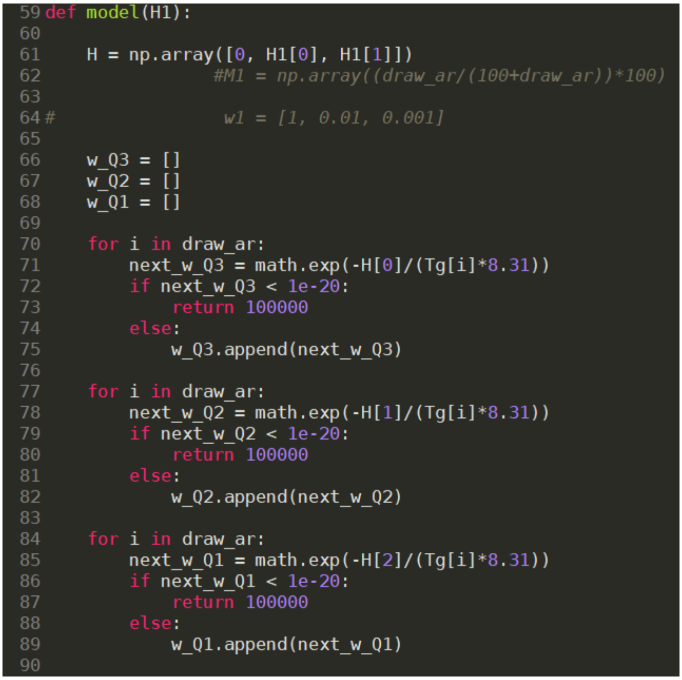

```
59 def model(H1):
60
61     H = np.array([0, H1[0], H1[1]])
62                 #M1 = np.array((draw_ar/(100+draw_ar))*100)
63
64 #                w1 = [1, 0.01, 0.001]
65
66     w_Q3 = []
67     w_Q2 = []
68     w_Q1 = []
69
70     for i in draw_ar:
71         next_w_Q3 = math.exp(-H[0]/(Tg[i]*8.31))
72         if next_w_Q3 < 1e-20:
73             return 100000
74         else:
75             w_Q3.append(next_w_Q3)
76
77     for i in draw_ar:
78         next_w_Q2 = math.exp(-H[1]/(Tg[i]*8.31))
79         if next_w_Q2 < 1e-20:
80             return 100000
81         else:
82             w_Q2.append(next_w_Q2)
83
84     for i in draw_ar:
85         next_w_Q1 = math.exp(-H[2]/(Tg[i]*8.31))
86         if next_w_Q1 < 1e-20:
87             return 100000
88         else:
89             w_Q1.append(next_w_Q1)
90
```

Still inside the “model” function, the prediction of each Q^n specie is defined as empty lists, except for the starting value at draw/modifier content 0. Then a loop is run for each number in the “draw” list. For each loop, the probabilities for each interaction is calculated based on the last value in the prediction list and the weighting factors at the given draw nr. Then the change in population for each Q^n unit is calculated as “next_Qn” and “appended” (added to the end) to their respective lists.

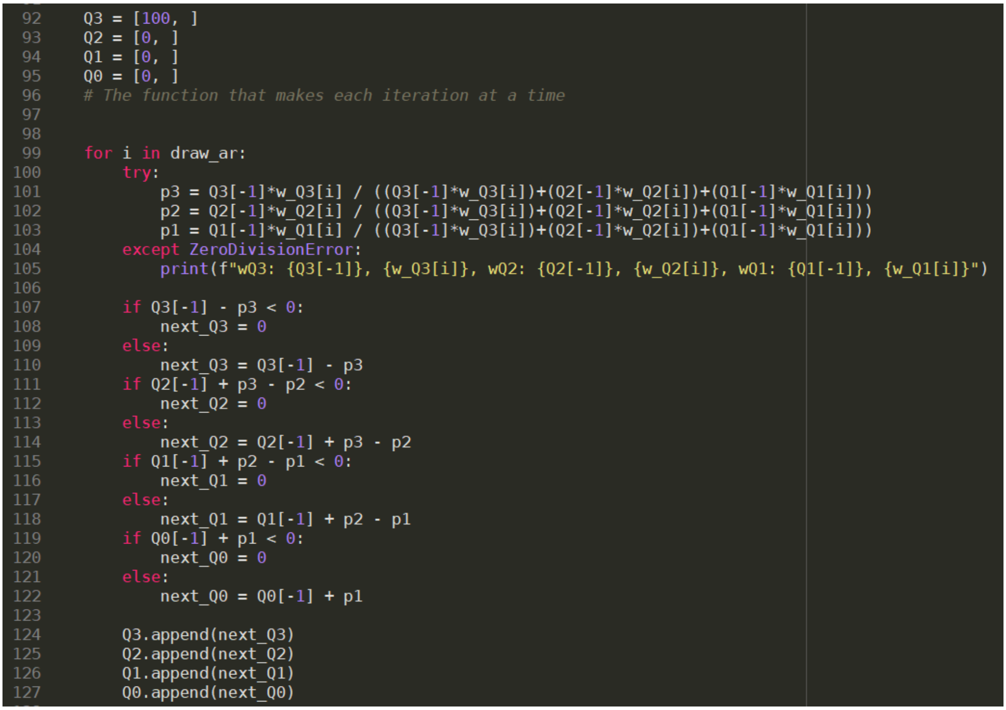

```python
    Q3 = [100, ]
    Q2 = [0, ]
    Q1 = [0, ]
    Q0 = [0, ]
    # The function that makes each iteration at a time


    for i in draw_ar:
        try:
            p3 = Q3[-1]*w_Q3[i] / ((Q3[-1]*w_Q3[i])+(Q2[-1]*w_Q2[i])+(Q1[-1]*w_Q1[i]))
            p2 = Q2[-1]*w_Q2[i] / ((Q3[-1]*w_Q3[i])+(Q2[-1]*w_Q2[i])+(Q1[-1]*w_Q1[i]))
            p1 = Q1[-1]*w_Q1[i] / ((Q3[-1]*w_Q3[i])+(Q2[-1]*w_Q2[i])+(Q1[-1]*w_Q1[i]))
        except ZeroDivisionError:
            print(f"wQ3: {Q3[-1]}, {w_Q3[i]}, wQ2: {Q2[-1]}, {w_Q2[i]}, wQ1: {Q1[-1]}, {w_Q1[i]}")

        if Q3[-1] - p3 < 0:
            next_Q3 = 0
        else:
            next_Q3 = Q3[-1] - p3
        if Q2[-1] + p3 - p2 < 0:
            next_Q2 = 0
        else:
            next_Q2 = Q2[-1] + p3 - p2
        if Q1[-1] + p2 - p1 < 0:
            next_Q1 = 0
        else:
            next_Q1 = Q1[-1] + p2 - p1
        if Q0[-1] + p1 < 0:
            next_Q0 = 0
        else:
            next_Q0 = Q0[-1] + p1

        Q3.append(next_Q3)
        Q2.append(next_Q2)
        Q1.append(next_Q1)
        Q0.append(next_Q0)
```

For the optimization, the program needs an error between the experimental data which was loaded into the script in the beginning and the predicted values. To do so, a new set of lists are created in line 132-135 “Qn_m” which is going to be the predicted values that has the same modifier content as the imported data. In lines 137 to 139, the mod_m list is built to consist of values from the predicted modifier list that are as close as possible to the values in the mod_data list. In lines 141 to 159, we find the index in the predicted modifier list, that corresponds to each value in the mod_m list. That is, we are going to know at which position in the list of numbers, the modifier concentrations that correspond to the experimental data is found. We then take the value from the predicted Q^n units at that same index and append them to the “Qn_m” lists. Hence, the “Qn_m” lists are going to consist of a value for each experimental data that corresponds to the prediction at the same modifier content as the experimental data.

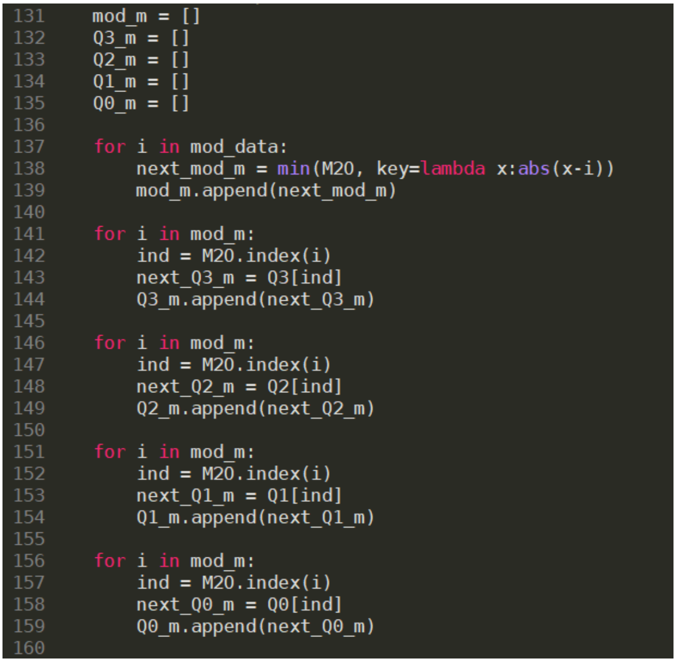

```
131     mod_m = []
132     Q3_m = []
133     Q2_m = []
134     Q1_m = []
135     Q0_m = []
136 
137     for i in mod_data:
138         next_mod_m = min(M20, key=lambda x:abs(x-i))
139         mod_m.append(next_mod_m)
140 
141     for i in mod_m:
142         ind = M20.index(i)
143         next_Q3_m = Q3[ind]
144         Q3_m.append(next_Q3_m)
145 
146     for i in mod_m:
147         ind = M20.index(i)
148         next_Q2_m = Q2[ind]
149         Q2_m.append(next_Q2_m)
150 
151     for i in mod_m:
152         ind = M20.index(i)
153         next_Q1_m = Q1[ind]
154         Q1_m.append(next_Q1_m)
155 
156     for i in mod_m:
157         ind = M20.index(i)
158         next_Q0_m = Q0[ind]
159         Q0_m.append(next_Q0_m)
160 
```

Finally, we define an SSE value that is calculated by summing the squared differences between the experimentally obtained- and predicted values. The function then returns the value so when the function is run with a set of parameters as input, the SSE is returned only.

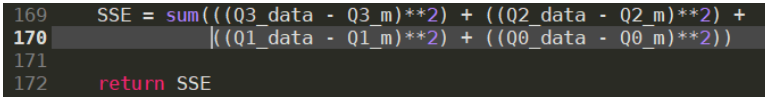

```
169     SSE = sum(((Q3_data - Q3_m)**2) + ((Q2_data - Q2_m)**2) +
170               ((Q1_data - Q1_m)**2) + ((Q0_data - Q0_m)**2))
171 
172     return SSE
```

With the model defined, all we need to do is run the optimization with the enthalpy values as free parameters. In line 174, we define two random starting values of 55 and 85 kj/mol (the unit is due to the value chosen for the Boltzman constant in lines 71 to 89). In line 189, we define “res” to be the results after running the scipy.optimize.basinhopping function, using the “model” function as we defined and the “H1” parameters. The basinhopping function will start by running a standard optimization of the starting parameters, where the values are changes in a direction that returns a lower value when running the “model” function until it reaches a minimum. Since such an optimization process may have several local minima, the basinhopping function attempts to get to another minima by redoing the optimization but with a new set of starting values (hence the name “Basin-Hopping”). It will keep redoing the optimization with new starting values “niter” number of times, in the below code, 10 times. For the results published, all simulations were done with at least

5000 iterations and repeated at least 10 times. Once finished, the results in the “res” parameter may be used to plot the best prediction of the data.

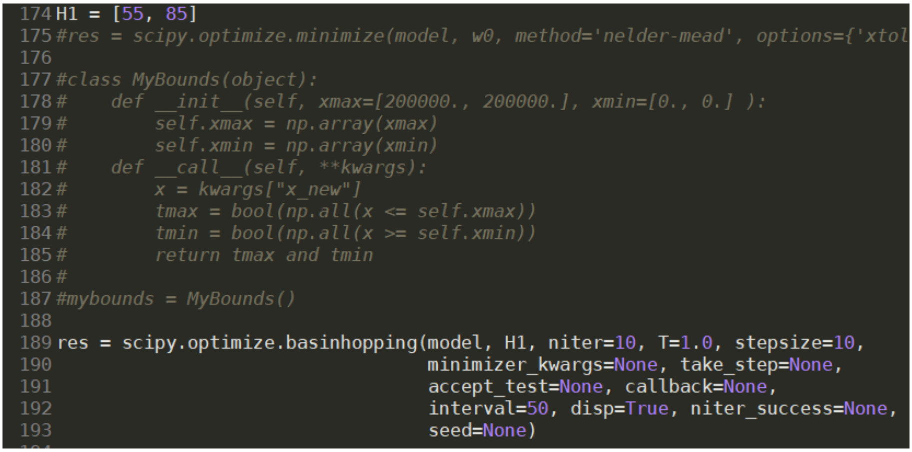

```
H1 = [55, 85]
#res = scipy.optimize.minimize(model, w0, method='nelder-mead', options={'xtol

#class MyBounds(object):
#    def __init__(self, xmax=[200000., 200000.], xmin=[0., 0.] ):
#        self.xmax = np.array(xmax)
#        self.xmin = np.array(xmin)
#    def __call__(self, **kwargs):
#        x = kwargs["x_new"]
#        tmax = bool(np.all(x <= self.xmax))
#        tmin = bool(np.all(x >= self.xmin))
#        return tmax and tmin
#
#mybounds = MyBounds()

res = scipy.optimize.basinhopping(model, H1, niter=10, T=1.0, stepsize=10,
                                  minimizer_kwargs=None, take_step=None,
                                  accept_test=None, callback=None,
                                  interval=50, disp=True, niter_success=None,
                                  seed=None)
```